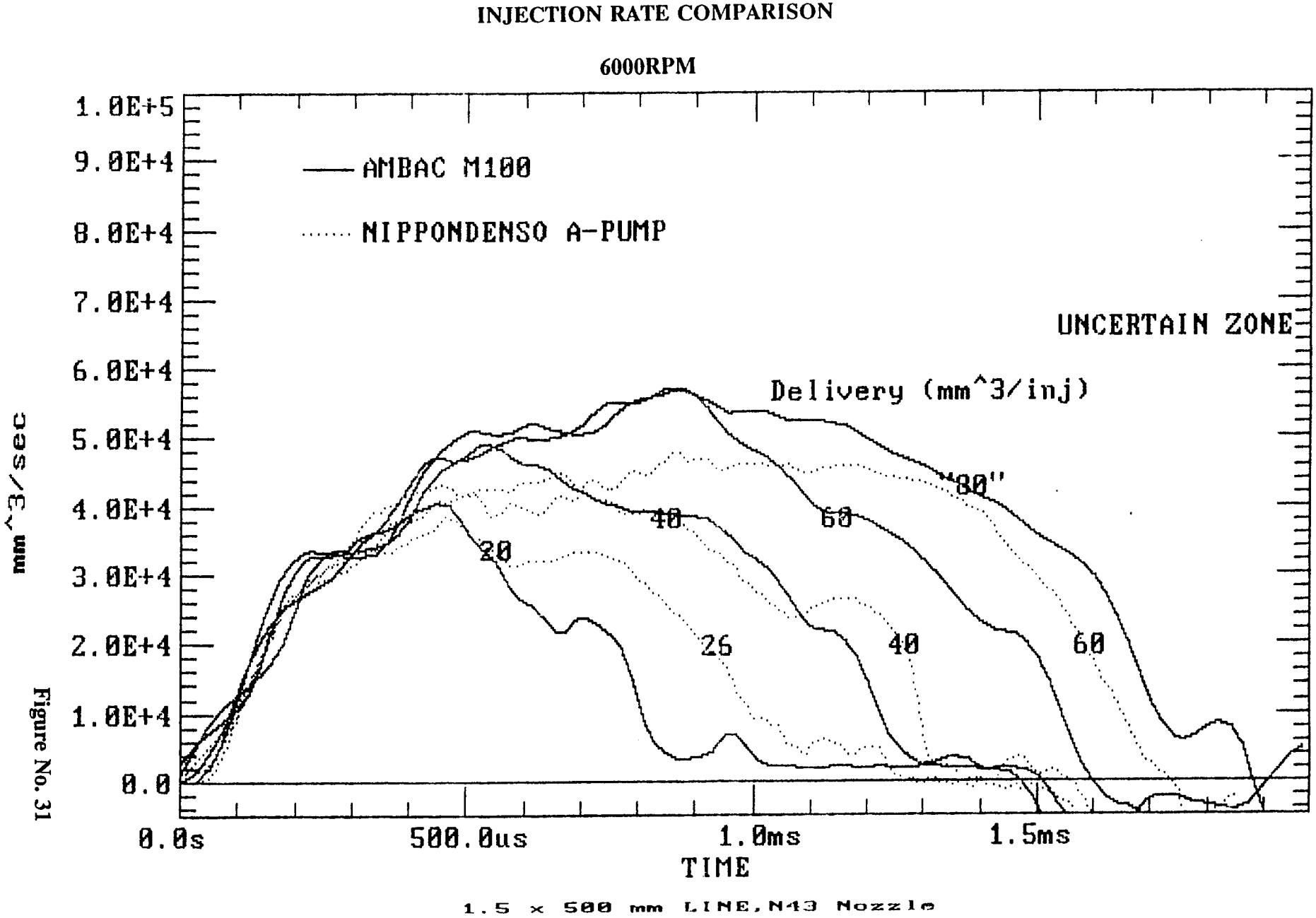

INJECTION RATE COMPARISON
6000RPM
AMBAC M100
NIPPONDENSO A-PUMP
UNCERTAIN ZONE
Delivery (mm^3/inj)
mm^3/sec
TIME
1.0E+5
9.0E+4
8.0E+4
7.0E+4
6.0E+4
5.0E+4
4.0E+4
3.0E+4
2.0E+4
1.0E+4
0.0
0.0s
500.0us
1.0ms
1.5ms
80"
60
40
20
60
40
26
1.5 x 500 mm LINE,N43 Nozzle

Figure No. 31

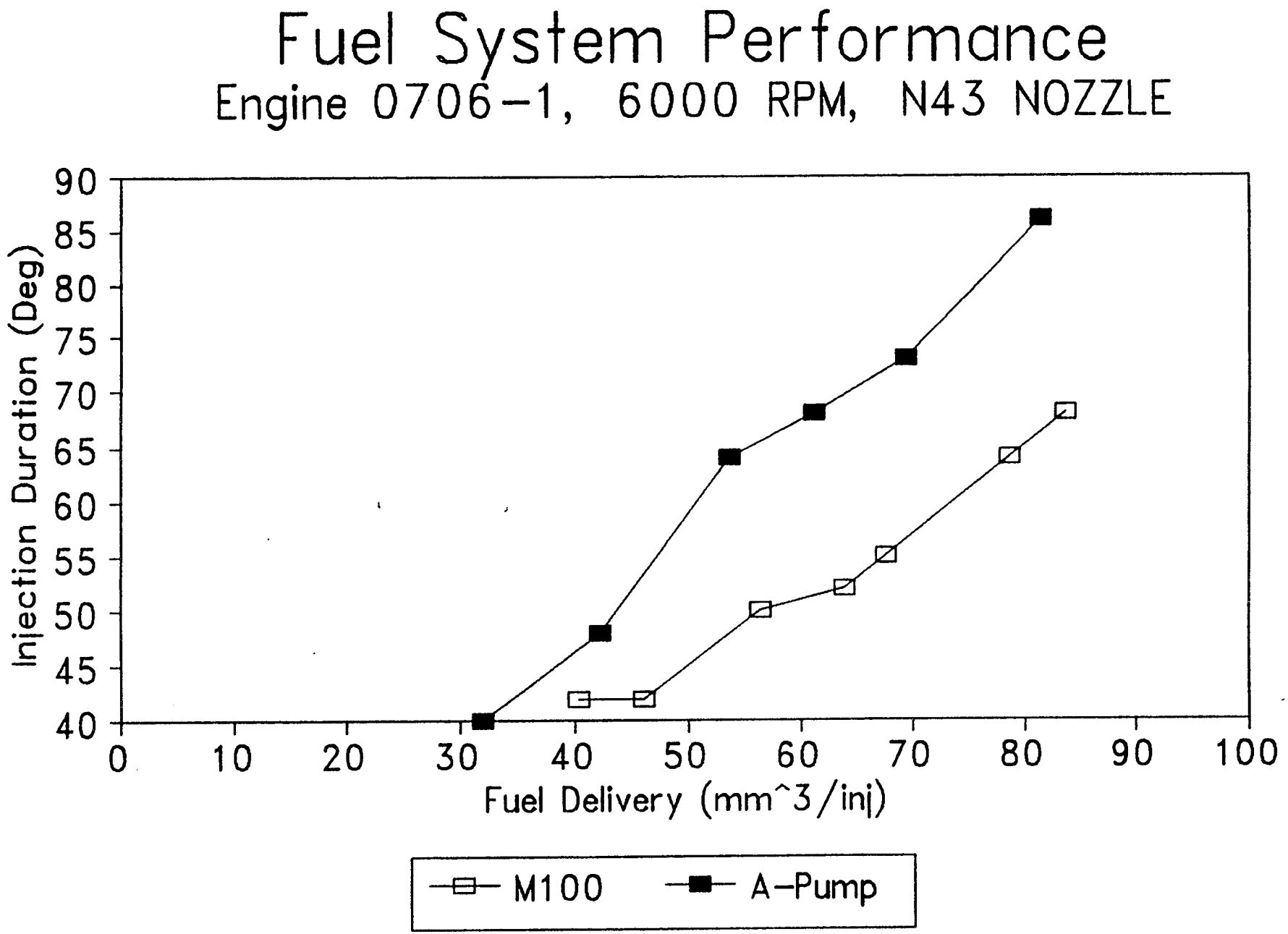


Figure No. 32A

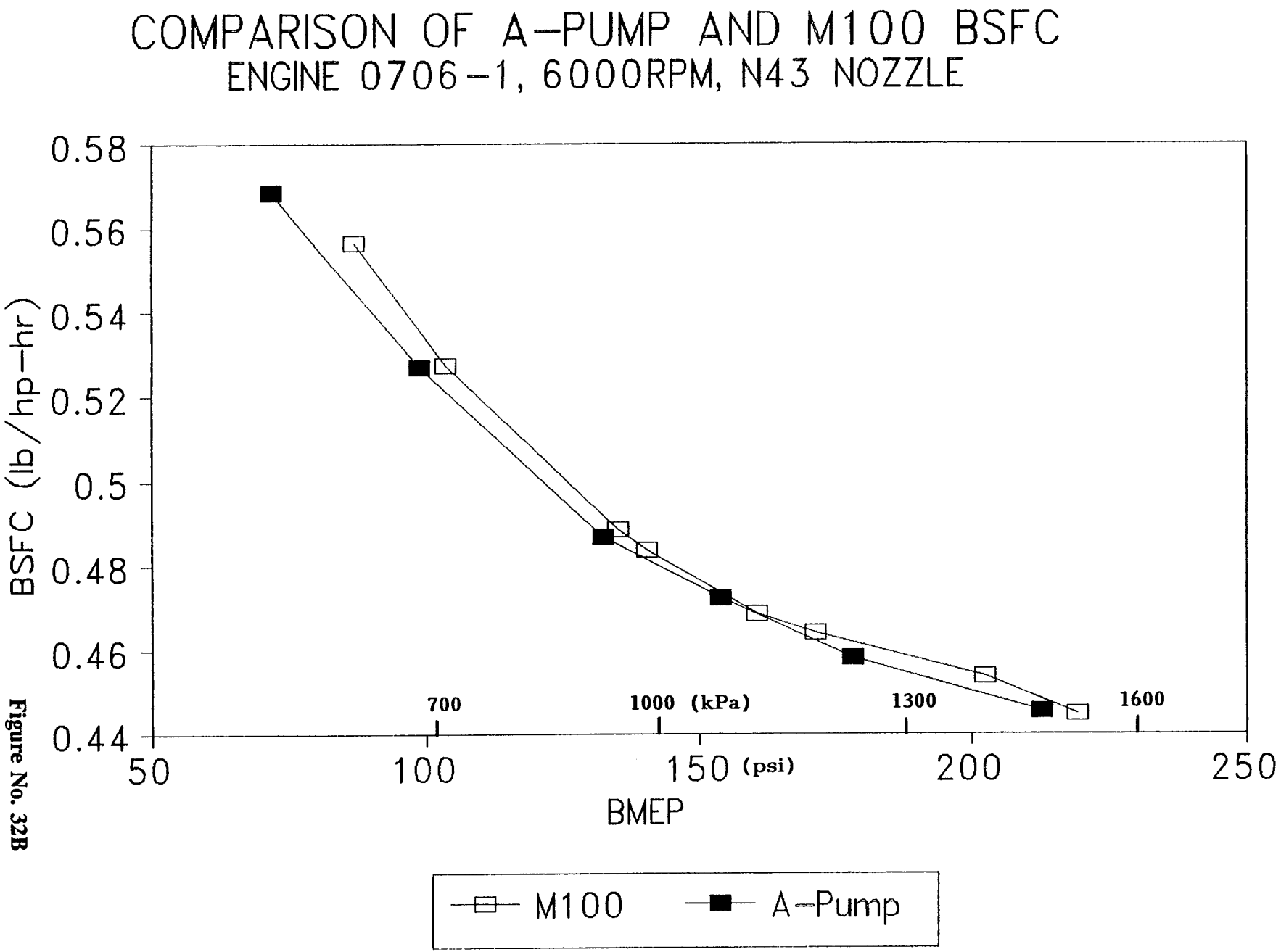


Figure No. 32B

4.2 REDUCED FRICTION/IMPROVED TRIBOLOGY/SEALING

PRECEDING PAGE BLANK NOT FILMED

INTRODUCTION

Improvements in the tribological systems of the Stratified Charge Rotary Engine (SCRE) are required to improve efficiency and assure adequate durability at the desired aviation power ratings. Activities in this program focused on: a) measuring and reducing friction, b) measuring and reducing side seal leakage, c) improving sealing system durability, and d) improving the lubrication of the gas sealing system.

Engine tests were performed to measure friction, seal leakage and wear. Seal system materials were screened and engine tested, showing a fourfold improvement in apex seal durability. New seals were designed which analytically show promise for further reductions in wear and friction. An advanced synthetic lubricant was tested. Apex seal temperature was measured in a firing engine during an attempt to improve lubricant usage efficiency.

The specific objectives, technical approach, results and conclusions are discussed in the sections that follow.

OBJECTIVES

The objectives of the reduced friction and improved tribology/sealing methods task are listed below:

1. Reduce Engine Friction:

   a. Establish a method for measuring engine friction to facilitate comparison of test configurations.

   b. Measure engine friction for the baseline single rotor rig.

   c. Design sealing systems which lower friction by reducing loads and promoting the formation of elastohydrodynamic or hydrodynamic films.

   d. Validate new sealing system designs in engine tests, measuring friction and wear.

2. Improve Engine Sealing at the Design Point:

   a. Design sealing systems that control seal loading under high combustion pressure conditions to minimize wear.

   b. Design sealing systems with improved compliance to reduce combustion gas leakage.

c. Select and test lubricants which can tolerate the expected high surface temperatures without forming detrimental deposits.

d. Enhance delivery of lubricant to the wear surfaces to minimize consumption and deposit formation.

e. Identify promising low wear material pairs using wear rigs and engine tests.

TECHNICAL APPROACH

The technical approach for reducing engine friction and improving engine sealing consisted of developing and utilizing an analytical seal dynamics model, bench screening and engine tests of new seal materials, and engine tests to evaluate present (and proposed) sealing grid friction and performance. The specific elements of this activity are described in the following paragraphs.

SEAL DYNAMICS MODEL

An existing apex seal dynamics model was available for use in this activity. This model calculates apex seal to trochoid loading based upon inputs of engine geometry, coefficients of friction, and measured or predicted combustion pressure indicator diagrams. This model was extensively modified to allow analysis of configurations other than the standard bar type apex seal. Corrections were made to the subroutine which calculates the contribution of slot friction to total apex seal load.

An example of the apex seal dynamics model output is shown in Figure 1. The two curves represent the two possible loading conditions which are dependent upon the direction of radial apex seal motion (or impending motion) relative to the rotor.

The inner curve represents the seal to trochoid load when the seal is moving out of the rotor slot, in which case slot friction is subtracted from the seal to trochoid load. The outer curve represents the loading when the seal is moving into its slot, and friction is added to the seal to trochoid load. Seal motion relative to the rotor occurs due to manufacturing and assembly tolerances, thermal and pressure distortions, bearing clearances, gear backlash and crankshaft deflections. Because of the complex nature and small magnitudes of these interacting causes, it is not possible at this time to predict with confidence the direction of seal motion at any point in the cycle. The objective when utilizing the dynamics model in the design process is to ensure that seal to trochoid load magnitudes are reasonable for both directions of seal motion throughout the cycle.

The apex seal dynamics model was used to determine the required dimensions of an apex seal which is predicted to offer improvements in friction and wear. The proposed new seal design is discussed in detail in the Results section of this report.

MATERIALS SCREENING TESTS

An Alpha LFW-1 wear rig was used to screen potential seal and counterface materials. The Alpha rig is a block-on-ring type tester that tests for basic material compatibility under dry sliding conditions. Previous investigations have shown the apex seals to operate under mixed lubrication conditions: a lubrication regime in which material compatibility is important in preventing catastrophic wear. The Alpha rig has shown, over decades of use, the ability to screen materials with sufficient accuracy to identify promising pairs for engine testing.

ENGINE TESTS

Engine tests were developed and run to obtain baseline data on rotor side seal gas leakage, engine power section friction, gas seal wear, and apex seal lubrication requirements. The individual test methods are described below.

Side Seal Leakage Test

A side seal leakage (blowby) test was developed to determine the volumetric flow of combustion gases past the rotor side sealing grid. The leakage test was run using a commercial configuration SCORE 70 (0.7 liter) single rotor engine. The power section of the engine did not differ significantly from the NASA 1007R rig engine except for the inclusion of special features intended to reduce blowby.

A blowby test cycle was devised to monitor the effect of speed, load, and test duration on side seal leakage. Blowby gas was directly measured by routing all crankcase blowby gases through a public utility type gas meter.

Friction Measurement Test

Engine friction was measured under firing conditions to determine the Friction Mean Effective Pressure (FMEP) of the present NASA rig engine configuration power section. The FMEP was obtained by calculating Indicated Mean Effective Pressure (IMEP) from the combustion pressure indicator diagrams and subtracting from this derived IMEP the Brake Mean Effective Pressure (BMEP) calculated from the engine dynamometer load cell. The resulting value is representative of the FMEP.

The IMEP calculations were found to be very sensitive to the assumed position of engine top center. Small changes in the location of engine top center produced large changes in calculated FMEP. The variability in FMEP with assumed top center location is shown in Figure 2. To improve confidence in the FMEP measurements, the actual rotor position at assumed top center was measured and compared to true top center (found by measuring the actual position of the rotor housing dowels). The top center position used to determine IMEP was then adjusted accordingly.

Seal Lubrication Test

Sacrificial lubricant consumption can be minimized by selecting a lubricant introduction location that promotes the deposition of the lubricant on the wear surfaces, while minimizing airstream entrainment or deposition on the rotor surface. The optimum lubricant introduction method can be determined by testing several lubricant introduction locations. The lubrication method which allows use of the lowest lubricant flow without causing breakdown of apex seal lubrication would be the preferred method. Monitoring the apex seal temperature for temperature increases while decreasing lubrication flow rates would provide the required indication of incipient lubricant film breakdown.

A pre-existing instrumentation system for measuring apex seal temperature in SCORE 580™ engines was used to attempt to select an improved lubricant introduction method. The SCORE 580 engine (5.8 litres per rotor) was used because the small size of the SCORE 70 engine's rotor precluded the installation of the required instrumentation. It is believed that lubricant delivery trends, if not absolute brake specific oil consumption requirements, will translate between the two engine sizes.

Instrumentation for the lubricant introduction test was configured with six apex seal thermocouples - two per apex seal - located as shown in Figure 3. The thermocouple voltages were processed by a signal conditioner module mounted in the rotor. Temperature signals were output from the module via a slip ring on the rotor side to a pair of carbon brushes mounted in one end housing, and ultimately to a decoder circuit in the control room. The decoder circuit provided synchronization pulses to the rotor module to control the sequence of the thermocouple channels that were monitored. Temperatures were displayed on a digital indicator, and were also recorded from the decoder's analog output onto a strip chart. The basic rotor instrumentation is shown in Figure 4.

The engine was configured to allow introducing seal lubricant in several locations;

- Intake port drip bar (standard location).
- Four axially spaced holes on the trochoid surface just after the intake port closing edge.

- Three additional sets of axially spaced trochoid holes, two sets in the intake quadrant, one set just before the cold minor axis.

- Single holes, one on each end housing, at locations similar to those shown in Figure 5, taken from General Motors Patent No. 3,814,555. (This patent claimed a 33% reduction in lubricant requirements compared with a fuel-oil mixture technique.)

Lubricant was supplied by a variable speed, variable displacement laboratory metering pump (Fluid Metering Inc., Model QV-0). The lubricant flow rate was monitored with a Pierburg Model PLU-103A High Precision Flowmeter.

RESULTS

The results of the engine tests for side seal leakage, friction measurement, and apex seal lubrication will be presented first. The results of the seal materials screening test and engine test of new seal materials will follow. The new sealing system design, which incorporates inputs from engine and materials tests, in addition to dynamic seal analysis, will be presented last.

ENGINE TESTS

Side Seal Leakage Test Results

The side seal leakage test was performed on a commercial configuration SCORE 70 (0.7 liter per rotor) single rotor engine, number 1007P001-4. The power section of this engine was essentially the same as the NASA rig engine, except for several features included specifically to reduce side seal leakage. The specific features and design rationale for inclusion of each feature are identified in Table 1.

The side seal leakage test consisted of the test cycle shown in Table 2. The test cycle was devised to determine the effects of speed, load, and cumalative engine operating time on side seal leakage. The total test time was 126 hours.

The crankcase blowby gas flow and the static leak-down test pressure were measured at the end of each test cycle. The results of the test are shown in Figure 6. The upper plot shows the increase in blowby over the duration of testing, while the lower plot shows the static leak-down test results. Static leak tests are routinely performed to give an indication of sealing system condition.

Crankcase gas blowby was not significantly reduced by the seal grid features designed to reduce blowby when compared with a standard configuration engine. The leak test results for engine 1007P001-4 are considered to be very good, indicating that the side seals and apex seals remained in good condition. The increase in blowby gas flow indicates that side seal gas leakage was likely worsening primarily due to factors affecting sealing during operation, and not due to degradation of the seal's physical condition.

TABLE 1

FEATURES TO REDUCE SIDE SEAL GAS LEAKAGE

Design Feature	Reason for Incorporation
Butt-Butt Side Seals	Reduce interaction of motion between side and button seals. Allow each element to respond to housing surface irregularities independently.
High aspect ratio side seals (Deep side seal grooves with matching tall side seals)	Reduce tilting tendency of side seals. Tilted side seals may not seat uniformly on side housing surface, and may have inhibited freedom of motion in rotor grooves.
Increased preload button springs.	Increase button seal actuation force against side housing.
Reduced axial rotor clearance. (Wet hub clearance)	Reduce relative motion between side seals and rotor by reducing rotor axial motion within engine.
Enlarged blow-by recovery annulus.	Improve the capability to internally recirculate blow-by gases.

Disassembly of engine 1007P001-4 revealed heavy carbonaceous deposits located inboard of the side seal grid, most heavily concentrated near the apex buttons. The deposits are clearly an indication of excessive side seal grid leakage. Faint patterns in the deposits suggest that the predominant leak paths may have been across the button seal faces. The rotor side deposits are shown in Figure 7. Despite the presence of the deposits all the seals were free in their slots. The deposits may, however, serve to inhibit seal performance during operation, perhaps by impeding the flow of gas to the underseal volumes, or by preventing the seals from achieving good contact against the seal slot walls. It is speculated that seal leakage is a self generating phenomenon; seal leakage promotes deposit formation which in turn further impairs seal performance.

Another possible contributor to rotor side deposits and side seal leakage is the narrow width of the SCORE 70 engine combustion chamber. The proximity of the end housings to the fuel spray may encourage partially combusted fuel to condense on the end housing surfaces and to collect in the side seal crevice volumes, promoting deposit formation and attendant seal leakage. JDTI's SCORE 580 engine with a similar side sealing grid has not exhibited any blowby or rotor side deposit problems in thousands of test hours. The SCORE 580 end housings are over twice the distance from the fuel sprays as in the SCORE 70 engine.

TABLE 2

SIDE SEAL LEAKAGE TEST CYCLE

SPEED (RPM)	ENGINE LOAD - BMEP PSI	kPa	CYCLE DURATION (HOURS)
4000	65	447	1
4000	120	827	1
5000	65	447	1
5000	120	827	1
6000	65	447	1
6000	130	896	1

Friction Measurement Test Results

Total engine friction was measured on the NASA rig engine 0706-1 under motoring and firing conditions. Engine 0706-1 was of the standard NASA rig engine configuration (0.7 liter per rotor) except for the inclusion of Ferrotic SK dual corner (clevite corners) apex seals mated against a Jetkote thermal spray applied Chromium Carbide-Nichrome (Cr_3C_2NiCr) trochoid coating, and the use of an experimental synthetic lubricant. These features were included because they represented the most likely near-term improvements in the sealing system which were anticipated to be incorporated into future engine builds.

Results of the Friction Test are shown in Figures 8, 9 and 10. These figures show the total measured FMEP for the engine's power section, accessory drive gearbox, and fuel injection pumps.

Friction (FMEP) was found to increase with engine speed, and to decrease with engine load. Possible reasons for the inverse relationship of friction and load involve the effect of combustion pressure on engine bearings and seal elements. Combustion pressure forces act on the rotor to counter centrifugal force. To a limited degree bearing friction will be reduced with increasing engine load. Combustion pressure also affects the sealing elements' friction. Combustion pressure acts to increase apex seal to slot friction. If the apex seal to rotor relative motion is outward during high pressure intervals of the combustion cycle, the effect of increased apex slot friction on the apex seal will be to reduce the apex seal load on the trochoid surface. Reducing the apex seal load on the trochoid directly reduces engine friction.

Seal Lubrication Test Results

Apex seal temperature during engine operation was monitored to determine the optimum method and flow rate of seal lubricant introduction. Apex seal temperatures were measured using instrumentation developed for and installed in a single rotor SCORE 580 engine.

The seal temperature data plotted against lubricant flow rate at an engine speed of 2400 rpm is shown in Figure 11. During engine operation at 2400 rpm and load of 120 psi 827 kPa) bmep, the seal lubrication rate was incrementally reduced to determine the minimum lubricant usage requirement. The minimum lubricant flow rate was to be indicated by a rise in apex seal temperature.

No temperature rise was indicated over the range of lubrication rates explored from 1% of fuel flow (the traditionally specified rate) down to 0.08% of fuel flow. The absence of a temperature rise at the low lubrication rate may be due to several factors:

1. Insufficient time may have been allotted for the depletion of lubricant introduced at relatively high rates. (0.08% rate was run for only five minutes to prevent undetected catastrophic wear.)

2. Thermocouple response time may not have allowed resolution of temperature transients.

3. Rotor oil seal leakage may have allowed sufficient lubricant to reach the seals, obviating the need for any additional seal lubricant. (At the condition run, fuel flow was 100 lbs/hr (45.36 kg/hr). At a seal leakage rate of 1% of fuel flow, sufficient lubricant would likely reach the apex seals without additional sacrificial supply. This leakage rate, one pound per hour, would not ordinarily be detectable with standard test cell instrumentation unless steady test points of approximately four hours or more were run.)

To improve test procedure sensitivity, it is recommended that any future apex seal temperature testing be run at higher engine loads, where oil seal leakage would be a smaller fraction of total apex seal lubrication requirements.

All six apex seal thermocouples failed before any additional testing was performed. The failure mode of the thermocouples has not been identified because the engine was not disassembled. Past failures in similar testing were due to fatigue or abrasion where the thermocouple wires exited the seals, looped inside machined cavities in the button seals, and attached to solder pads on the rotor. Larger diameter rotor buttons (which have been run in unrelated tests) are recommended to be fitted to the instrumented rotor to allow more room for wiring on any future builds.

MATERIAL SCREENING TESTS

Seal and trochoid coating material screening tests identified seven promising new material combinations, successfully engine tested one new material wear pair, and evaluated an experimental lubricant.

MATERIAL SCREENING

Twenty five apex seal and trochoid material pairs were screened in the materials bench testing process. The methodology and selection of the proposed materials are discussed in detail in Appendix 1.

The following material combinations were found to merit further evaluation in engine testing:

Seal Material	Trochoid Coating
PM-212	LW 1N-30 (Tungsten Carbide-Cobalt)
PM-212	Triballoy T-800
PM-212	Stellite 6
Si_3N_4	Triballoy T-800
Si_3N_4	44\430
Triballoy T-800	Triballoy T-800
NJS 234 (Gopalite)	Triballoy T-800

MATERIAL ENGINE TEST

One new material wear pair was tested in the NASA 1007R rig engine. The combination tested was Ferrotic SK apex seals running against Chrome Carbide-Nichrome, Jetkote applied, trochoid coating. The material pair performed extremely well with a seal wear rate of only 0.0017 inches (0.043 mm) per 100 hours of operation. The testing included engine operation at engine loads up to 277 psi (1.908 mPa) Brake Mean Effective Pressure (BMEP). No visible trochoid coating deterioration was detected. The standard material combination, Clevite apex seals and Tungsten-Carbide, Detonation Gun (D-Gun) applied trochoid coating has an historical average apex seal wear rate of 0.007-0.009 inches (0.178-0.229mm) per 100 hours.

LUBRICANT TEST

An experimental high temperature capability lubricant was tested in three engine tests. The lubricant is a proprietary formula manufactured by AKZO Corporation, designated E90046. Deposits formed on the rotor flanks and rotor faces were judged to be excessive relative to

the convential lubricants generally used. Evidence of the deposits interfering with side sealing function was not conclusive.

SEALING SYSTEM DESIGN

New rotor side and apex seals were designed to reduce seal related friction, wear, and gas leakage. Design inputs included engine test results of present grid configurations, seal dynamic analysis, and the objectives of reducing friction while improving gas sealing performance, and reducing seal loads to reduce seal wear.

Rotor Side Seal Design

The rotor side seal design includes features to increase side seal compliance with mating surfaces and to reduce effects of external seal tilting forces. Two side seal designs were prepared and one configuration was procured.

The standard configuration side seals are made to fit curved rotor grooves with a radius approximately parallel to and inboard of the rotor face contour. The seals' primary mating surface is the flat side housing. The side seals' curved shape will allow uniform contact with the side housing to be disturbed if the seals tilt in their groove. Conditions that may cause a tilting moment on the seal include: 1) uneven pressure distribution on the seal, 2) friction forces on the seal, 3) axial rotor motion, and 4) side housing distortion. Loss of uniform contact between the side seals and side housing will possibly allow gas leakage.

To eliminate the loss of uniform side housing contact when the seal tilts, several straight element side seal concepts were explored. A segmented side seal was proposed, with each curved seal replaced by two straight elements joined with a secondary button seal at the center. This configuration is shown in Figure 12. Design layout of this proposal revealed an interference with the side housing dummy port feature. The concept was modified as shown in Figure 13 to incorporate three straight segments per seal joined with two secondary buttons.

The three straight element segmented seal has two drawbacks: 1) there are four additional junctions per seal which may be leak paths for gas, and 2) the rotor grooves are difficult to machine.

The three straight element side seal configuration was procured for a proof of concept test. The test objective was to determine if improved side seal compliance would reduce leakage. This test was not performed because of the reduced scope of the NASA Phase III program.

Rotor Apex Seal Design

An apex seal system was designed to minimize wear and friction by controlling gas pressure loading and enhancing lubricant film formation. This seal configuration is shown in Figure 14 and is characterized by a mushroom shaped bar with a larger than standard (6x) tip radius and two secondary seal elements at the seal to slot interface.

The mushroom shape provides pressure balancing to control pressure induced seal to trochoid forces. The secondary seals prevent high gas pressure from creating high side loads and the attendant high seal to slot friction force which can disrupt seal behavior. The large tip radius enhances the formation of a lubricant film which can reduce friction and wear.

Figures 15 through 18 are plots of seal to trochoid forces for the standard and new mushroom apex seals at 160 HP (120kw) and 200 HP (150kw), as predicted by the apex seal dynamics model. Figures 15 and 16 compare the predicted seal forces for the standard and new design apex seals at 7000 RPM and 160 BHP (120kw). Figures 17 and 18 provide the same comparison at 8000 RPM and 200 BHP (150kw). Loads for the mushroom seal are predicted to be lower than for the standard seal for most of the cycle. Predicted peak seal loads are dramatically reduced by up to 50% for the 200 HP (150kw) operating condition.

Additional discussion of the benefits of the mushroom seal design is provided in Appendix 2. Seal analysis results for the mushroom seal configuration and two other candidate seal design systems are provided in Appendix 3.

CONCLUSIONS

1) The Score 70 NASA engine side and button seal performance deteriorates with increasing engine operating time. The deterioration is not due to wear or mechanical changes of the sealing elements. Deposit formation associated with seal leakage is the likely cause of the sealing performance degradation. The deposits appear to cause the deterioration by interfering with seal motion and/or impeding the flow of actuating gas pressure to the underseal volume.

2) The geometry of the SCORE 70 engine may contribute to the formation of deposits due to the proximity of the fuel sprays and partially combusted fuel to the crevice volumes.

3) Engine friction increases with engine speed, but decreases slightly with engine load. The inverse relationship of friction with load may be due to the following:

   A) Combustion pressure forces reducing peak engine bearing loads and thereby reducing bearing friction losses.

   B) Combustion pressure loading on the apex seals which is believed to reduce the seal to trochoid force. The combustion pressure reduces the load by increasing the seal to slot friction force while the seal moves outward relative to the rotor.

4) New apex seal designs are feasible which may reduce engine friction and wear. The new seal designs would reduce friction and wear by controlling pressure loading, increasing lubricant film thickness, decreasing contact stress, and providing a more favorable height to volume wear rate ratio.

5) New seal and trochoid coating materials offer the potential for greatly enhanced seal life. One apex seal and trochoid coating material pair (Ferrotic SK/Chrome Carbide-Nichrome) demonstrated a four-fold reduction in wear rate compared to the standard (Clevite/Tungsten Carbide) material combination. Other material combinations showed potential for excellent wear resistance in wear rig tests. These material combinations included such materials as the self lubricating, NASA developed, PM-212, Triballoy T-800, and Silicon Nitride.

RECOMMENDATIONS

1) Fabricate new gas sealing systems in accordance with the concepts discussed herein. Test the seal systems by measuring friction, wear and gas leakage.

2) Engine test the apex seal and trochoid coating material combinations judged most promising in the materials screening tests. Bench tests should also be performed to determine if any of the materials react with common lubricant additives to form anti-wear films.

3) Repeat the seal lubrication test after making the following instrumentation and engine improvements:

   A) Utilize new or reconditioned rotor oil seals.

   B) Incorporate larger diameter apex button seals to provide more space for the apex seal thermocouple wiring.

   C) Use stranded thermocouple wiring to increase durability.

   D) Devise a means for measuring crankcase oil consumption with greater sensitivity.

APPENDICES

1) Memo, Dan Newman to C.E. Irion, "LFW-1 Testing of Apex Seal Trochoid Coating Material Couples for Potential Reduced Friction," 3 December 1991.

2) Memo, Jon Lauter to Engineering, "Mushroom Apex Seal Rationale," 17 July 1991.

3) Memo, A. Leto to J. Lauter, "Mushroom Apex Seal Design," 29 October 1991.

RECOMMENDATIONS

1) Fabricate new gas sealing systems in accordance with the concepts discussed herein. Test the seal systems by measuring friction, wear and gas leakage.

2) Engine test the apex seal and trochoid coating material combinations judged most promising in the materials screening tests. Bench tests should also be performed to determine if any of the materials react with common lubricant additives to form anti-wear films.

3) Repeat the seal lubrication test after making the following instrumentation and engine improvements:

   A) Utilize new or reconditioned rotor oil seals.

   B) Incorporate larger diameter apex button seals to provide more space for the apex seal thermocouple wiring.

   C) Use stranded thermocouple wiring to increase durability.

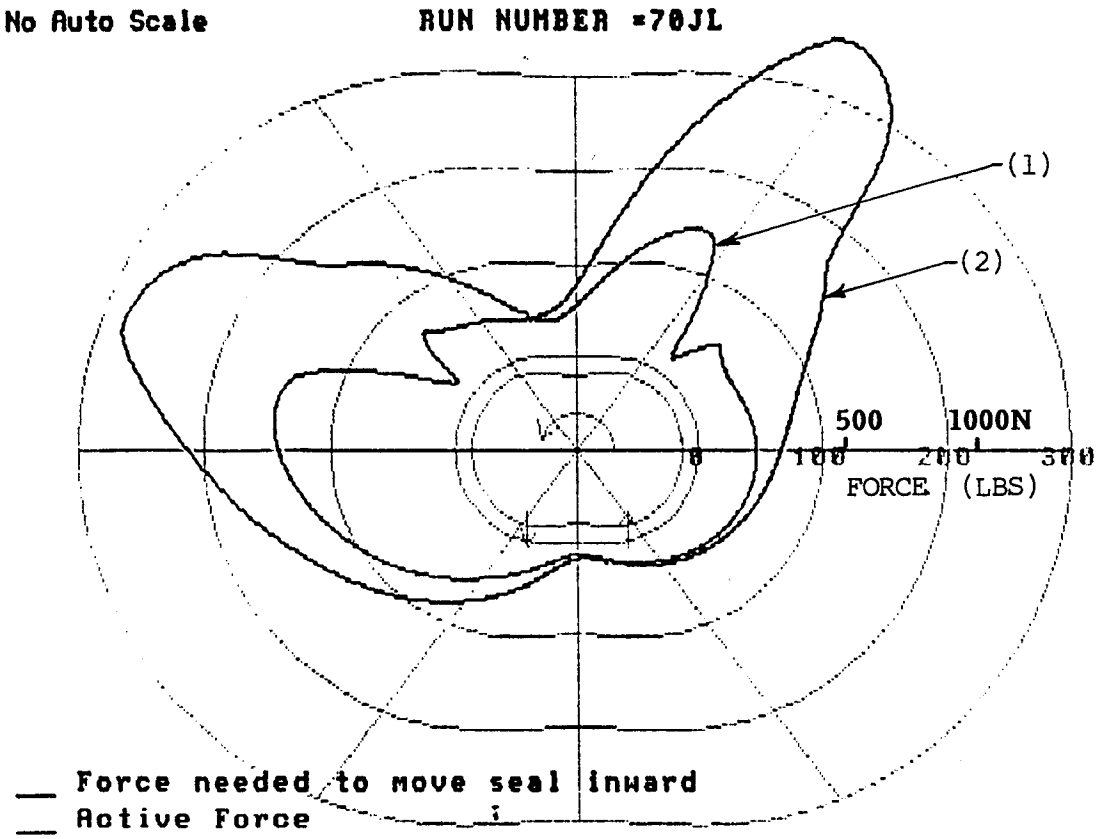
   D) Devise a means for measuring crankcase oil consumption with greater sensitivity.

APPENDICES

1) Memo, Dan Newman to C.E. Irion, "LFW-1 Testing of Apex Seal Trochoid Coating Material Couples for Potential Reduced Friction," 3 December 1991.

2) Memo, Jon Lauter to Engineering, "Mushroom Apex Seal Rationale," 17 July 1991.

3) Memo, A. Leto to J. Lauter, "Mushroom Apex Seal Design," 29 October 1991.



1) Seal Moving Outward Relative to the Rotor Slot

2) Seal Moving Inward Relative to the Rotor Slot

FIGURE 1

SAMPLE OUTPUT OF APEX SEAL DYNAMICS MODEL

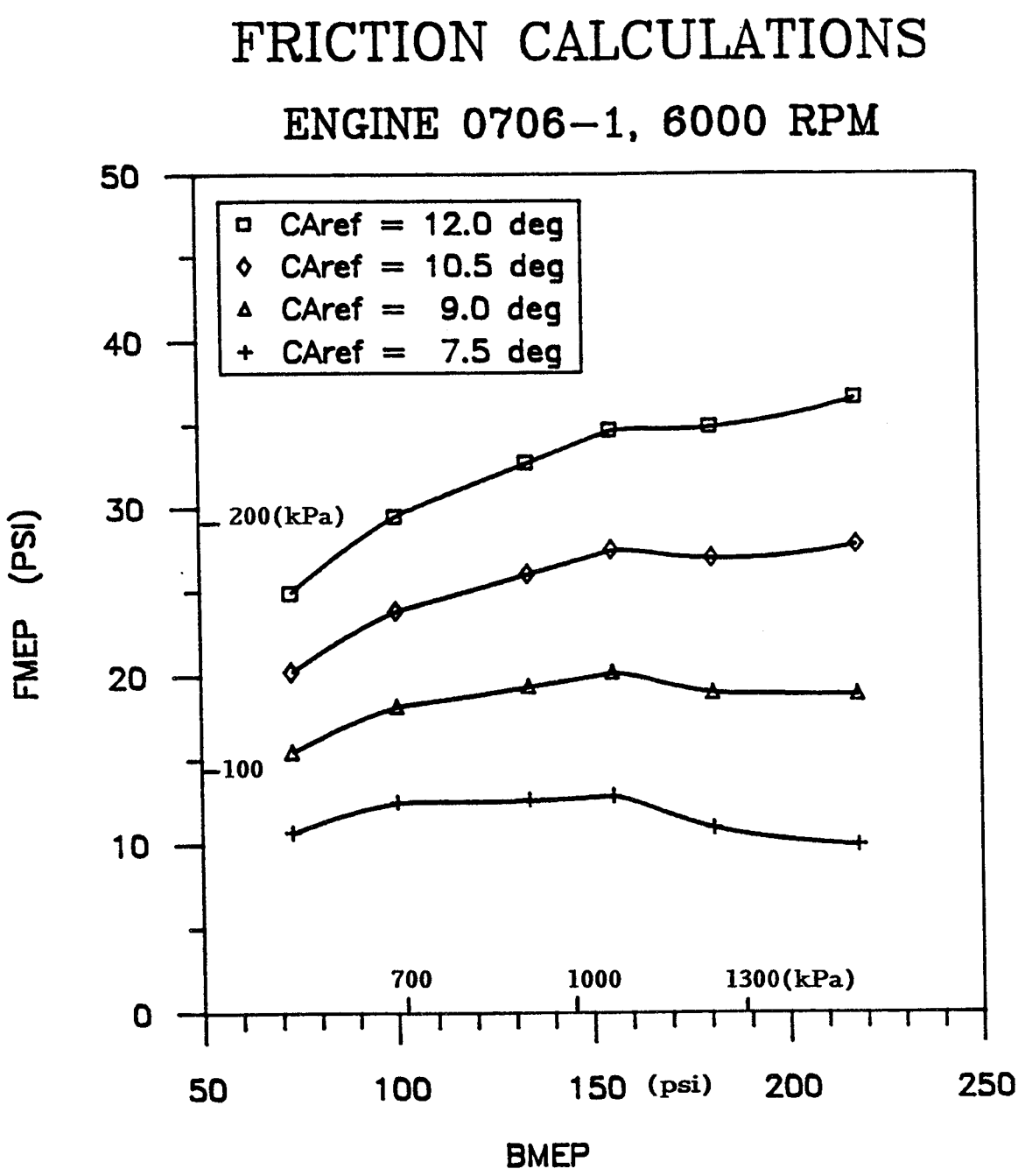


FIGURE 2

VARIABILITY OF FMEP WITH TDC POSITION

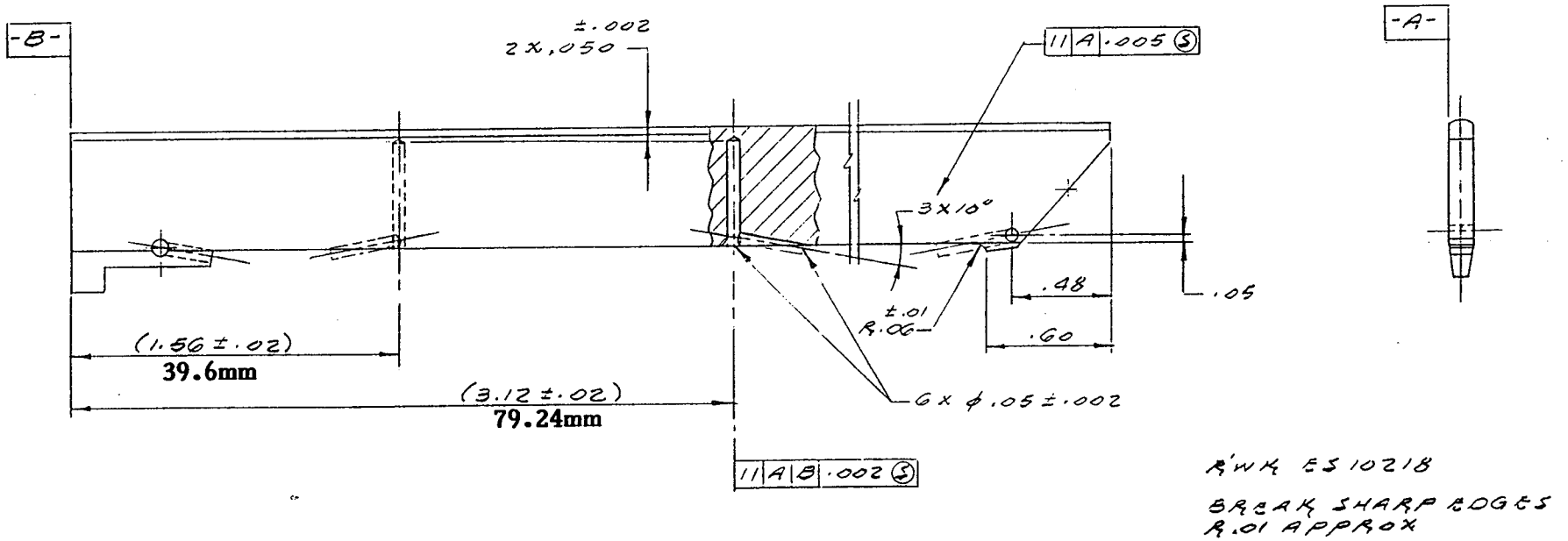


FIGURE 3

APEX SEAL THERMOCOUPLE LOCATION

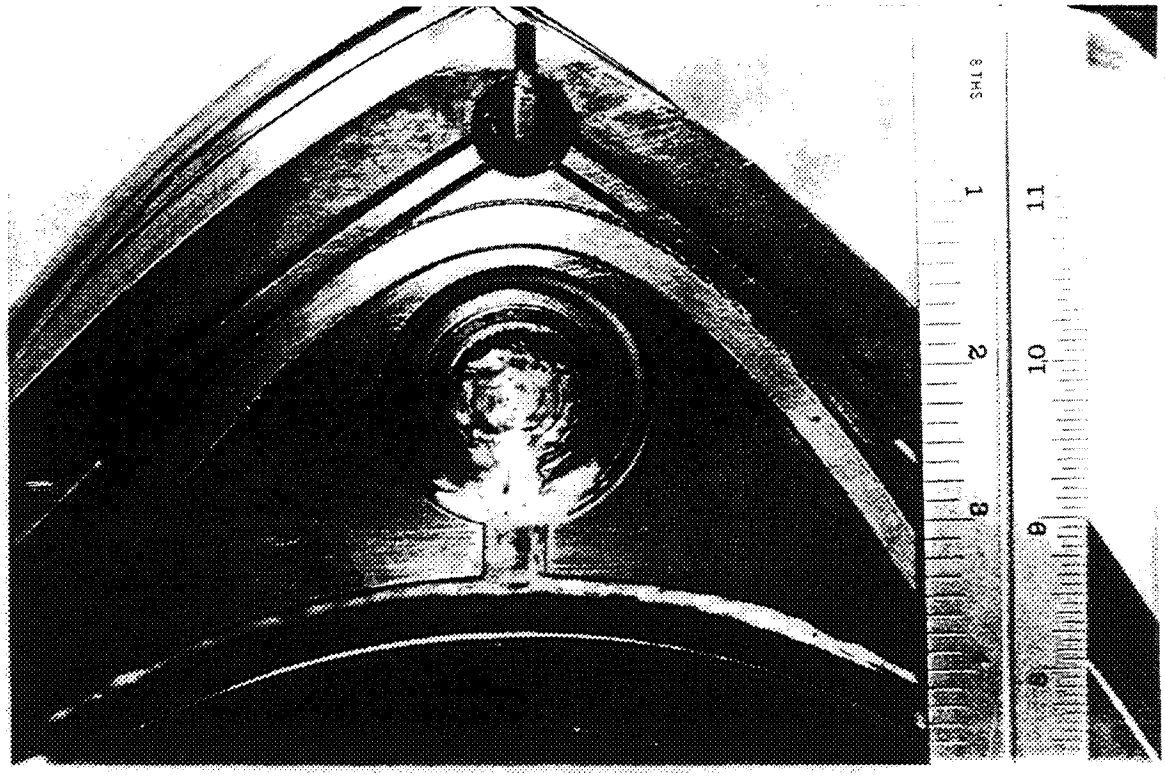


FIGURE 4

SIGNAL CONDITIONING

MODULE, INSTALLED

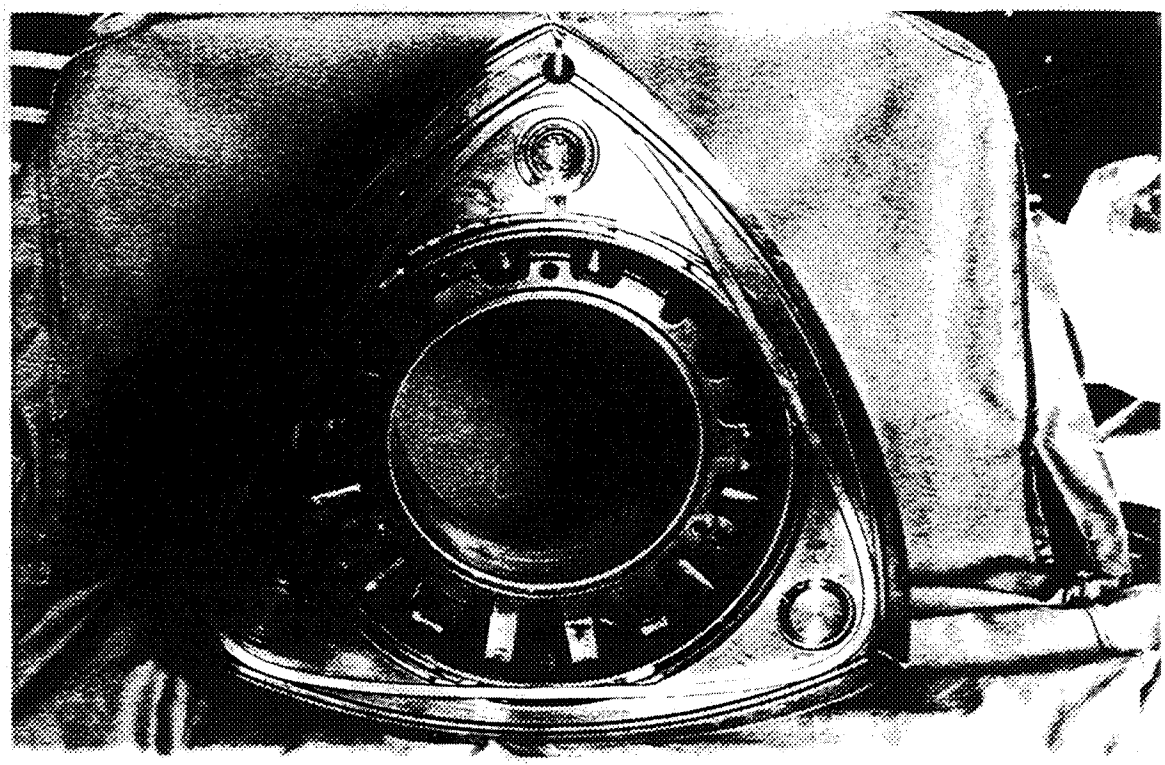


FIGURE 4

ROTOR INSTRUMENTATION

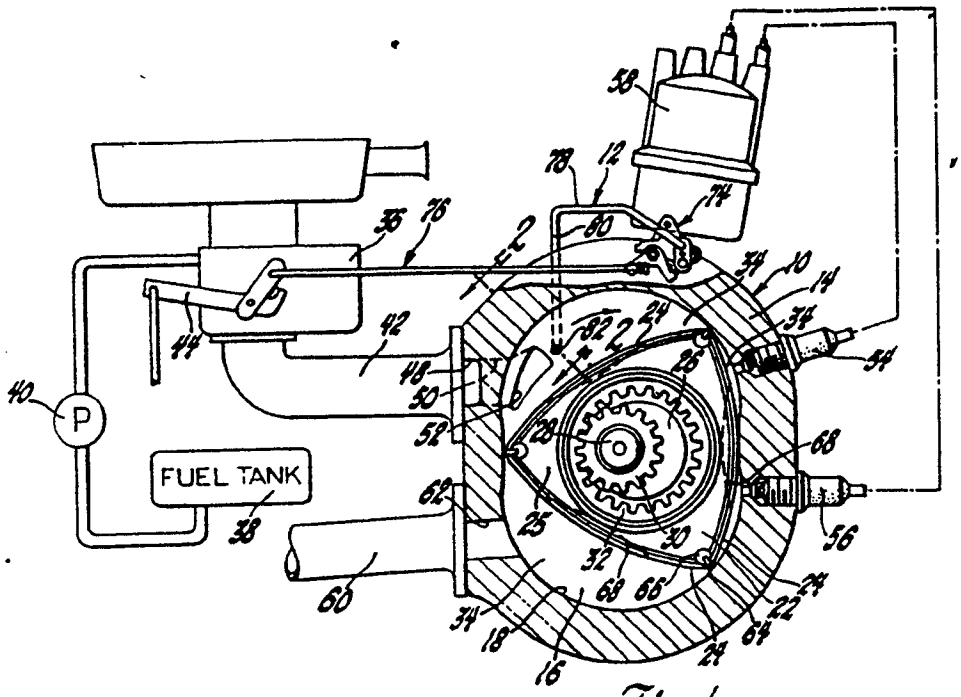


Fig. 1

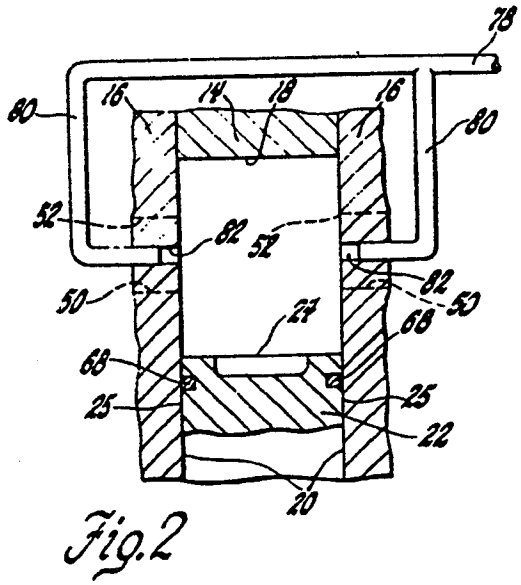


Fig. 2

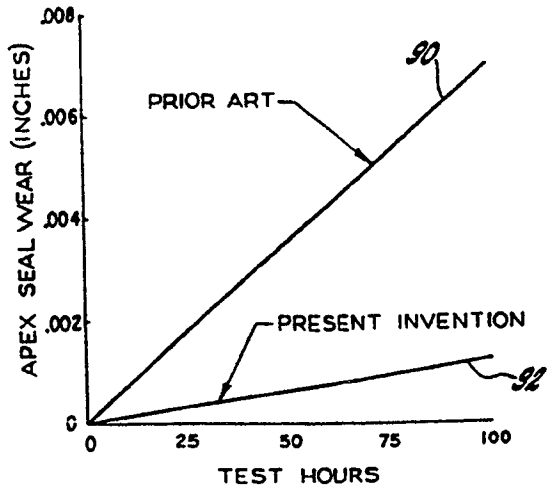


Fig. 3

FIGURE 5

END HOUSING OIL INTRODUCTION LOCATION:
Reference General Motors Patent # 3,814,555

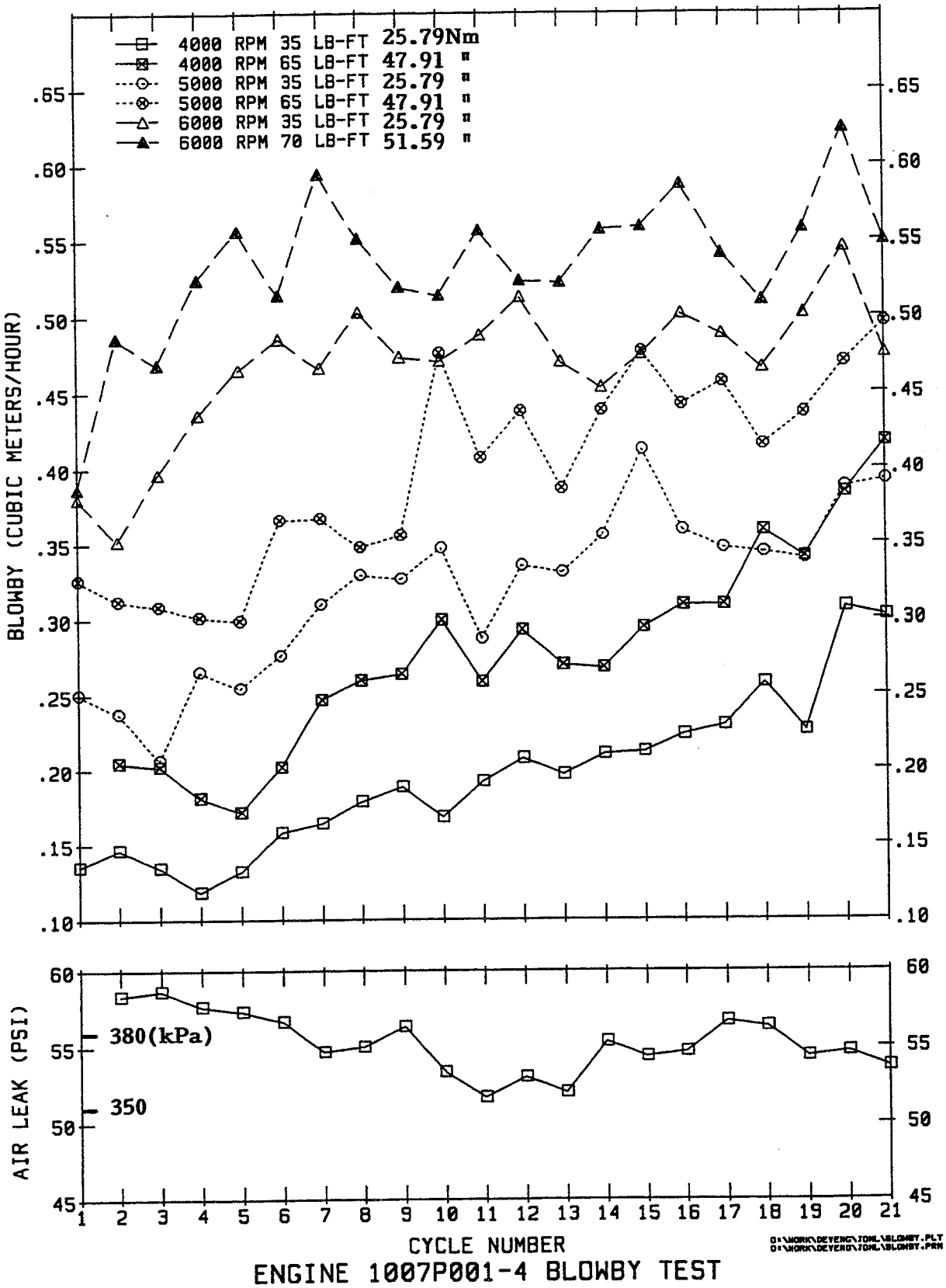


FIGURE 6

CRANKCASE BLOWBY GASES AND ENGINE AIR-LEAK TEST



FIGURE 7

ROTOR DEPOSITS - BLOWBY TESTS

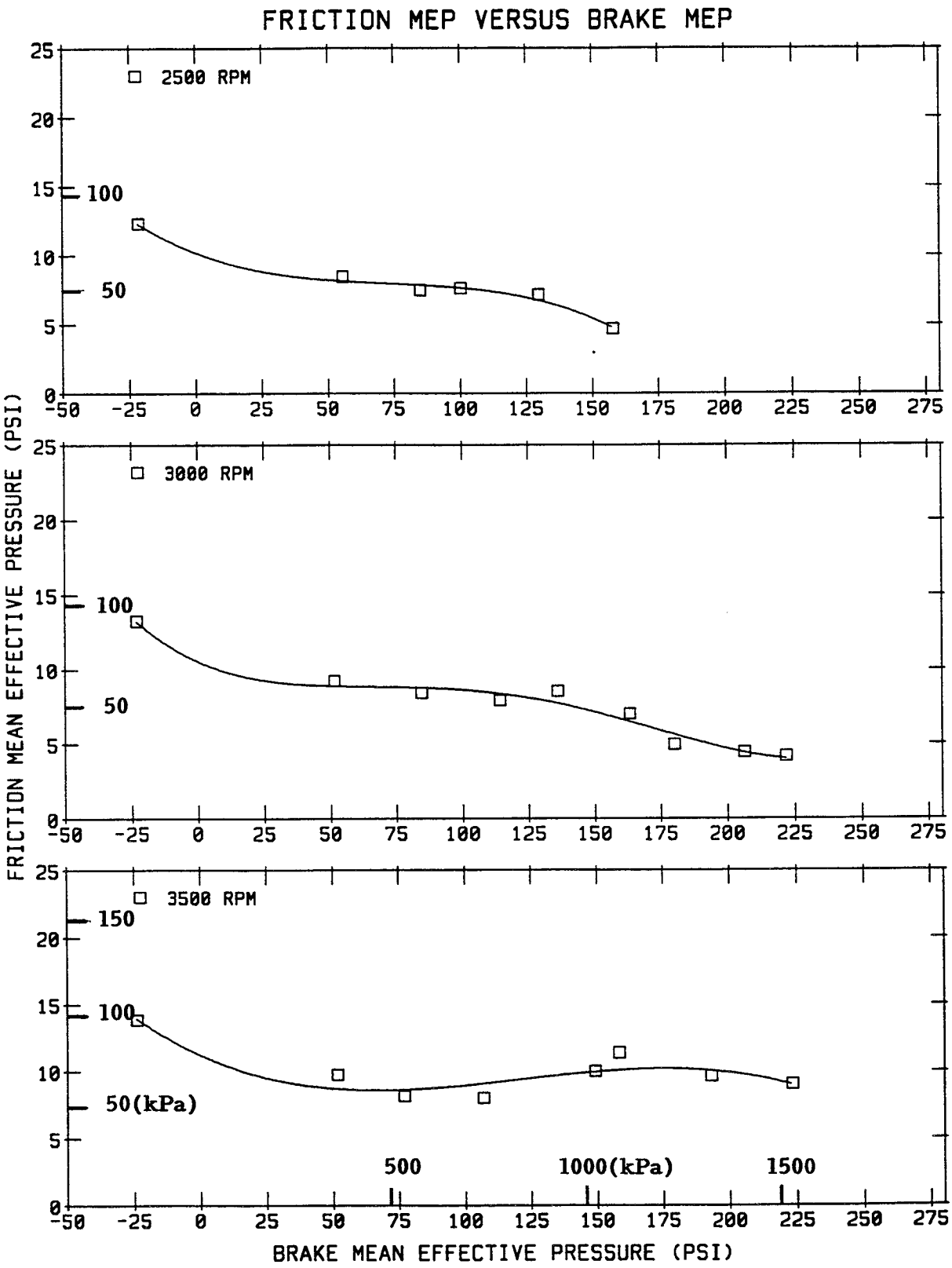

FRICTION MEP VERSUS BRAKE MEP
2500 RPM
3000 RPM
3500 RPM
100
50
150
50(kPa)
500
1000(kPa)
1500
FRICTION MEAN EFFECTIVE PRESSURE (PSI)
BRAKE MEAN EFFECTIVE PRESSURE (PSI)

FIGURE 8

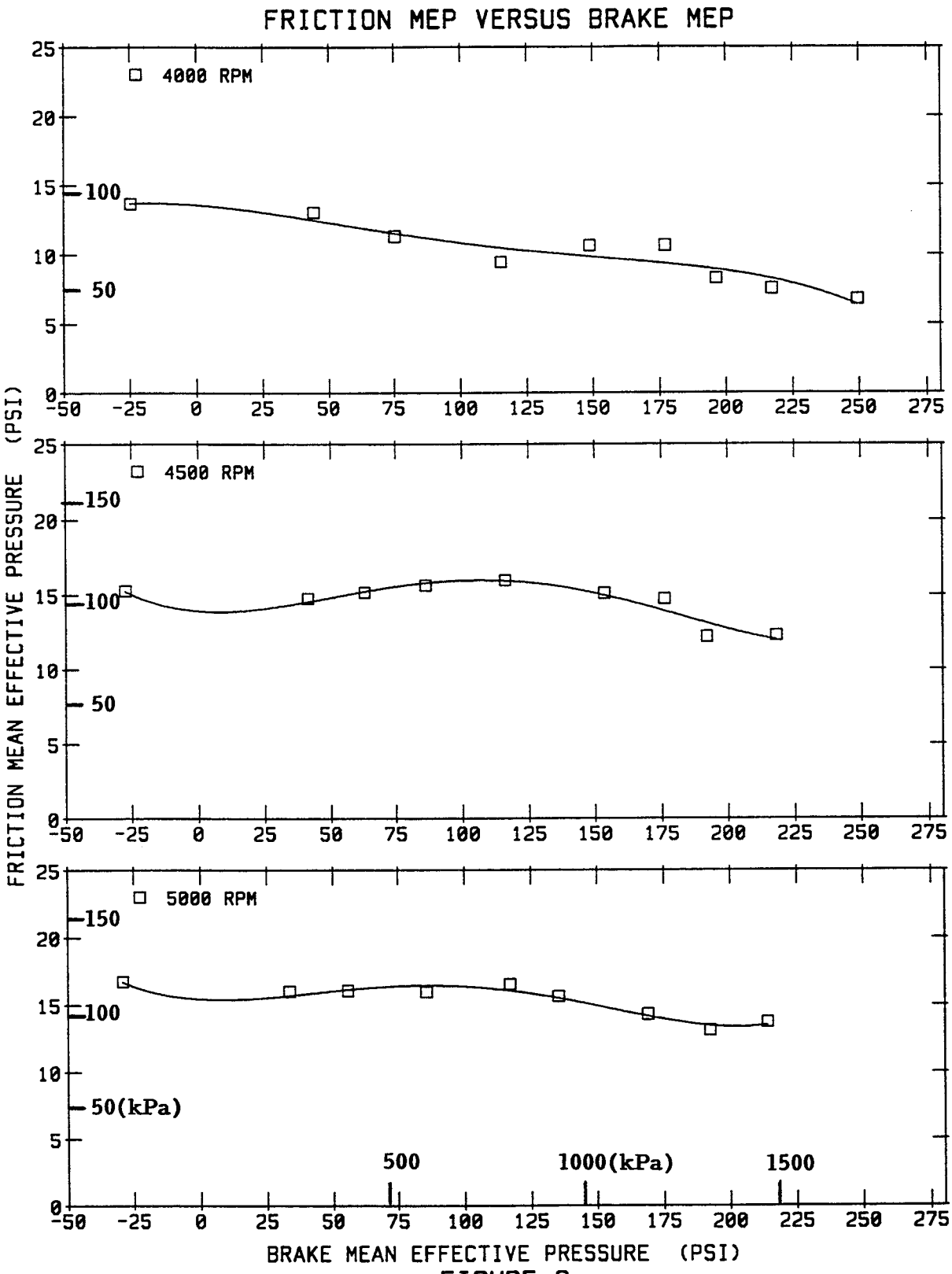

FRICTION MEP VERSUS BRAKE MEP
4000 RPM
4500 RPM
5000 RPM
FRICTION MEAN EFFECTIVE PRESSURE (PSI)
BRAKE MEAN EFFECTIVE PRESSURE (PSI)
50(kPa)
500
1000(kPa)
1500

FIGURE 9

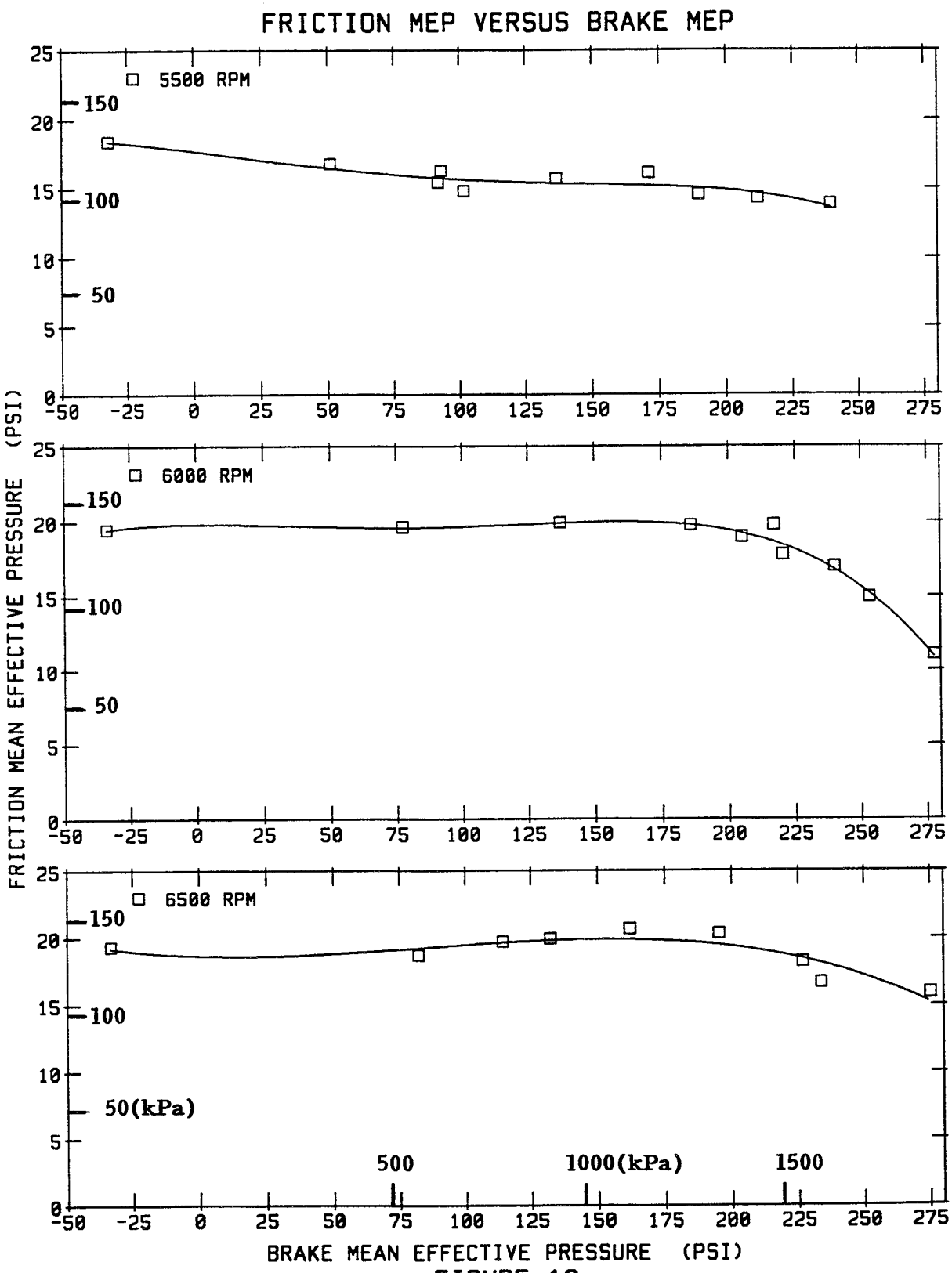

FRICTION MEP VERSUS BRAKE MEP
5500 RPM
6000 RPM
6500 RPM
150
100
50
50(kPa)
500
1000(kPa)
1500
FRICTION MEAN EFFECTIVE PRESSURE (PSI)
BRAKE MEAN EFFECTIVE PRESSURE (PSI)

FIGURE 10

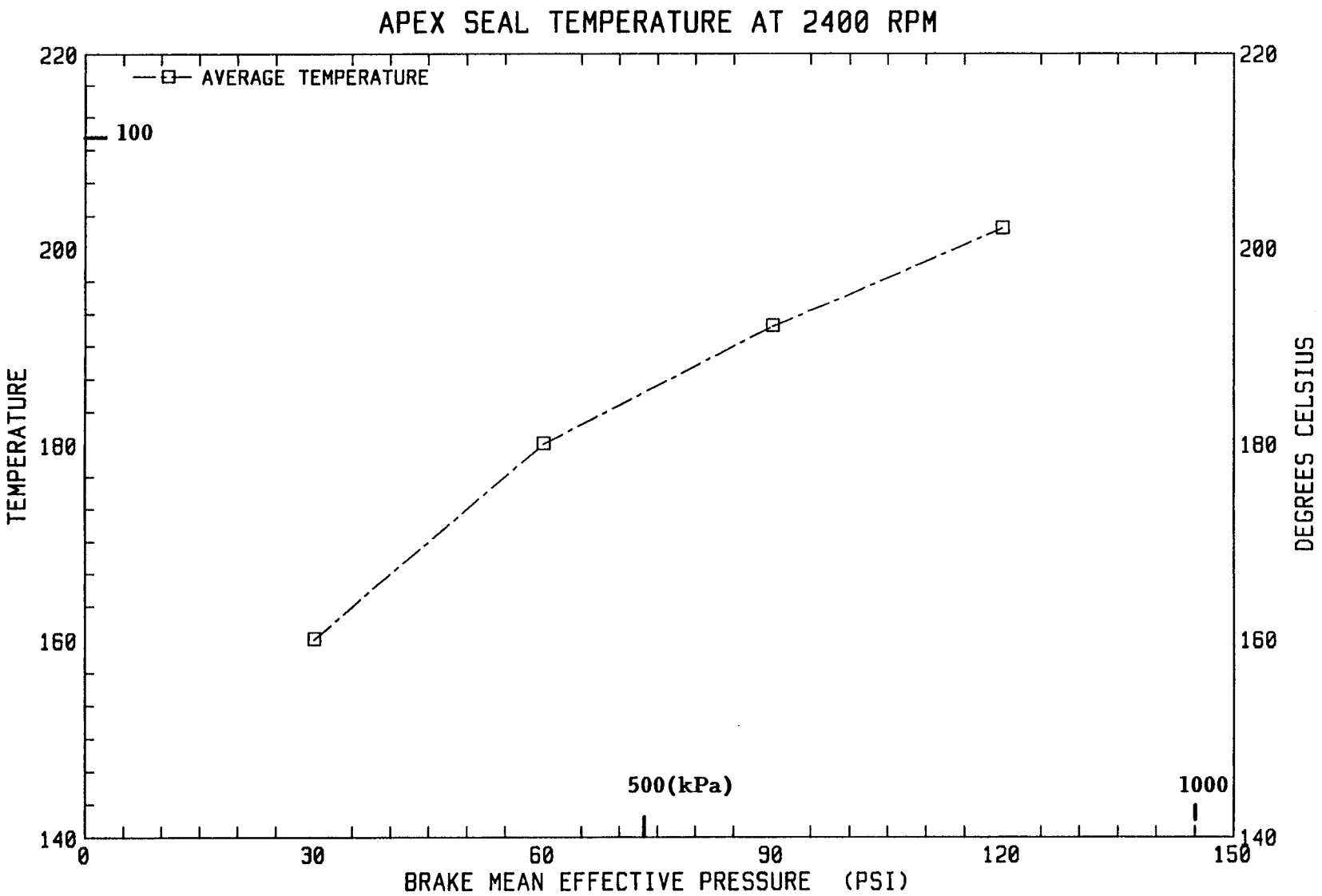

APEX SEAL TEMPERATURE AT 2400 RPM
AVERAGE TEMPERATURE
100
220
200
180
160
140
TEMPERATURE
DEGREES CELSIUS
0
30
60
90
120
150
500(kPa)
1000
BRAKE MEAN EFFECTIVE PRESSURE (PSI)

FIGURE 11

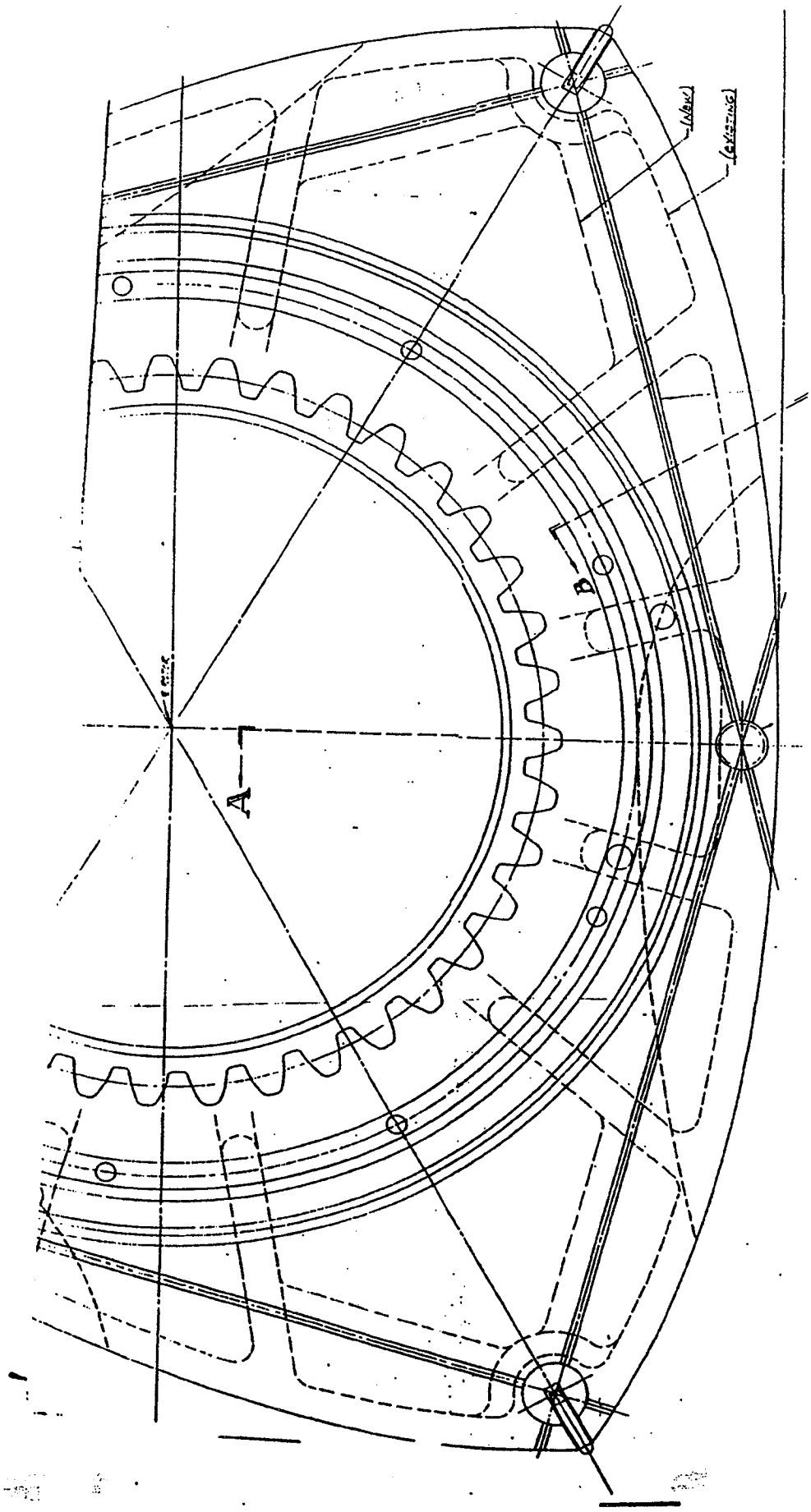


FIGURE 12

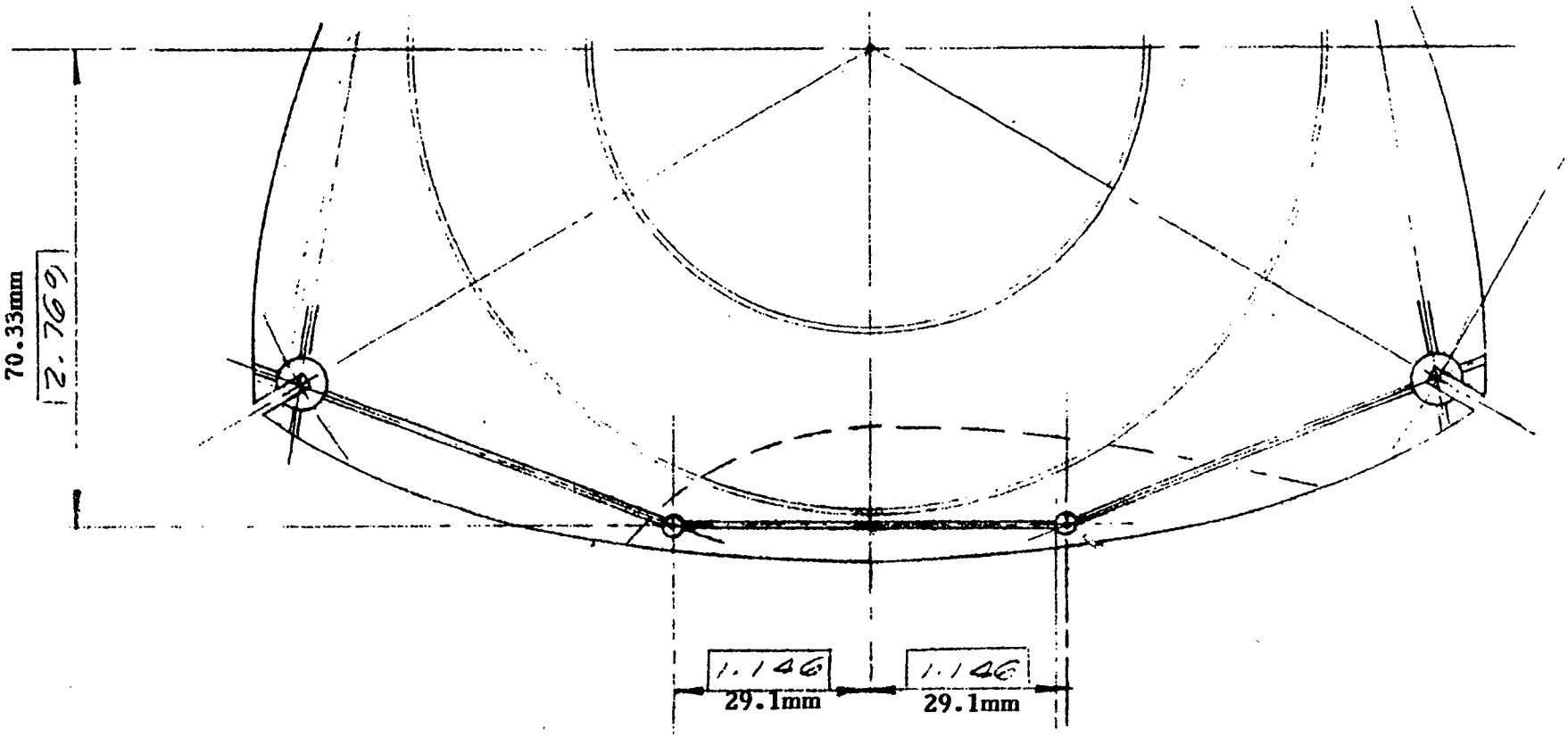


FIGURE 13

THREE-PIECE STRAIGHT SIDE SEALS

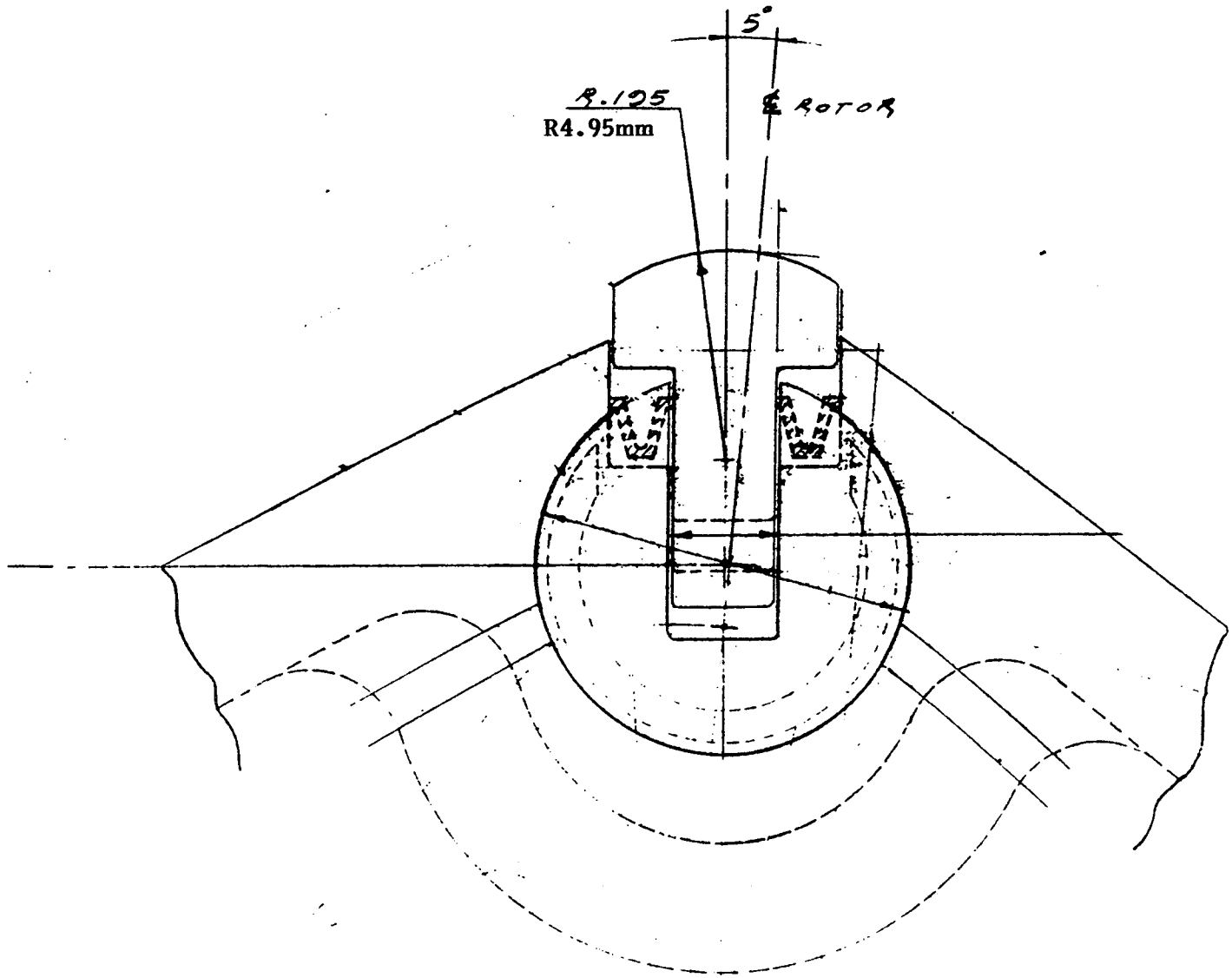
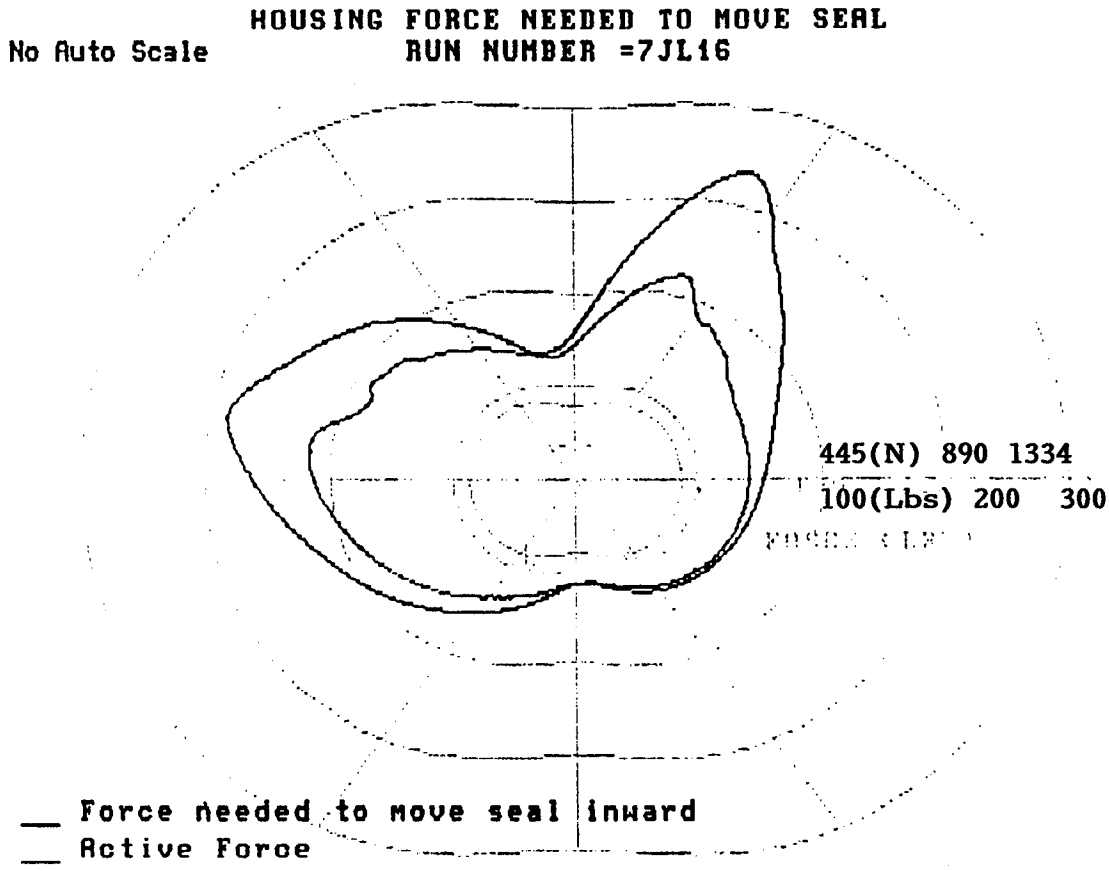


FIGURE 14

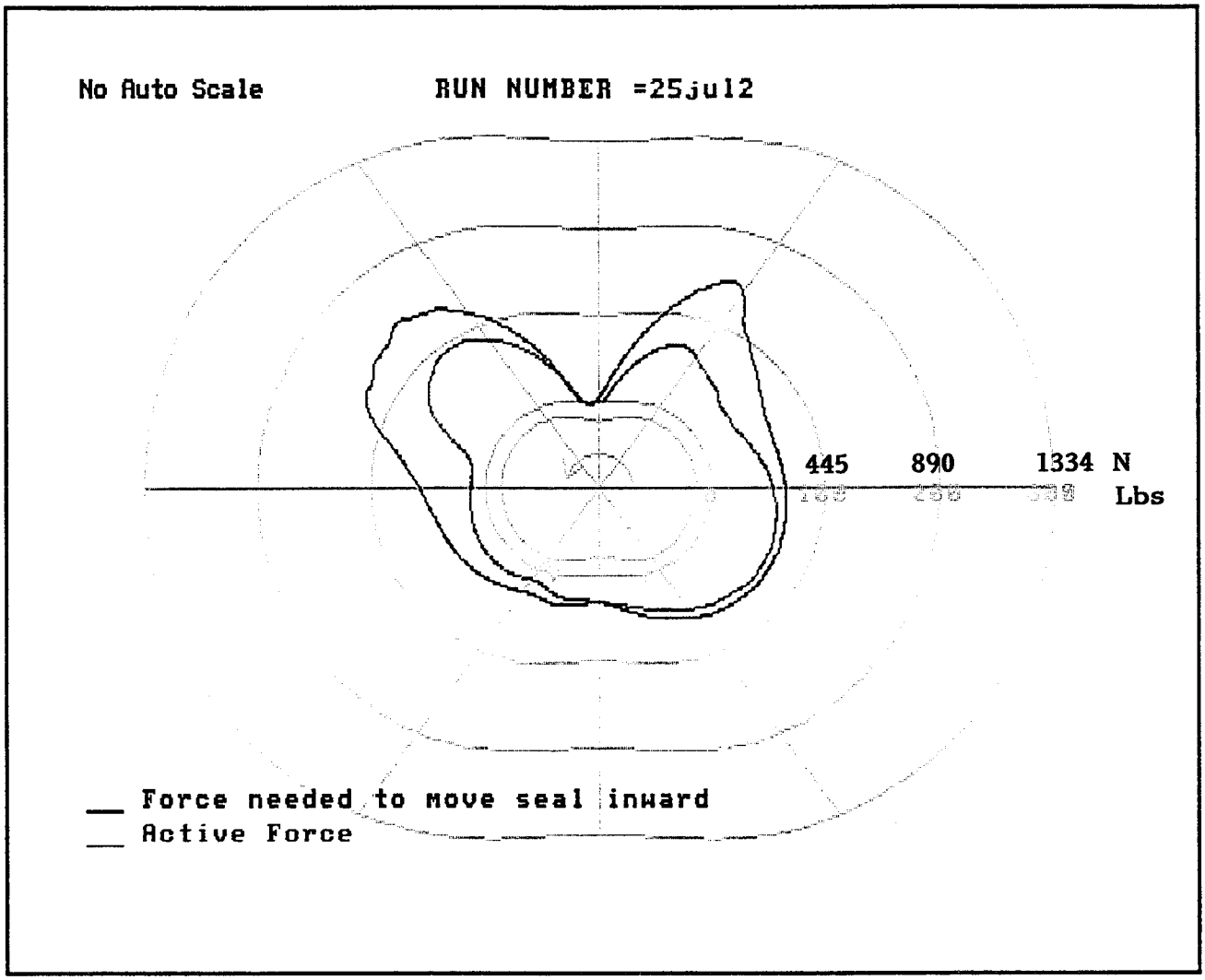
MUSHROOM SEAL WITH SECONDARY ELEMENTS



STD CONFIG, 160HP IND CRD,7000RPM
(120kW)

FIGURE 15

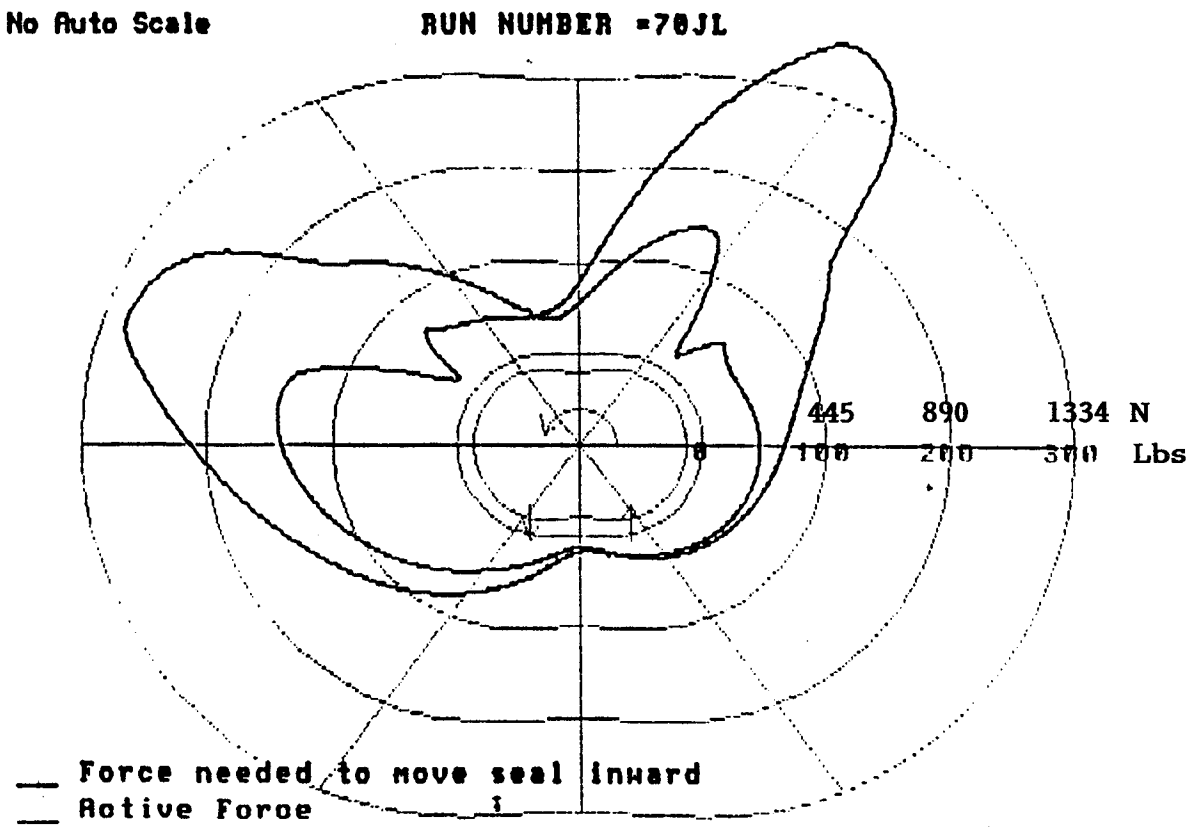
STANDARD SEAL CONFIGURATION:
SEAL TO TROCHOID LOADS AT 7000 RPM AND 160 BHP
(120kW)



7000rpm 160hp 5deg tilt ferrotic .096 stem, .195 radius
(120kW)

FIGURE 16

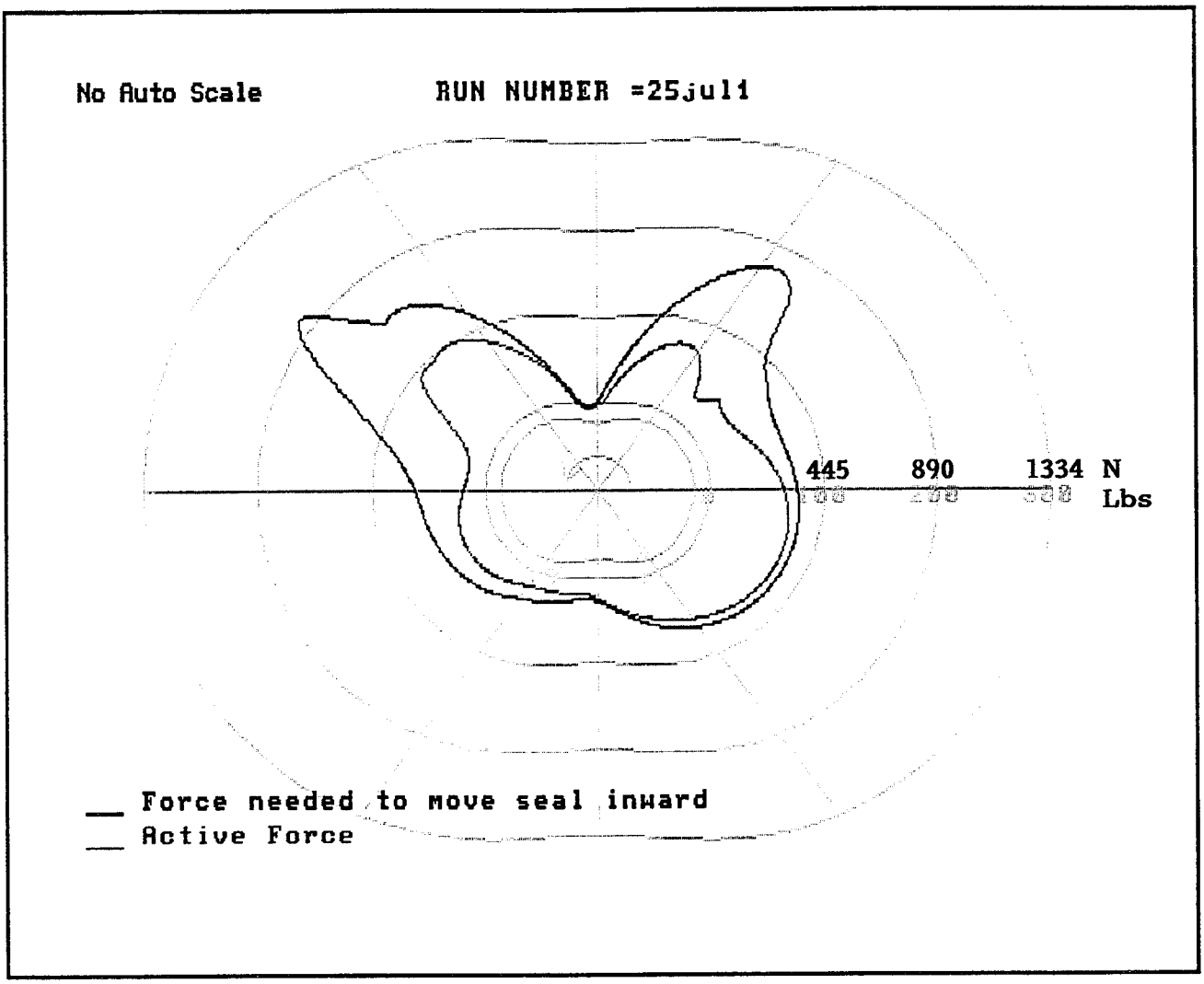
NEW MUSHROOM SEAL DESIGN:
SEAL TO TROCHOID LOADS AT 7000 RPM AND 160 BHP
(120kW)



STD. CONFIG., 200HP @ 8000RPM
(150kW)

FIGURE 17

STANDARD SEAL CONFIGURATION:
SEAL TO TROCHOID LOADS AT 8000 RPM AND 200 BHP
(150kW)



8000rpm 200hp 5deg tilt ferrotic .096 stem, .195 radius
150kW 2.44mm 4.95mm

FIGURE 18

NEW MUSHROOM SEAL DESIGN:
SEAL TO TROCHOID LOADS AT 8000 RPM AND 200 BHP
(150kW)

4.3 LIGHTWEIGHT/LOW CONDUCTIVITY PARTS

PRECEDING PAGE BLANK NOT FILMED

4.3 LIGHTWEIGHT/LOW CONDUCTIVITY PARTS

INTRODUCTION

Several Lightweight/Low conductivity components for the Stratified Charge Rotary Engine were identified during the NASA Phase III sixth month program review. The Lightweight/ Low Conductivity engine components, proposed for the rotary engine critical technology enablement program, were anticipated to provide improved engine performance. The components identified were:

a. Lightweight Rotor - Titanium

b. Composite Structural Material End Housing

Subsequently, due to the restructuring of the Phase III contract only the Lightweight Rotor was continued into final design, hardware procurement and parts readied for testing. The Composite Structural Material End Housing effort was terminated after completion of a conceptual design layout. A brief discussion of the Composite End Housing design and benefits is provided.

LIGHTWEIGHT ROTOR

OBJECTIVE

Conduct a candidate material screening study and select the best applicable material to provide the lightest rotor assembly configuration while operating at the NASA Enablement Rig Engine design conditions.

TECHNICAL APPROACH

A wide variety of rotor designs and rotor constructions were considered in selecting the best Lightweight Rotor design candidate. The search included a review of three decades of rotor design and a review of recently developed material technologies.

Primary considerations in selecting the Lightweight Rotor design were the capability to withstand the NASA rig engine design operating conditions, the potential for maximum weight reduction, and the probability of successful fabrication.

The design operating conditions anticipated for the stratified charge rotary engine are shown in Figure 1. Figure 1 is an estimated indicator card for engine operations at 160 bhp (120kw)

PRECEDING PAGE BLANK NOT FILMED

PAGE 188 INTENTIONALLY BLANK

and 8000 rpm. The indicator card depicts a peak combustion pressure of 1110 psi (7.65 mPa) and a peak combustion chamber temperature of 3500° R (1671° C).

Candidate rotor materials and design configurations which were considered are listed in Figure 2.

Selection of the most promising Lightweight Rotor candidate material and design is described in detail in JDTI Rotary Engine Division Report "Lightweight Rotor Candidate Material Screening Study" 25 March 88, NAS3-24628.

The selection report recommended a titanium material rotor as the lightest rotor configuration having a relatively high probability for successful fabrication of a prototype rotor. The report's recommendation was approved by the NASA Project Manager for design and fabrication.

Rotor design layout effort was initiated and was supported by design analysis which drew on the successful experience of JDTI Series 70 engine rotor design, analysis, fabrication and test experience. Finite element stress analysis utilizing ANSYS method code was employed to examine temperature distributions, resulting thermal stresses, inertial loading, and pressure loading. The maximum stress range throughout the rotor structure was determined for all rotor positions and predicted engine operating conditions. Design considerations included rotor fabrication, assembly, bearing retention, and thermal conductivity amongst others.

RESULTS

The Lightweight Rotor design effort resulted in the release of detail design drawings for a Titanium Rotor. The following drawings describe the complete rotor design:

TITLE	DRAWING NO.
Rotor & Bearing Assembly, ADE	NR10252
Rotor, Titanium, Gear & Adapter Assembly, ADE	NR10251
Rotor, Titanium, ADE	NJ12479
Rotor & Bearing Assembly, DE	NR10447
Rotor, Titanium, Gear & Adapter Assembly, DE	NR10446
Rotor, Titanium, DE	NJ12870

As discussed in Section V of the referenced report, the Howmet Ti-Cast Division was selected to provide investment rotor castings. The casting material selection was titanium 6-2-4-2 (Ti-6Al-2Sn-4Zr-2Mo). This decision was based on additional material studies (after the screening report) that revealed the 6-2-4-2 has a higher strength/density ratio for elevated temperature applications than the titanium 6-4 material. Howmet proceeded to develop investment patterns for both ADE and DE rotor castings.

Trial machining of the cast titanium 6-2-4-2 alloy material was initiated concurrent with the rotor pattern development so that the methods of machining the rotor casting material were developed when castings became available.

Both ADE and DE rotor assemblies have been completed and are available for testing in either the NASA 1007R Enablement Rig Engine or the NASA 2013R Rig Engine.

Figure 3 illustrates the rotor assembly cross-section and major components. Also provided are actual weight savings when compared to the original 17-4PH material workhorse rotor assembly designed for the NASA 1007R Enablement Rig Engine. Figure 4 lists the advantages of lightweight rotor assemblies when incorporated into the rotary engine power section.

Figure 5 shows the rotor casting and completed rotor assembly. The surface of the casting is the final chemical-milled surface. The completed rotor assembly includes the bolted-in rotor gear and oil seal adapter (not visible).

An additional benefit of the titanium Rotor design is the low thermal conductivity of the titanium. The thermal conductivity of the titanium 6-2-4-2 material is only 30% of the thermal conductivity of the 17-4PH material. The selection of titanium as the rotor material provides a means to examine reduction of heat transfer to the rotor cooling oil.

The titanium 6-2-4-2 material has several drawbacks which must be taken into account. The investment castings of titanium are expensive, and the as-cast parts require chemical milling. The chemical milling is required to remove an approximate 0.030 inch (0.762mm) thick case of alpha-phase titanium to ensure the desired metallurgical properties are obtained. Titanium is difficult to machine. The titanium rotors also require NiBron plating of the apex seal slots and rotor gear mating surfaces to prevent galling.

COMPOSITE DRIVE END HOUSING

Restructuring of the NASA Phase III contract eliminated the final design, hardware procurement and testing of the composite drive end housing. Figure 6 illustrates the end housing conceptual design configuration and Figure 7 presents comparative material data. An approximate 27% weight saving was estimated for this lightweight end housing design.

CONCLUSIONS

1. A lightweight, Titanium 6-2-4-2, Rotor has been successfully designed, investment cast and machined to provide finished rotor assemblies ready for engine testing. The Titanium 6-2-4-2 rotor provided a 35% rotor assembly weight reduction relative to the 17-4PH stainless steel rotor previously used.

2. Composite construction methods for the rotary engine End Housing application may provide substantial weight savings.

RECOMMENDATIONS

Engine test the titanium rotor assemblies to determine their performance and mechanical capabilities.

SCRC1-40T
ESTIMATED INDICATOR CARD
160BHP (120Kw)/8000RPM

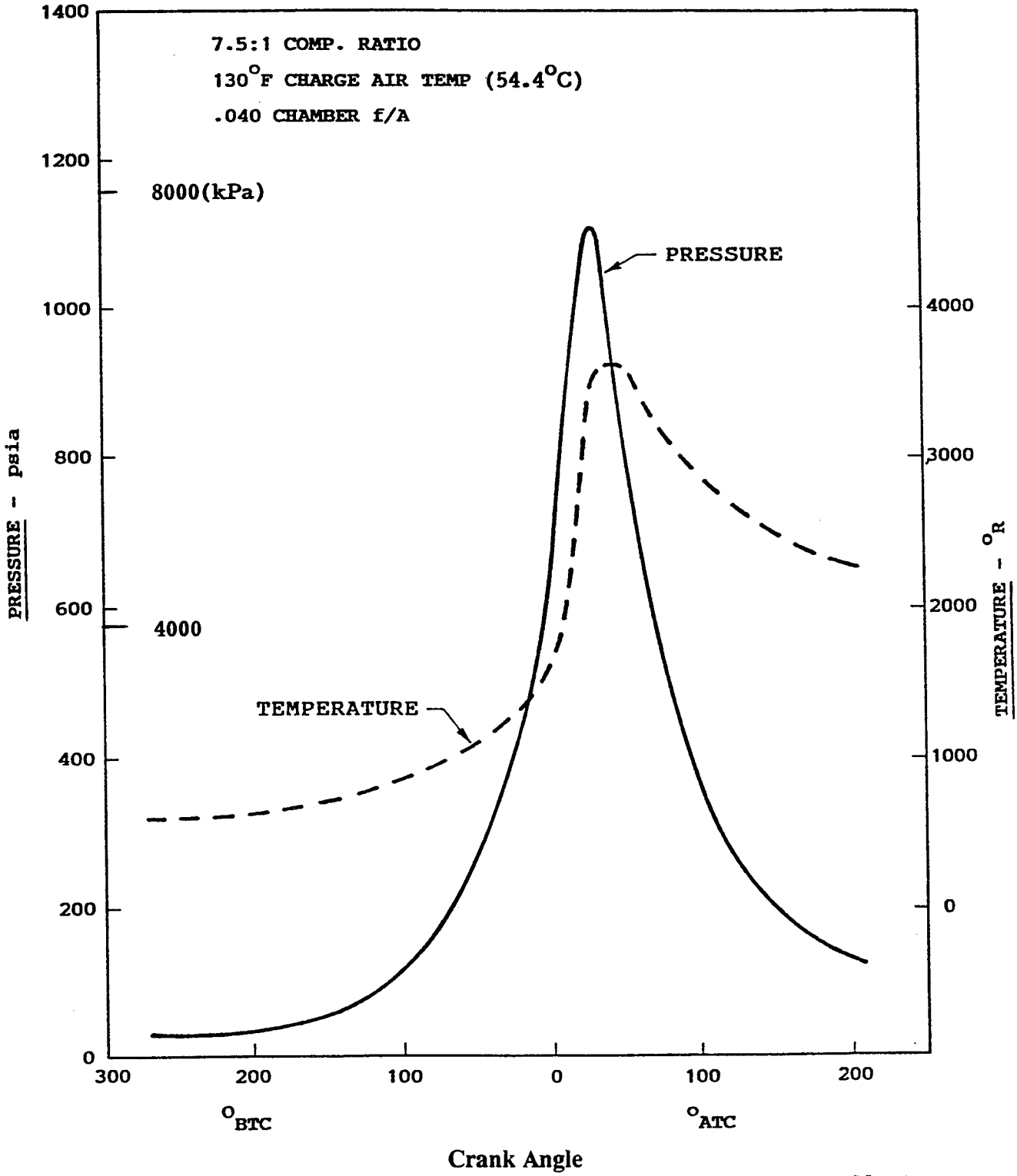


Figure No. 1

CANDIDATE MATERIALS AND CONFIGURATIONS

17-4 OPTIMIZED, (BASELINE) DETAIL, 7.7 LB (3.49kg)

INVESTMENT CAST TITANIUM 6-4

SAND CAST ALUMINUM

SQUEEZE CAST ALUMINUM

FORGED ALUMINUM (3 PIECE)

METAL MATRIX COMPOSITE

REINFORCED PLASTIC (TORLON) & METAL HOT SECTION

CERAMIC (MONOLITHIC)

THREE PIECE ROTOR

SELF BROACHING BEARING SUPPORT

SEMI-FLOATING BEARING

THERMAL BARRIER

INTEGRAL GEAR

Figure No. 2

ROTOR ASSEMBLY WEIGHT COMPARISON

17-4PH Workhorse Rotor Weight 10.7 Lbs. (4.536kg)
Titanium Rotor Weight 7.0 Lbs. (3.175kg)

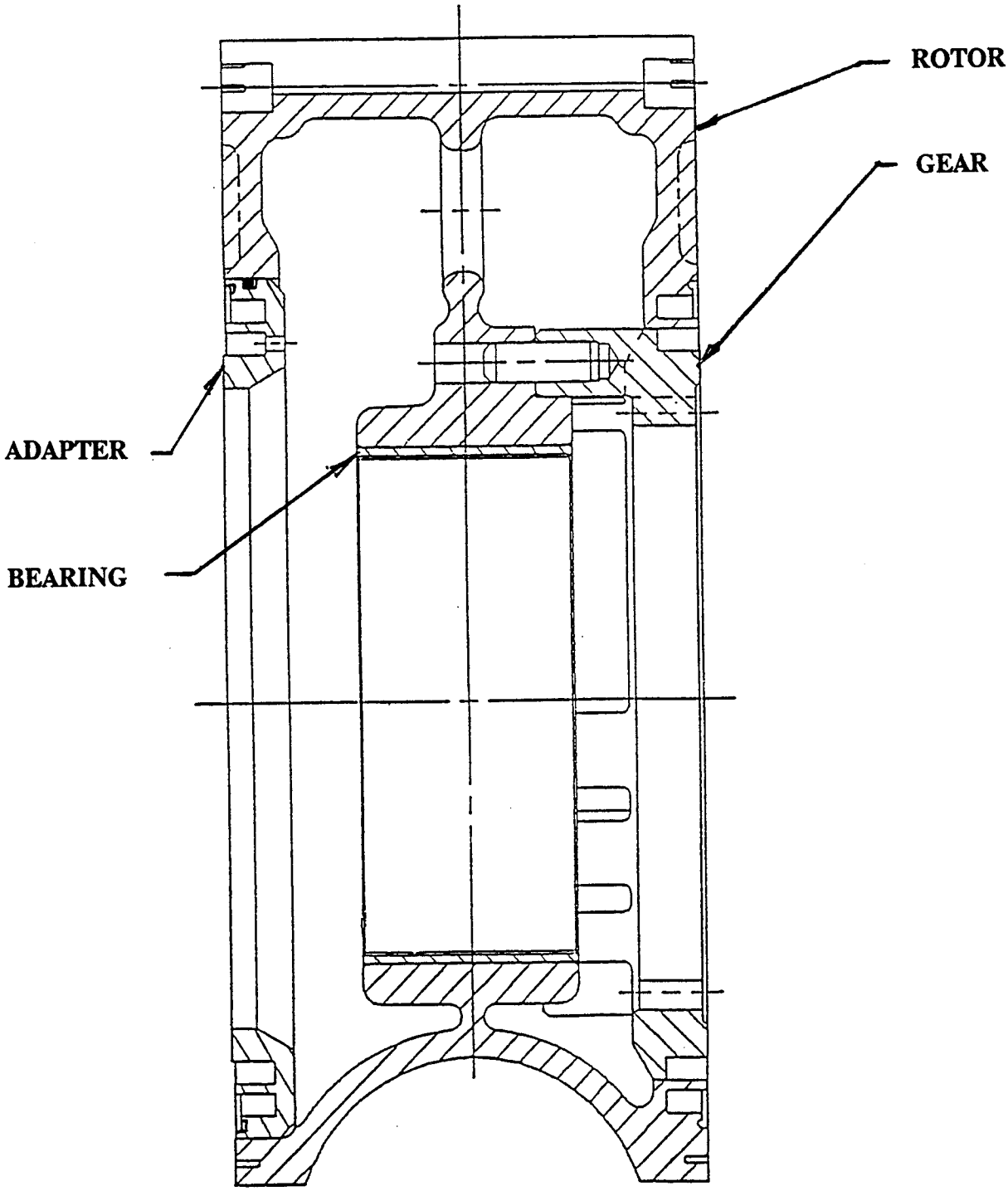


Figure No. 3

ADVANTAGES OF LIGHTWEIGHT ROTORS

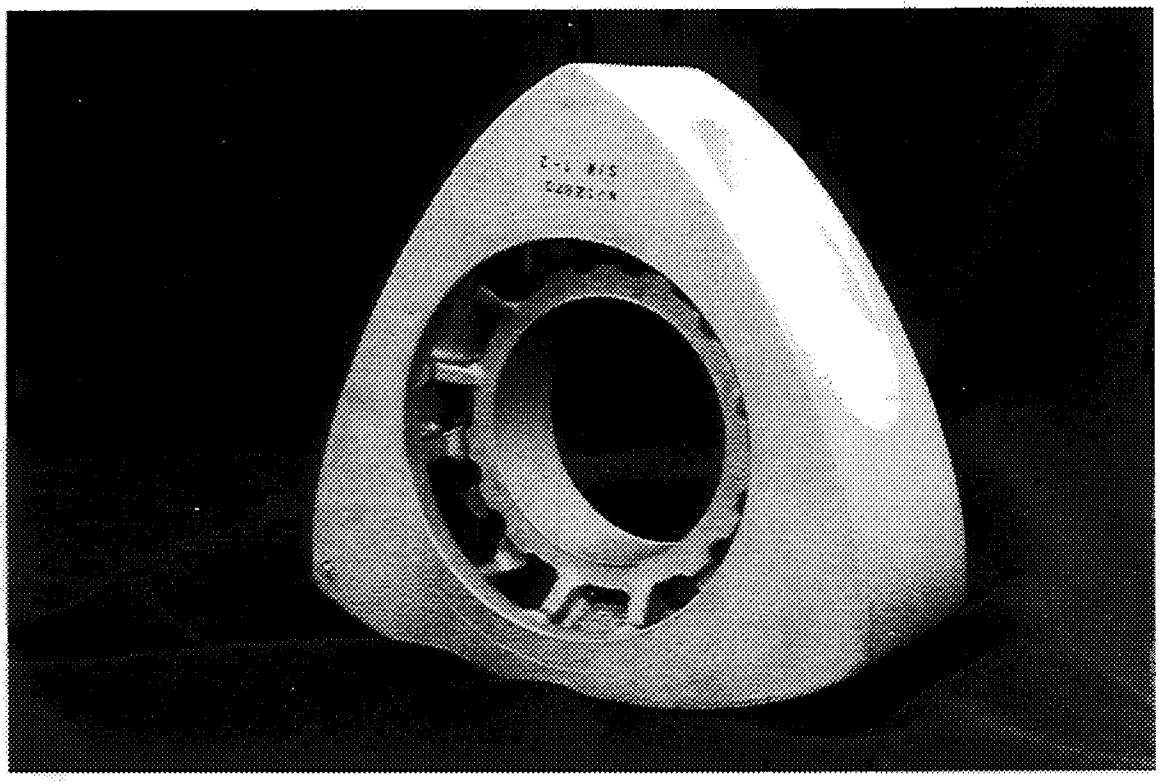
CRANKSHAFT ASSEMBLY WEIGHT SAVINGS

REDUCED CRANKSHAFT SLOPES

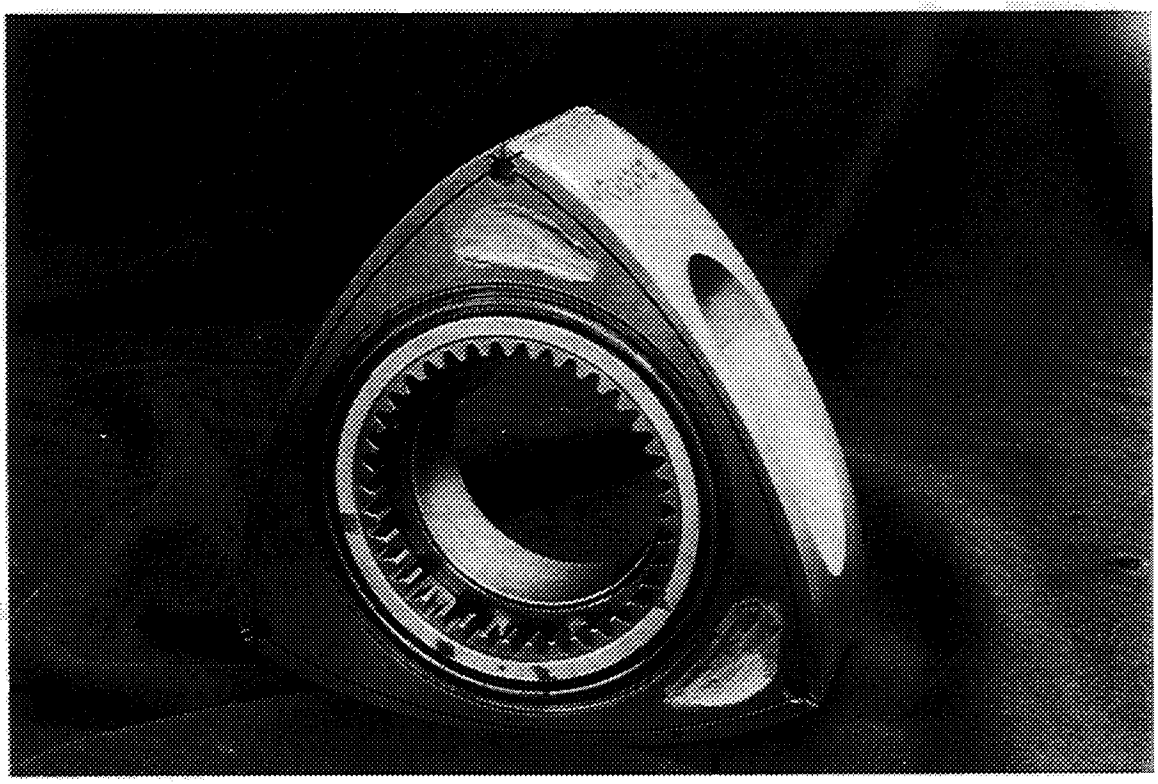
REDUCED ROTOR & MAIN BEARING LOADS

IMPROVED ENGINE ACCELERATION

Figure No. 4



TITANIUM ROTOR CASTING



ROTOR, GEAR, AND BEARING ASSEMBLY
DRAWING NUMBER NR10252
TITANIUM 6-2-4-2 ROTOR
FIGURE 5

COMPOSITE DRIVE END HOUSING

PRESENT WT. 14.4 Lbs. (6.53kg) **COMPOSITE WT. 10.5 Lbs. (4.76kg)**

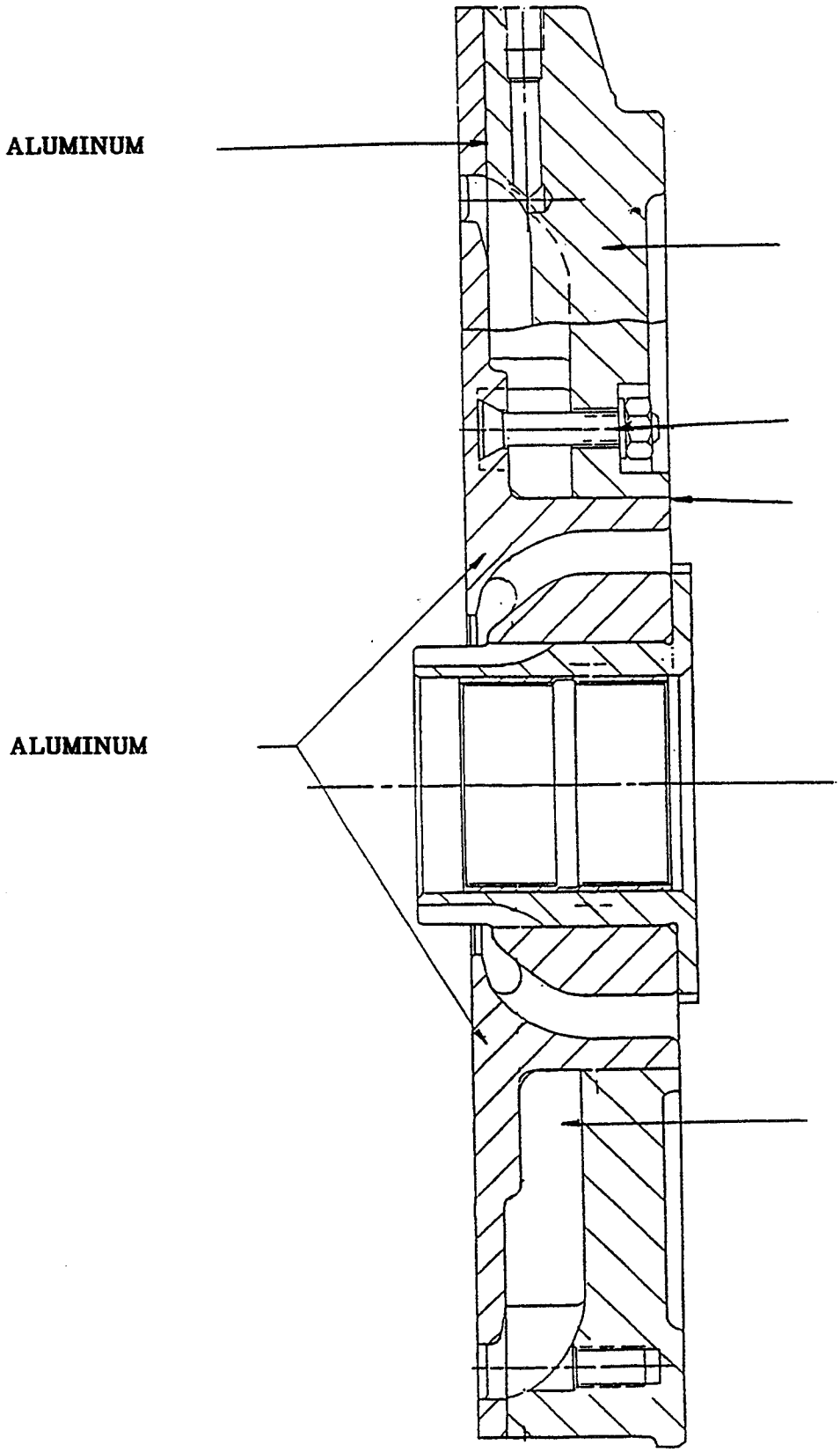


Figure No. 6

ALUMINUM - PLASTIC MATERIAL COMPARISON

MATERIAL	TENSILE STRENGTH 10^3psi(kPa)	ELONGATION %	TENSILE MODULUS 10^6psi(kPa)	DENSITY #/in.^{3}(kg/cm^3)
ALUMINUM A356 - T6	38(262kPa)	5	10.3(71kPa)	0.097 (.0027kg/cm^3)
REINFORCED PLASTIC TORLON 5030	32.1(221kPa)	2.3	2.1(14.47kPa)	0.058 (.0016kg/cm^3)

Figure No. 7

4.4 CATALYTIC SURFACES

PRECEDING PAGE BLANK NOT FILMED

CATALYTIC SURFACE COMPONENT DEVELOPMENT

INTRODUCTION

One goal of the NASA Technology Enablement program is to develop new materials for major components and heat barrier coatings to reduce rotary engine heat rejection rates. A numerical goal of a 40% reduction in heat rejection from the baseline 1988 Series 70 engine was set forth in the NASA Phase III Technical Proposal. A related goal was investigating a catalytic surface coating on various combustion chamber components to enhance combustion efficiency and turn-down capability.

Engine testing of the thermal barrier coated rotor had been conducted in the NASA Phase II contract. The test used a 17-4PH stainless steel rotor coated with a .005 inch (0.127mm) thick bond coat and .025 inch (0.635mm) thick zirconia coating. Figure 1 shows the detail of the ceramic thermal barrier coating as applied by Adiabatics, Inc. The barrier was intended to reduce heat transfer through the rotor to the engine oil, and to increase rotor surface temperatures for increased engine operating efficiency.

Engine performance data comparing the thermal barrier rotor installed in Engine 0704 -3, and a conventional 17-4PH uninsulated rotor installed in Engine 0704-1, are provided in Figures 2 and 3. Figure 2 shows that less than a 2% difference in observed Brake Specific Fuel Consumption (BSFC) was noted between the two builds of the engine. The BSFC performance data was taken at 5500 RPM using the N41 (4x0.009 inch (0.229mm) orifice) main nozzle. Figure 3 compares the heat rejection to the oil of the same two engines at 4400 RPM. At loads up to 133 psi (916 kPa) BMEP the oil heat rejection for Engine 0704-1 (standard rotor) was higher than for Engine 0704-3 (thermal barrier rotor). However, at high load (approximately 148 psi (1019 kPa) BMEP) the oil heat rejection of Engine 0704-3 was 5% higher than for 0704-1. This reversal in trend is not well understood, but is attributed to factors other than the thermal barrier coating. The increased oil flow is attributed to the increased bearing clearance of Engine 0704-3.

No reduction in engine BSFC or heat rejection to the engine oil was believed to be attributable to the thermal barrier coating applied to the rotor. Further testing of the thermal barrier coating was pursued in the Phase III Contract in conjunction with evaluation of the catalytic surface rotor.

PAGE 202 INTENTIONALLY BLANK

PRECEDING PAGE BLANK NOT FILMED

OBJECTIVE

To establish the potential for catalytic surfaces to improve combustion rates and to improve engine operating efficiencies. The investigation will test the effect of introducing a catalytic surface into the combustion chamber. The investigation is a cooperative effort with Precision Combustion, Inc. (PCI).

TECHNICAL APPROACH

Testing of the catalytic surface concept consisted of engine testing catalyst coated components and examining changes in engine fuel consumption performance and exhaust emissions.

To determine the effect of catalytic surfaces the thermal barrier coated rotor from Engine 0704-3 was coated with a catalyst and rebuilt as engine 0705-2. The catalytic coating was applied to the rotor flank and rotor pocket surfaces over the thermal barrier coating.

The catalytic coating is intended to promote combustion of fuel in close proximity to the rotor face and pocket. The catalytic coating, by promoting the oxidation process, is intended to reduce fuel ignition delay and to promote combustion stability at lower temperatures than would be required for non-catalytic surfaces. The catalytic coating is a proprietary coating developed and applied by Precision Combustion (reference SAE paper 890326).

RESULTS

Engine performance testing of the catalytic coated, thermal barrier rotor was conducted in the NASA enablement single rotor rig engine 0705-2. Comparison to the performance of engine 0704-3, which tested the thermal barrier rotor previously, revealed no significant change to the engine fuel consumption. Comparisons of the fuel flow versus the engine load for the two engines are provided in Figures 4 and 5. The fuel consumption of the two engines was nearly identical throughout the load range tested at engine speeds of 4000 and 6000 RPM.

Differences in turbine inlet and turbine outlet temperatures and exhaust energy were apparent for the two engines 0704-3 and 0705-2, as shown in Figure 6. The catalytic surface rotor engine 0705-2 featured an exhaust port enlarged by 18% relative to engine 0704-3. The differences in turbine inlet temperature observed are believed to be attributable to this engine configuration change. No effect on engine BSFC is attributed to the enlarged exhaust port.

Overall, no significant change in engine fuel consumption performance is believed to be attributable to the catalytic rotor surfaces.

Exhaust emissions were measured for Engine 0705-2 with the catalytic surface rotor. However, due to problems with the exhaust gas sampling system, the emission data obtained are believed to be invalid. The emissions-based calculations for air-to-fuel ratios were twice the observed values. The exhaust sampling probe was found to be plugged with carbon which suggests that the exhaust sample was diluted with air.

CONCLUSIONS

Application of the catalytic coating to the rotor flank and pocket did not measurably change the fuel efficiency of the rotary engine. No conclusion regarding the catalytic coatings' effect on exhaust emissions can be reached due to the test difficulties encountered.

RECOMMENDATIONS

Consider applying the catalyst coating to a rotor which would provide a higher surface temperature. Candidate designs for providing higher surface temperatures include the titanium rotor and/or a thicker thermal barrier on the rotor surfaces.

ROTOR WITH THERMAL BARRIER COATING

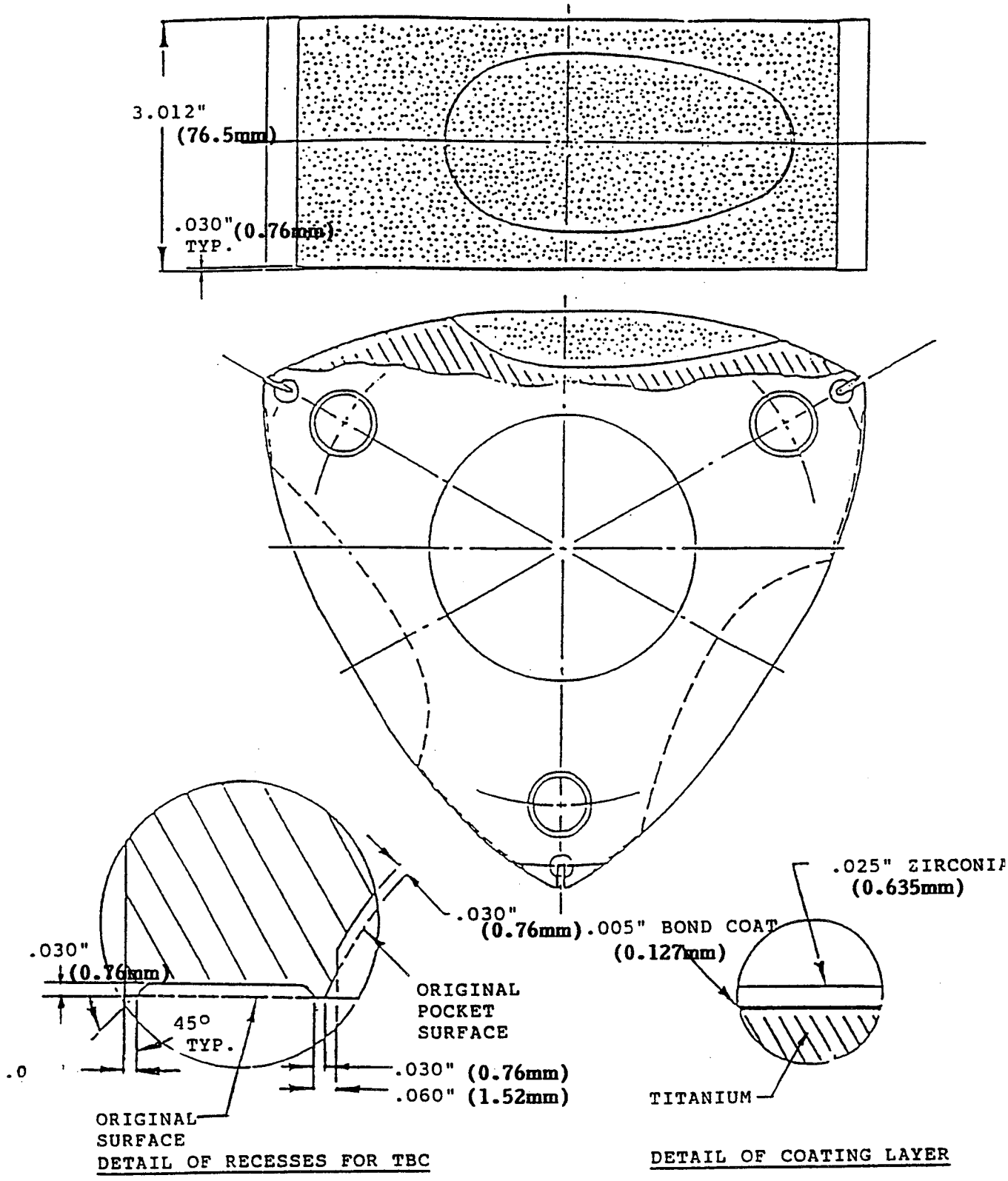


Figure No. 1

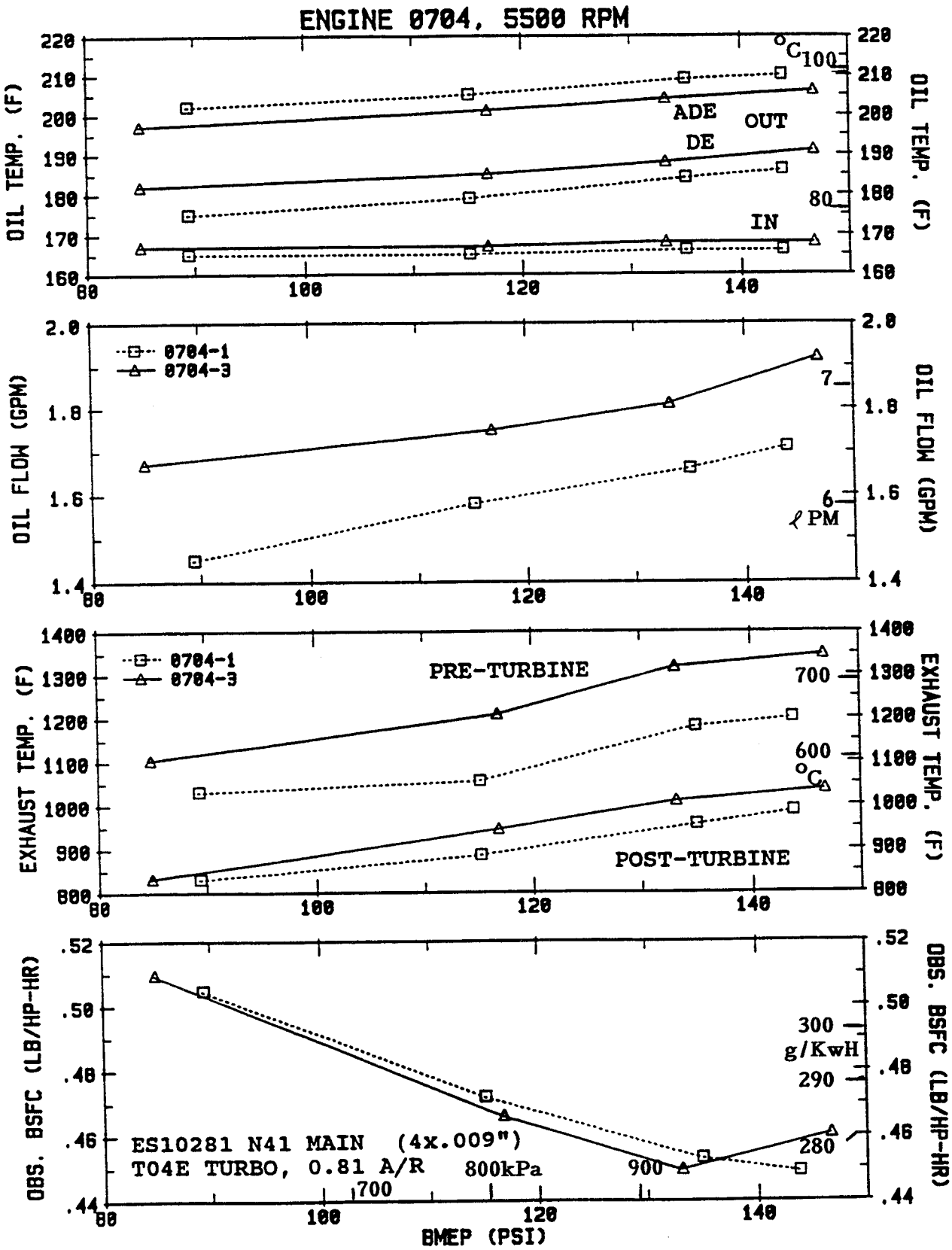


Figure No. 2

C 3

ENGINE PERFORMANCE

ENGINE 0704, 4400 RPM
ES10281N41 MAIN (4x.009")

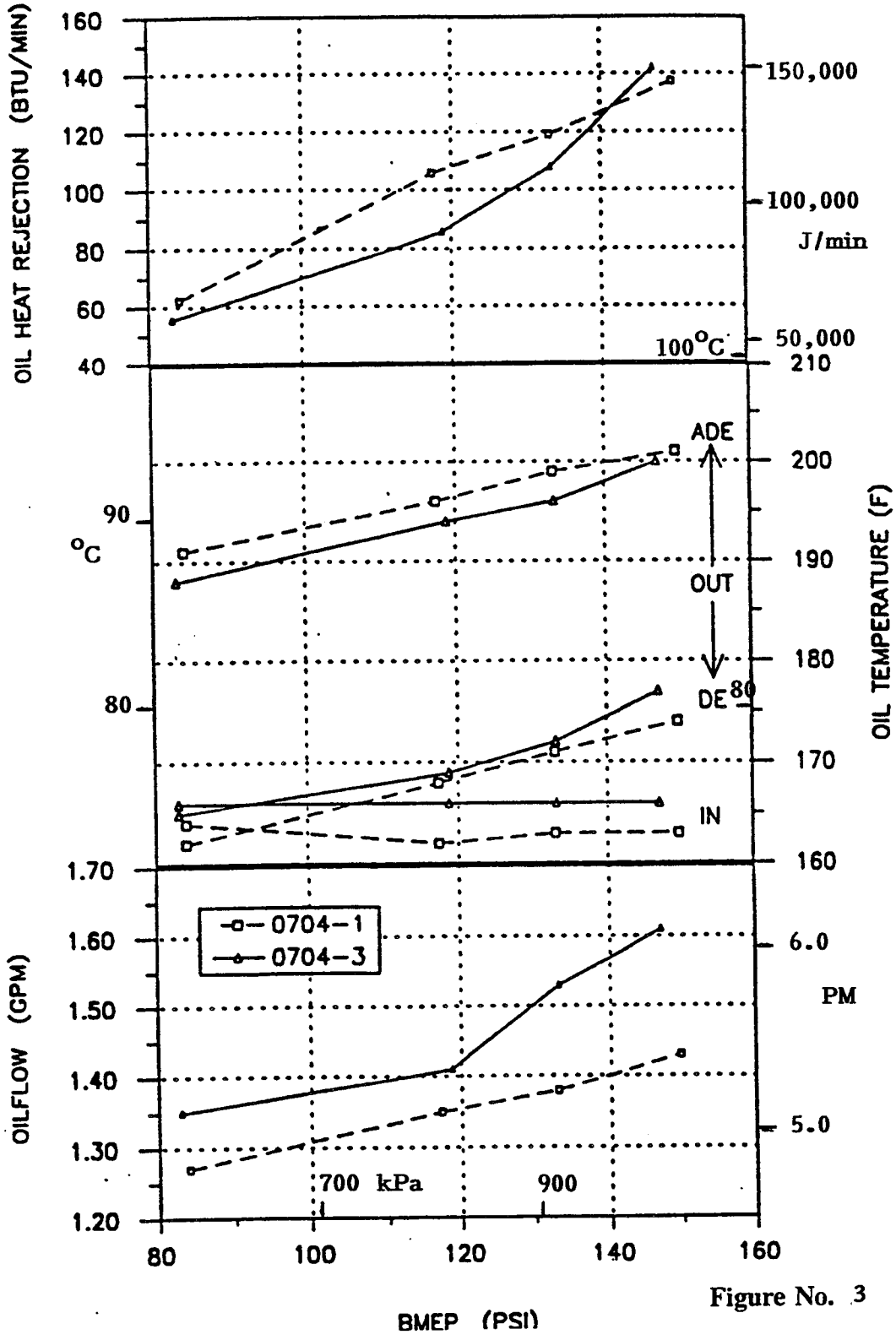


Figure No. 3

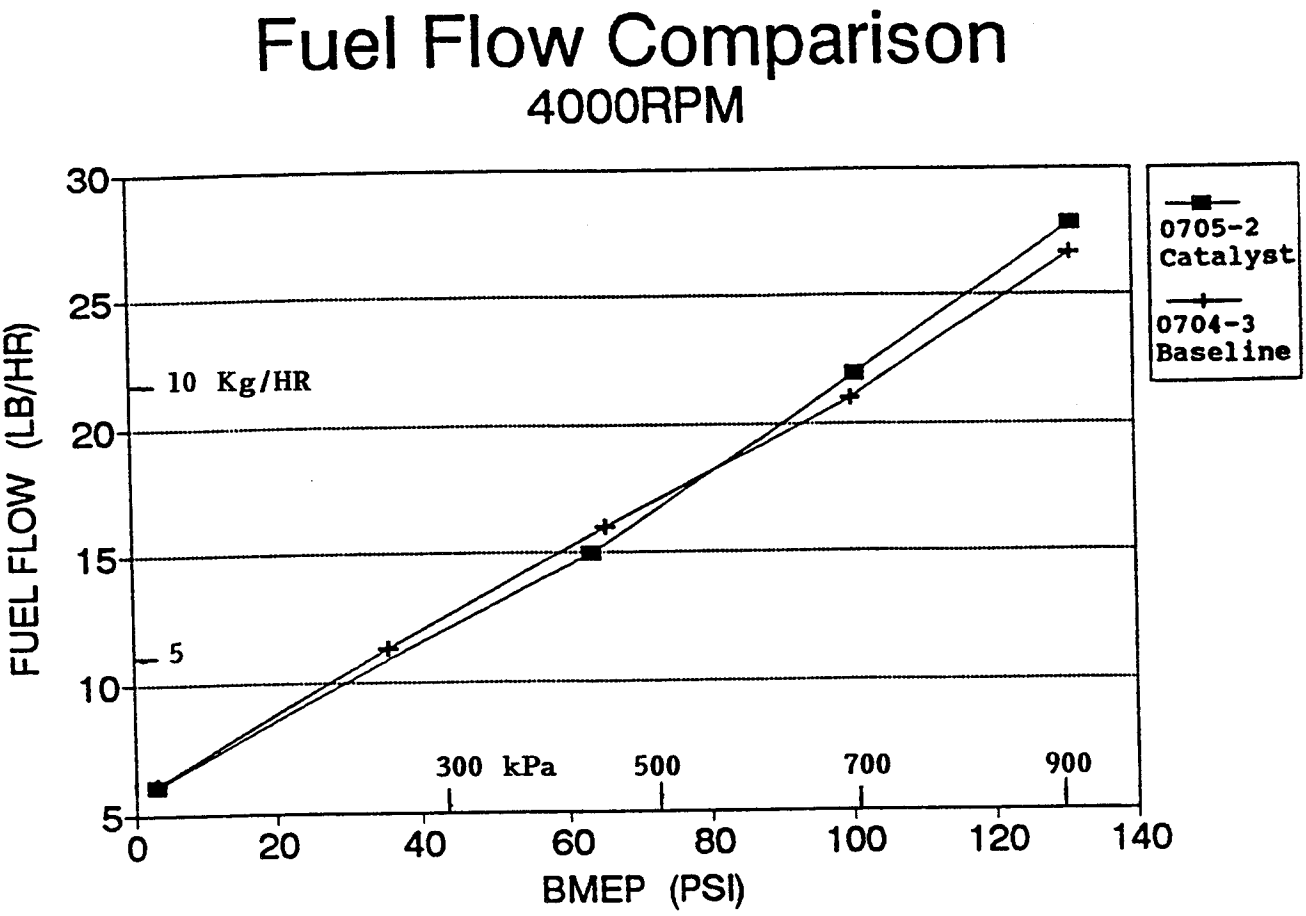

Fuel Flow Comparison
4000RPM
FUEL FLOW (LB/HR)
30
25
20
15
10
5
10 Kg/HR
5
0
20
40
60
80
100
120
140
300 kPa
500
700
900
BMEP (PSI)
0705-2
Catalyst
0704-3
Baseline

Figure No. 4

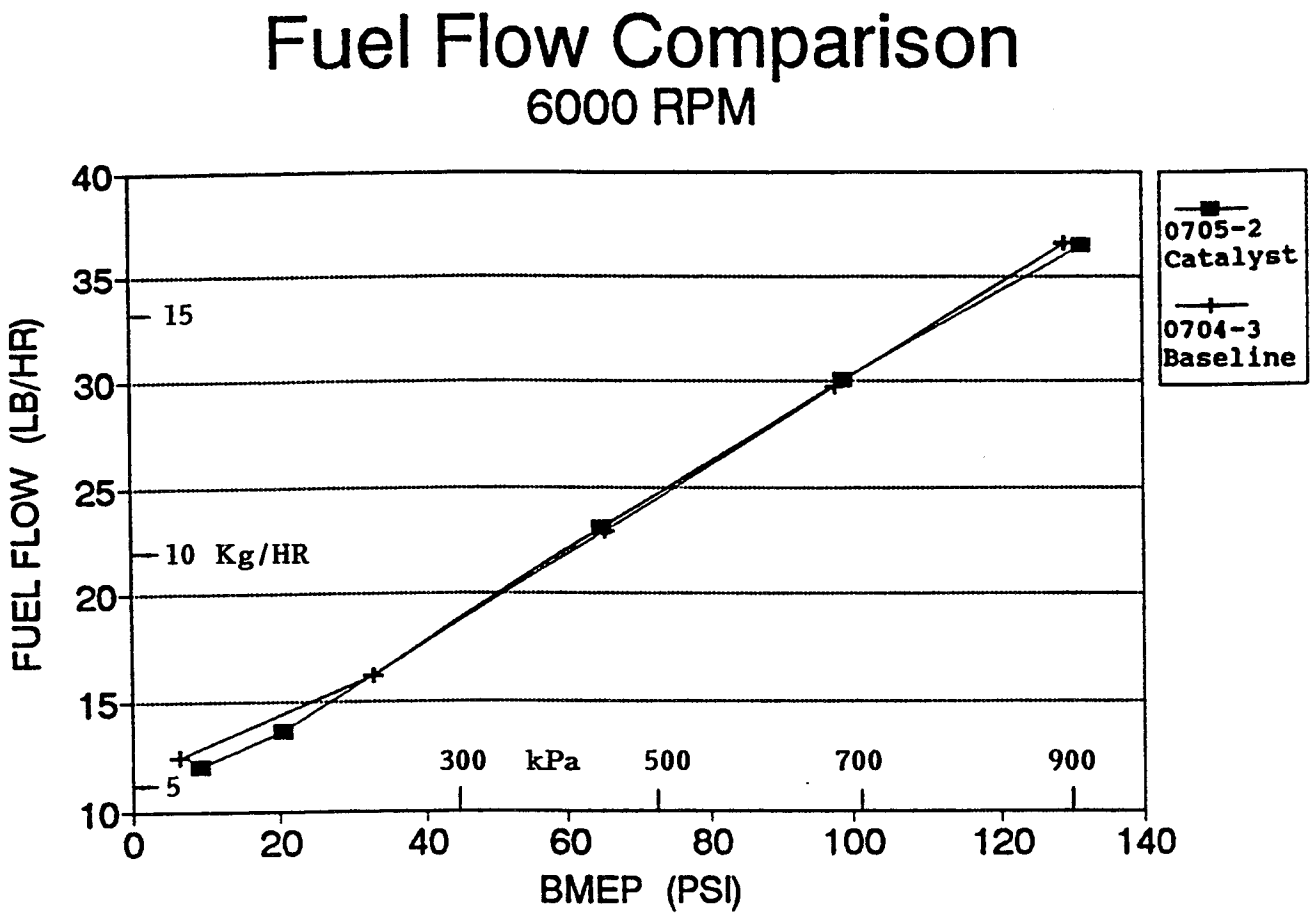

Fuel Flow Comparison
6000 RPM
FUEL FLOW (LB/HR)
BMEP (PSI)
40
35
30
25
20
15
10
5
15
10 Kg/HR
0
20
40
60
80
100
120
140
300 kPa
500
700
900
0705-2 Catalyst
0704-3 Baseline

Figure No. 5

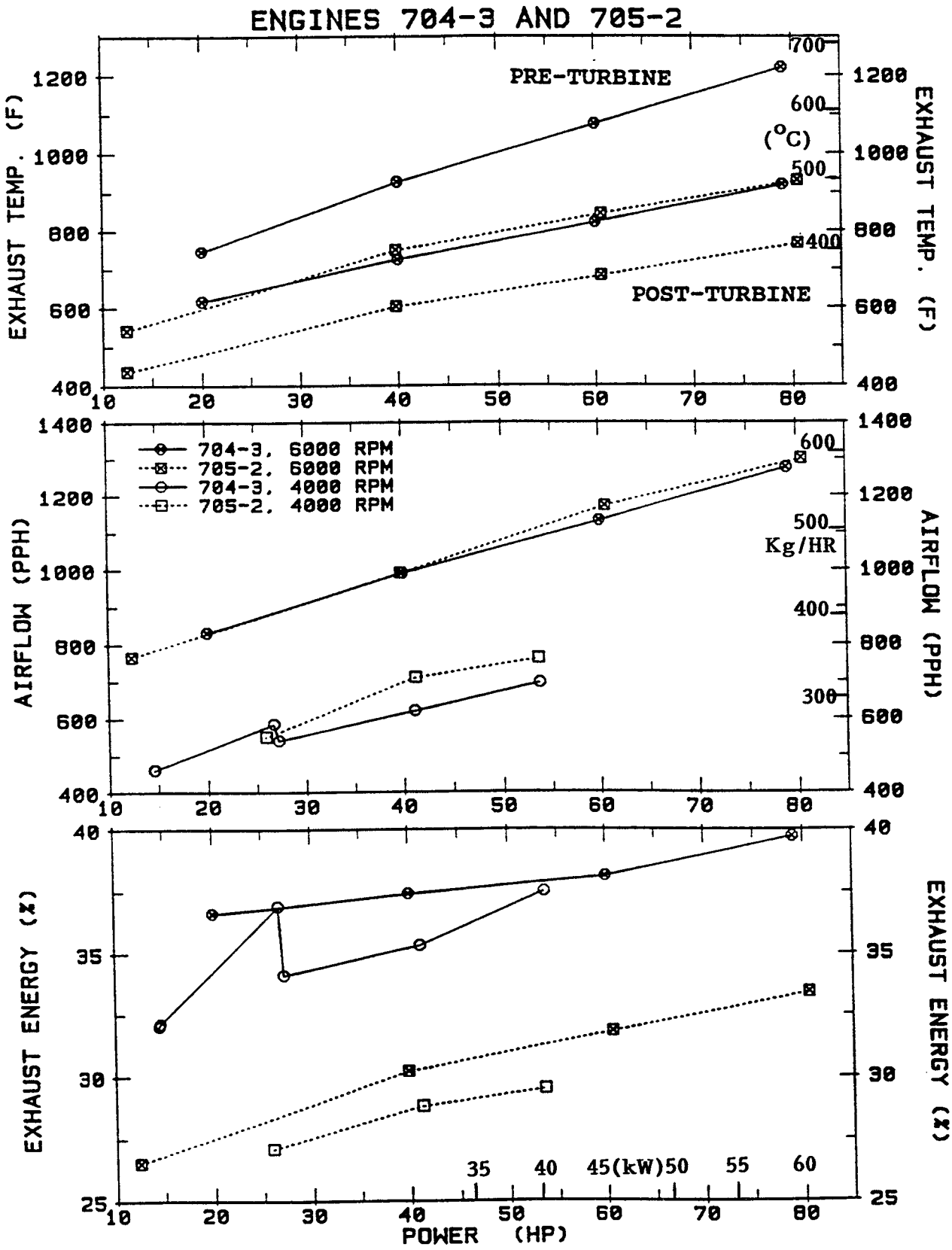

ENGINES 704-3 AND 705-2
EXHAUST TEMP. (F)
PRE-TURBINE
POST-TURBINE
(°C)
EXHAUST TEMP. (F)
704-3, 6000 RPM
705-2, 6000 RPM
704-3, 4000 RPM
705-2, 4000 RPM
AIRFLOW (PPH)
Kg/HR
AIRFLOW (PPH)
EXHAUST ENERGY (%)
EXHAUST ENERGY (%)
45(kW)
POWER (HP)

Figure No. 6

4.5 REFERENCE ENGINE DESIGN

PRECEDING PAGE BLANK NOT FILMED

INTRODUCTION

The purpose of the 2013R Reference Engine Design is to define a Stratified Charge Rotary Engine (SCRE) configuration as a baseline aircraft engine. The design is intended to reflect the advanced technologies, engine components, design analyses and assessments established in the performance of the NASA Phase III contract. The Reference Engine Design was initiated in June 1990 and completed by September 1990. The continued Reference Engine Design update effort was curtailed with program re-direction as discussed in Section 2.0 Executive Summary.

OBJECTIVE

Conduct a SCRE aircraft Reference Engine Design for an engine with the capability of 400 horsepower at takeoff with a 40% brake thermal efficiency at best cruise power, and a 2,000 hour TBO (time between overhaul) service life. The Reference Engine Design shall address components, subsystems and technologies considered in the technology enablement program and critical to meeting the objectives. The Reference Engine Design shall also consider where appropriate current and anticipated light aircraft design practices and utilize general aviation type accessories suitable for light aircraft use.

TECHNICAL APPROACH

Design of the Reference Engine was based upon a twin rotor, 70 Series core power section, 40 cu. in. (0.7ℓ /rotor displacement) and integrated into a complete general aviation engine configuration. Component sections of the core rotary power plant were defined on the basis of overall rotary engine expertise, consultations with accessory suppliers, major air framer's, turbomachinery and control suppliers and consideration of advanced technologies anticipated as a result of the critical technology enablement effort.

The basic design parameters considered were:

- 400 BHP (300 kw) at Take-Off
- 300 BHP (225 kw) at Maximum Cruise
- 2000 Hr. Time Between Overhauls (TBO)
- Jet-A Fuel (Primary); DF-2, AVGAS (Alternate)
- Planetary Reduction Gear
- Clockwise and Counterclockwise Prop Rotation
- Crankshaft Speed 8500 RPM
- Propeller Speed 2500 RPM (approx.)
- Cruise Altitude Capability 33,000 Ft. (10km)
- Lightweight components deriving from the technology enablement program.
- Consideration of a high commonality family of engines having 1-6 rotors.
- Manufacturing technologies for cost, quality and durability/performance considerations.

PRECEDING PAGE BLANK NOT FILMED

PAGE 214 INTENTIONALLY BLANK

- Integration of core stratified charge rotary engine power section and accessory components into a complete aircraft engine package for single and twin aircraft installation.
- Providing a baseline configuration for reference wherein critical component technology enablement items can be integrated and evaluated as the component technologies are advanced.
- Torsional damping provisions, propeller shaft and reduction gearing for adaptability of conventional light aircraft propellers.

The design effort included layout of the internal power section components including rotors, rotor housings, side and intermediate housings, crankshaft and counterweights. To this core power unit, provisions for the propeller shaft, reduction gear and torsional damper were added. Accessory drives for the required-to-run engine accessory components (fuel injection, ignition, coolant and oil) were integrated. Also, drives for accessories related to aircraft installation were provided. Coolant and oil coolers, turbomachinery and mounting considerations were addressed. Weight calculations for detailed components and the overall package (dry) were completed and the center-of-gravity defined. Performance characteristics were estimated at Take-off, 75% cruise, 65% cruise, 55% cruise, approach, taxi and idle conditions. These projections defined anticipated performance capabilities that could be achieved (if a full-up aircraft engine package was prepared and tested) utilizing technologies to be derived from re-directed technology enablement program as discussed in Section 2.0, Executive Summary.

RESULTS

Reference Engine Design

A Reference Engine Design, which includes a propeller reduction gear assembly, power section, and engine accessories was completed. The Reference Engine Design provides a Stratified Charge Rotary Engine configuration for aircraft application representative of the requirements for aircraft application and includes consideration of the advanced technologies pursued in the technology enablement program.

The Reference Engine is designed and packaged as an aircraft engine which will fit within a tapered nacelle inside diameter of 21.0 to 26.0 inches (533 to 660mm) from behind the propeller to the rear accessory end respectively. The Reference Engine will have an overall length of 57.6 inches (1463 mm) and a total weight of 480 pounds (dry) (218 kg).

The general construction and layout of the Reference Engine Design is shown in Figure 1, Basic Arrangement; Figure 2, Accessory End View; and Figure 3, Propeller End View. The aircraft nacelle diameters are superimposed on the End Views for reference.

The complete engine installation and location of the engine accessories is shown in Figure 4, Preliminary Installation Drawing, Left Side; Figure 5, Preliminary Installation Drawing, Right Side; and Figure 6, Preliminary Installation Drawing, Accessory End View.

A description and illustration of some of the major Reference Engine Design components are provided in the following paragraphs.

PROPELLER REDUCTION GEAR ASSEMBLY

The Propeller Reduction Gear Assembly is shown in Figure 7. The Assembly includes the Reduction Gear Housing and Nose Cone, the Propeller Shaft Assembly, Torsional Coupling, Planetary Reduction Gearing, and Vacuum and Propeller Governor Drives. The Reduction Gear Assembly serves the following functions:

a. Enclosure of the reduction and accessory drive gear trains, and torsional coupling.

b. Lubrication supply for the gearing and attendant bearings, and propeller thrust bearing.

c. Structural support for the propeller shaft, torsional coupling, reduction gear and pinion, and loads imposed by propeller thrust and aircraft maneuver conditions.

d. Oil supply through the propeller shaft from the prop governor to control propeller pitch.

The propeller shaft torsional coupling is shown in Figure 8. The planetary reduction gear propeller drive provides the capability for clockwise or counterclockwise rotation as required for twin engine aircraft installation. Figure 9 shows the clockwise prop reduction gearing. Figure 10 shows the counterclockwise reduction gearing. Both mechanisms provide a gear ratio of 3:39 to 1.0, for a resulting propeller speed of 2511 rpm at take-off conditions.

TURBOMACHINERY

A major installation concern of the Reference Engine Design is location, configuration, and support of the turbomachinery. To maintain the minimum nacelle diameter of 26 inches the turbocharger must be mounted on a truss support system bolted to the Accessory Housing. The truss support is shown in Figure 11. The turbocharger is mounted to the support plates and connected to the intercooler as shown in figure 12.

ENGINE COOLANT SYSTEM

The engine coolant system features a dual path coolant flow through the engine and a four pass coolant system through each set of paired end and rotor housings. The dual path coolant flow independently cools the Anti-Prop End and Prop End Rotor Housings by splitting the coolant flow at the coolant manifold integrally cast into the Anti-Prop End Housing. Both coolant paths then utilize a four pass cooling system through the End and Rotor housings as shown in Figures 13 and 14. The arrangement of the four pass system was developed to enhance cooling at regions of maximum heat flux, where the cooling mechanism is primarily nucleate boiling. The coolant flow circuitry is designed to locate the regions of maximum heat flux near the end of an axial series flow where coolant static pressure is lower. The lower coolant static pressure enhances the formation of nucleate boiling.

ENGINE LUBRICATION SYSTEM

The Reference Engine Lubrication System schematic is shown in Figure 15. The Lubrication System shows the oil cooler incorporated into the engine oil pressure system. The following advantages are attributed to the pressurized oil cooler:

a. The oil cooler core size is reduced.

b. The risk of cooler blockage due to air entrainment is reduced.

c. The scavenge system is simplified. Generally the oil scavenge system is the most temperamental and altitude sensitive section of the lubrication system.

d. Oil de-aeration in the oil tank is generally expected to be improved due to the increased temperature of oil in the tank.

FUEL PUMP TIMING

The Reference Engine Design includes a Fuel Pump Advance/Retard Mechanism. The pressure activated mechanism, activated by engine oil pressure, is shown in Figure 16.

ENGINE ENVELOPE

The Reference Engine total weight and center of gravity is shown in Figure 17. The engine total weight includes the Reduction Gear Assembly (but no propeller), the Engine Power Section, and the engine accessories. The present estimated engine weight is 480 lbs. dry (218

kg). A moderate weight reduction program is believed to be capable of providing an engine dry weight of just below 400 lbs (181 kg).

ENGINE PERFORMANCE

The estimated Performance Data for the aircraft Reference Engine Design are provided in Figures 18 and 19. Figure 18 provides an engine operation summary. Figure 19 provides estimated engine fuel consumption at typical aircraft mission duty cycle operating points.

CONCLUSIONS

The Reference Engine Design provides a realistic baseline definition of an advanced SCRE suitable for light aircraft usage.

RECOMMENDATIONS

1) Critical technology enablement advancements occurring during the latter stages of the NASA Phase III contract should be integrated into the Reference Engine Design. As noted previously, the design update activities originally planned were curtailed upon program re-direction. Some items which should be considered are:

   - The Dual Orifice Pilot Nozzle
   - The Titanium Rotor
   - Rotor Combustion Pocket configurations which provide lower cruise BSFC

2) A weight reduction program should be initiated to markedly lower the overall engine weight. This program should include a search for the lowest weight applicable engine accessories.

LIST OF FIGURES

FIGURE	TITLE
1.	BASIC ARRANGEMENT
2.	ACCESSORY END VIEW
3.	PROPELLER END VIEW
4.	PRELIMINARY INSTALLATION DRAWING: LEFT SIDE
5.	PRELIMINARY INSTALLATION DRAWING: RIGHT SIDE
6.	PRELIMINARY INSTALLATION DRAWING: ACCESSORY END VIEW
7.	REDUCTION GEAR HOUSING AND NOSE CONE
8.	PROPELLER SHAFT TORSIONAL COUPLING
9.	CLOCKWISE PROPELLER REDUCTION GEARING
10.	COUNTERCLOCKWISE PROPELLER REDUCTION GEARING
11.	TURBOCHARGER SUPPORT
12.	TURBOCHARGER/INTERCOOLER INSTALLATION
13.	COOLANT FLOW SCHEMATIC THROUGH ENGINE
14.	COOLANT FLOW THROUGH ROTOR HOUSING
15.	LUBRICATION SYSTEM
16.	FUEL PUMP ADVANCE/RETARD MECHANISM
17.	ENGINE WEIGHT AND CENTER OF GRAVITY LOCATION
18.	OPERATING DATA SUMMARY
19.	ESTIMATED FUEL CONSUMPTION

2013R NASA REFERENCE ENGINE

BASIC ARRANGEMENT

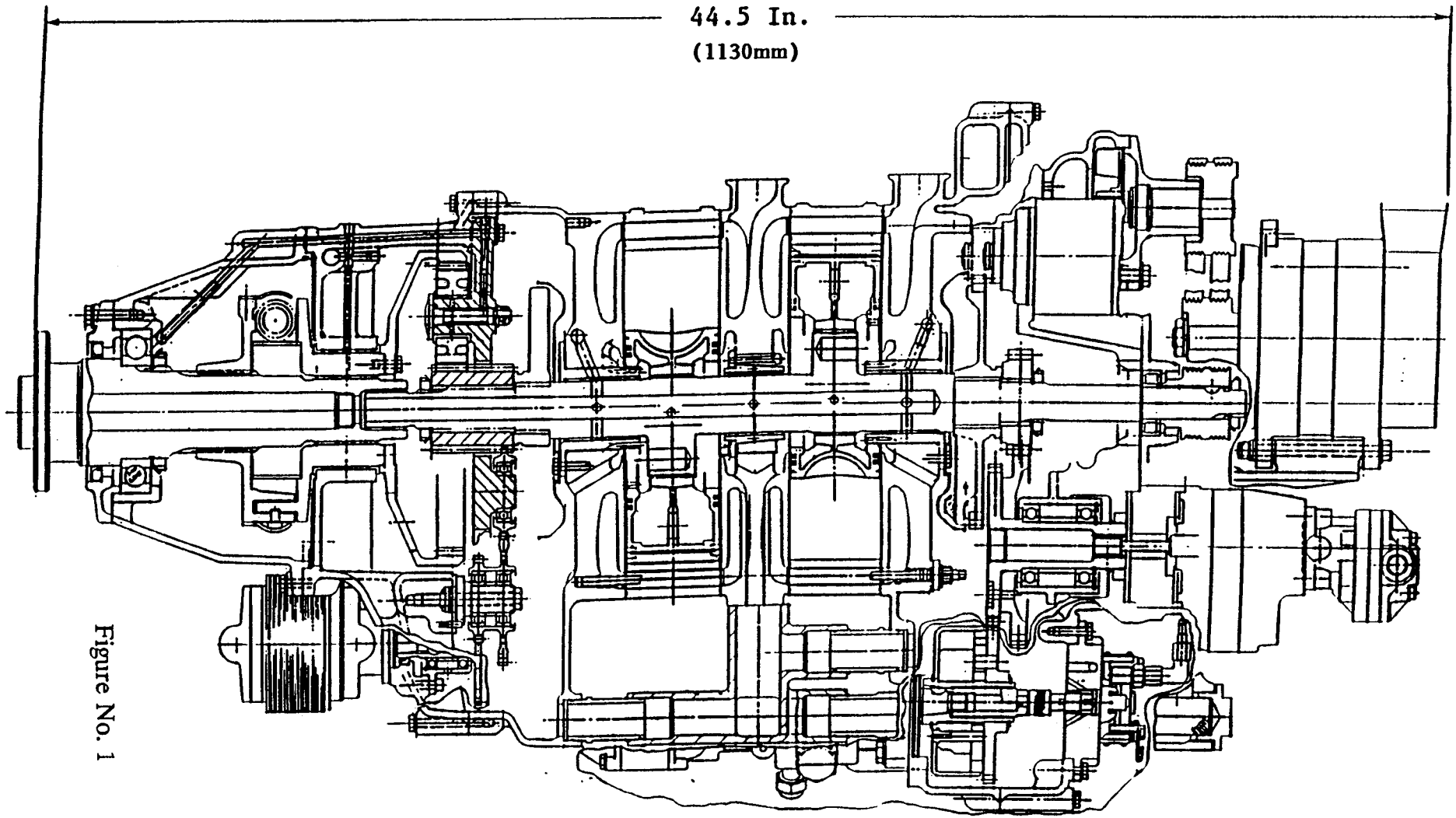


Figure No. 1

2013R NASA REFERENCE ENGINE

ACCESSORY END VIEW

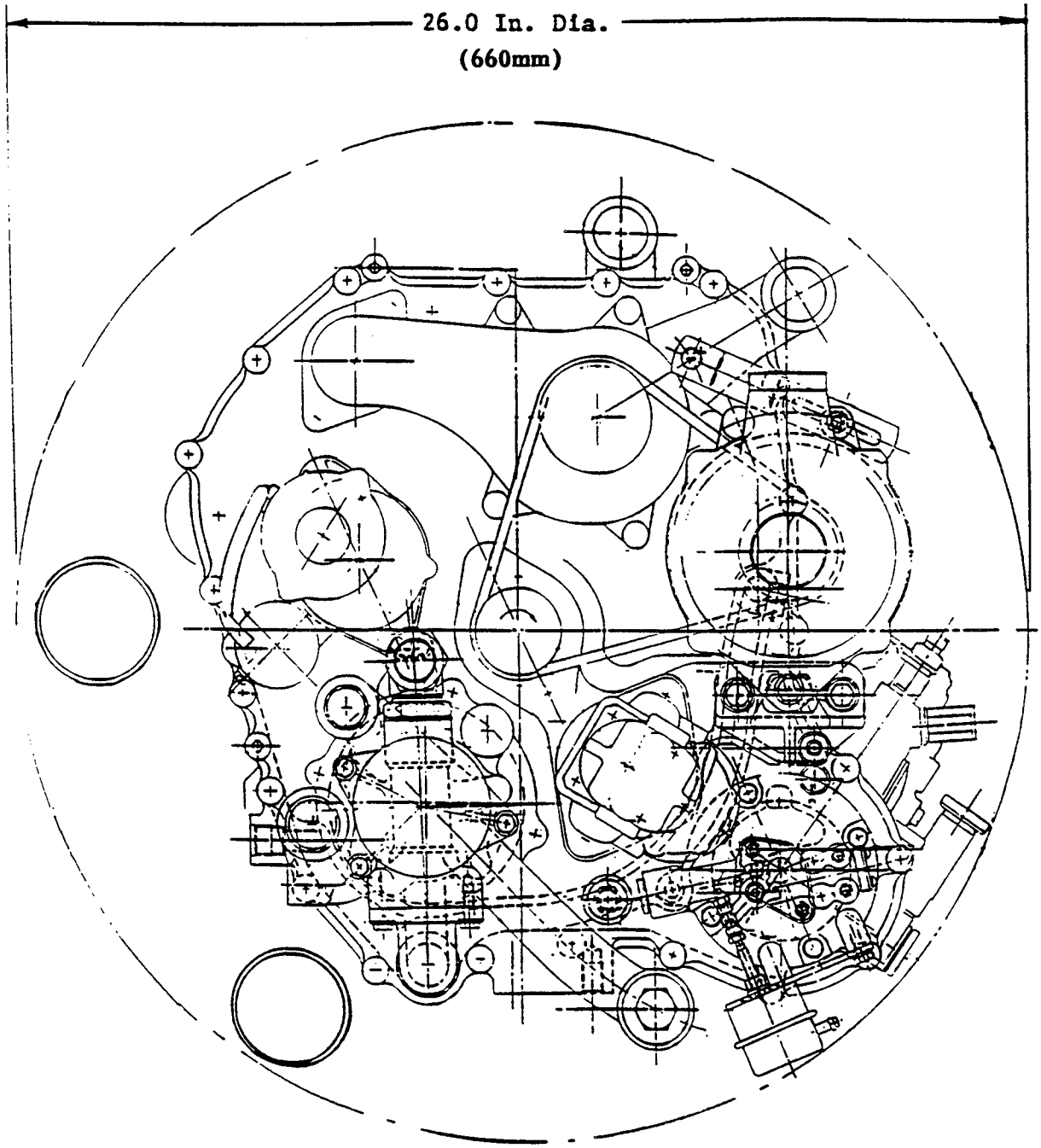


Figure No. 2

2013R NASA REFERENCE ENGINE

PROP END VIEW

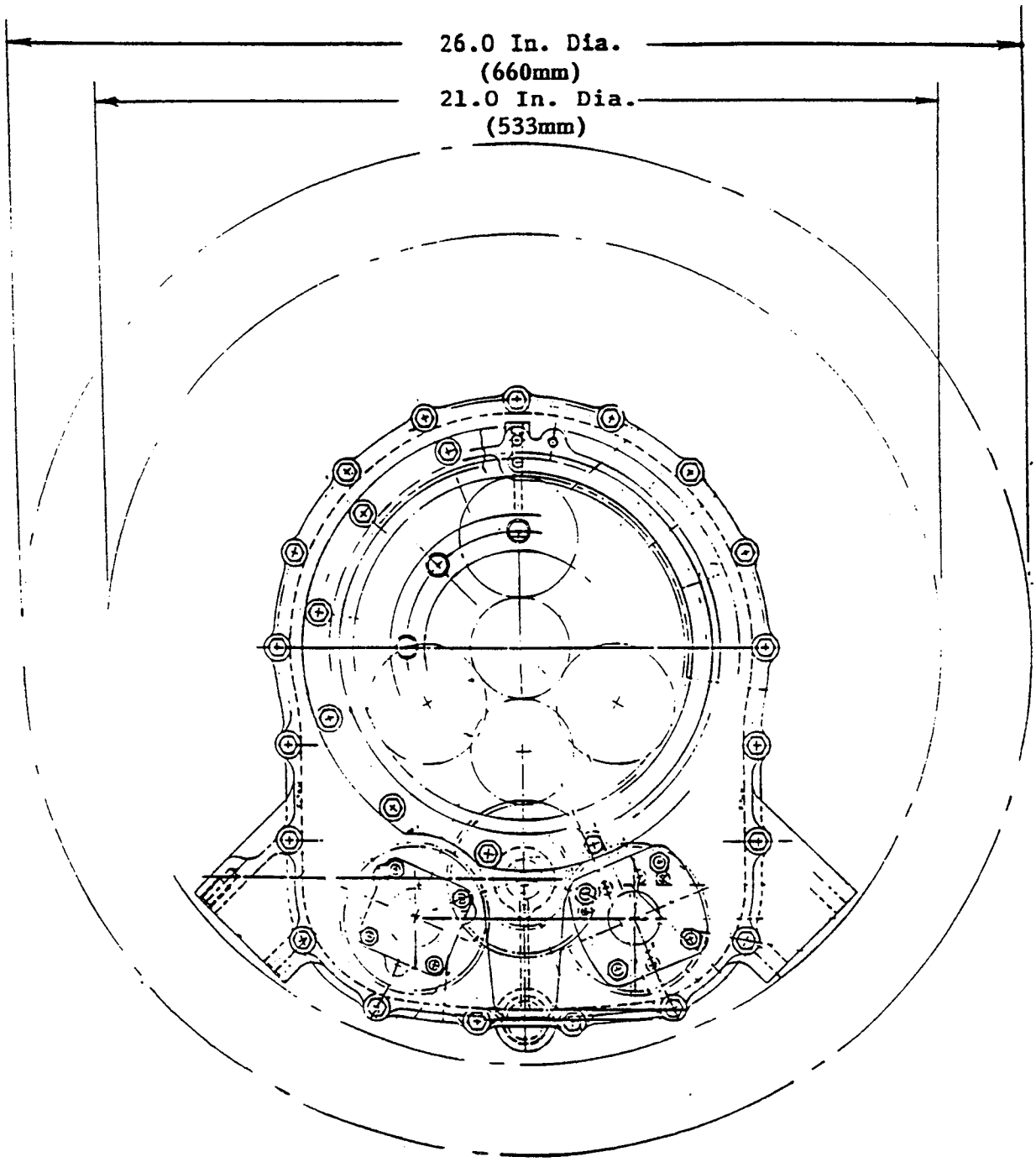


Figure No. 3

2013R NASA REFERENCE ENGINE

PRELIMINARY INSTALLATION DRAWING

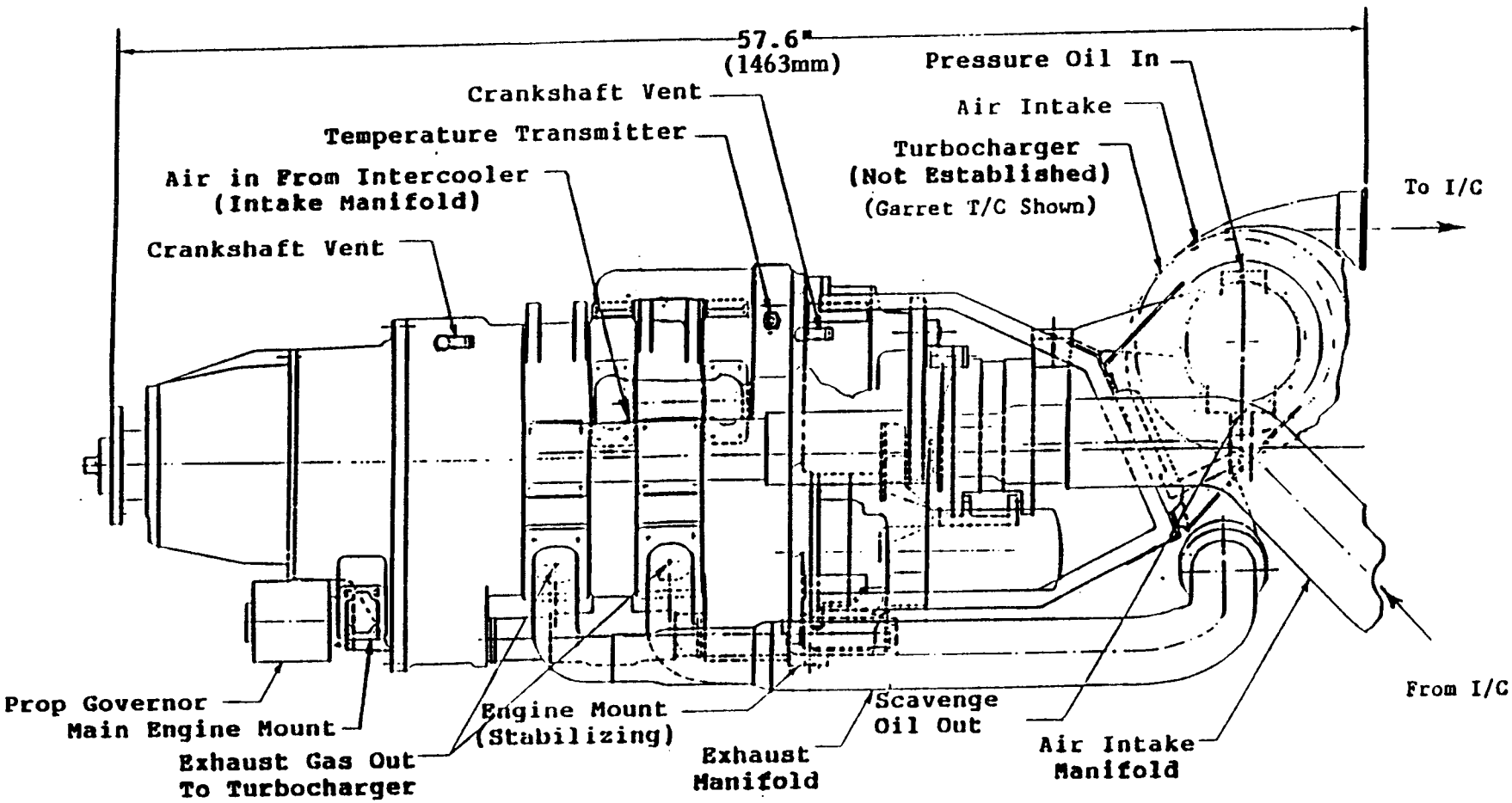


Figure No. 4

2013R NASA REFERENCE ENGINE

PRELIMINARY INSTALLATION DRAWING

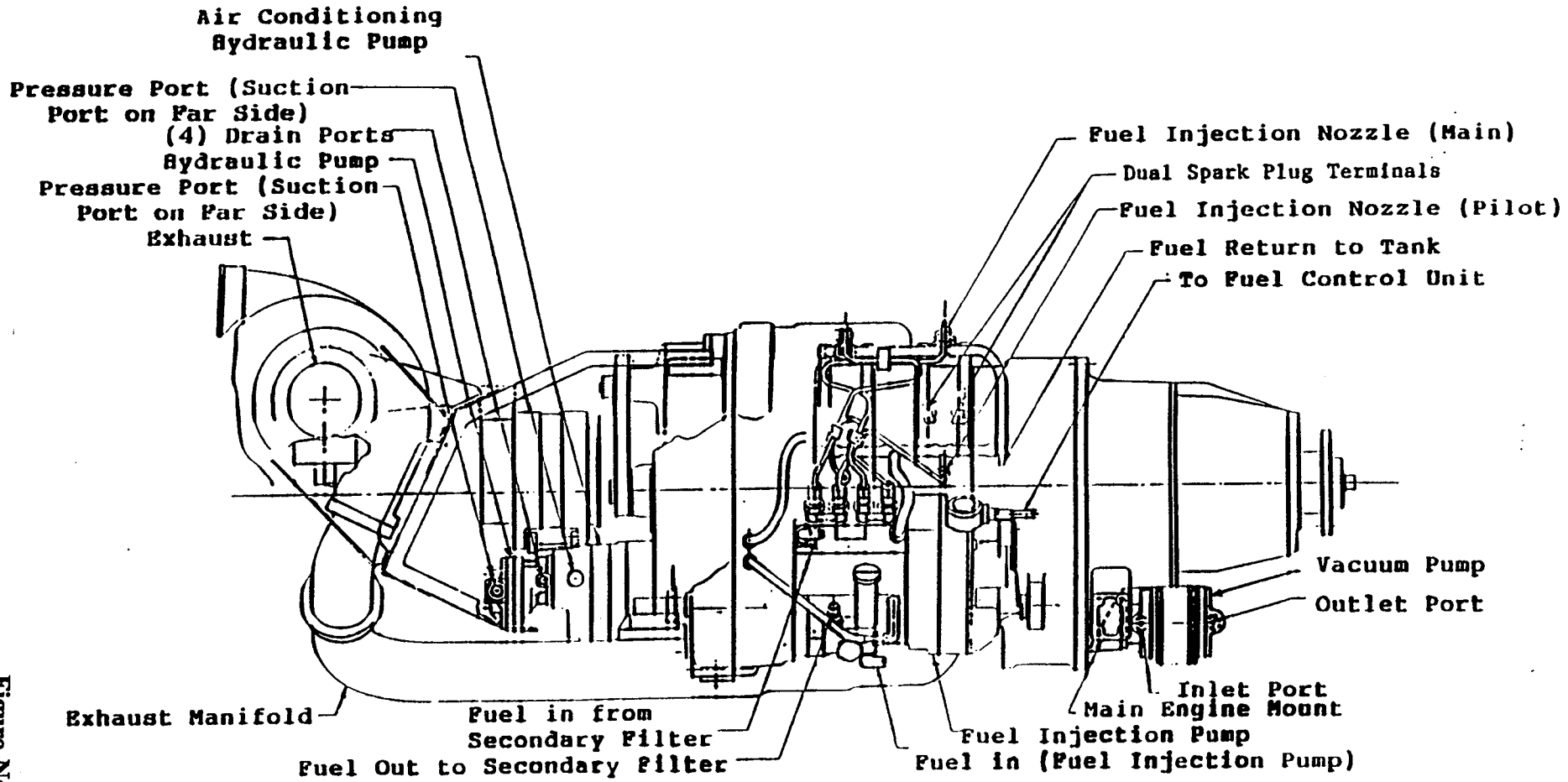


Figure No. 5

2013R NASA REFERENCE ENGINE

PRELIMINARY INSTALLATION DRAWING

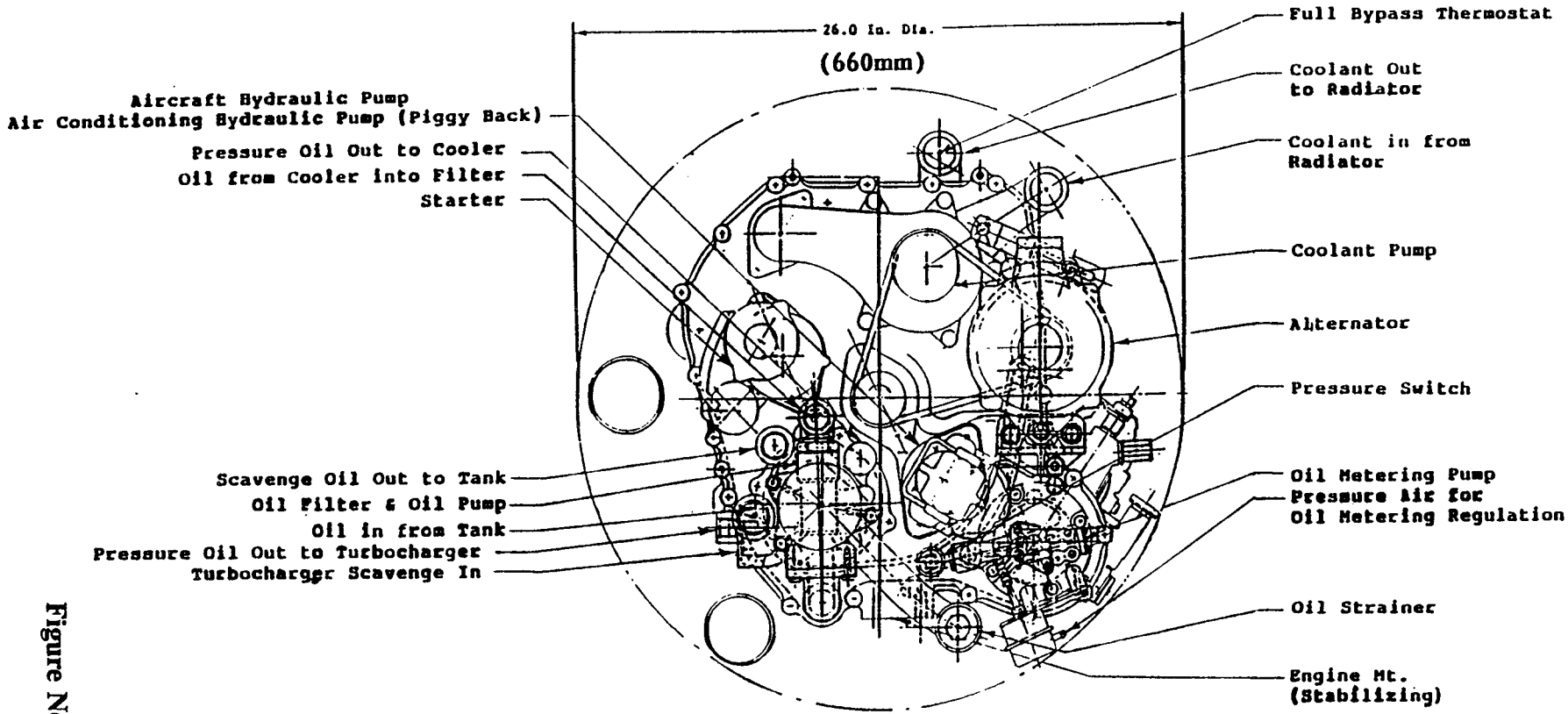


Figure No. 6

2013R NASA REFERENCE ENGINE

REDUCTION GEAR HOUSING AND NOSE CONE

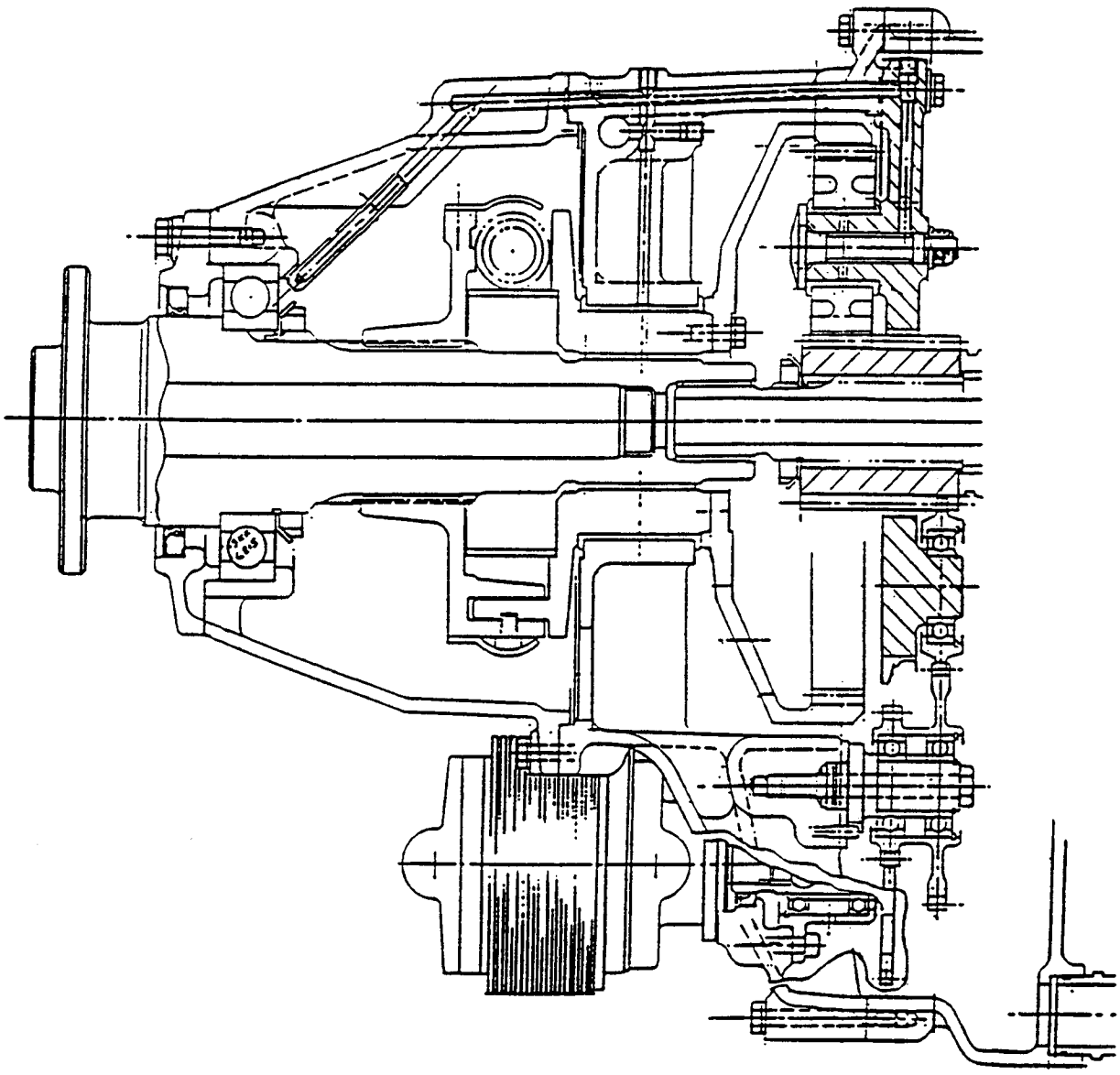


Figure No. 7

2013R NASA REFERENCE ENGINE

PROP SHAFT TORSIONAL COUPLING

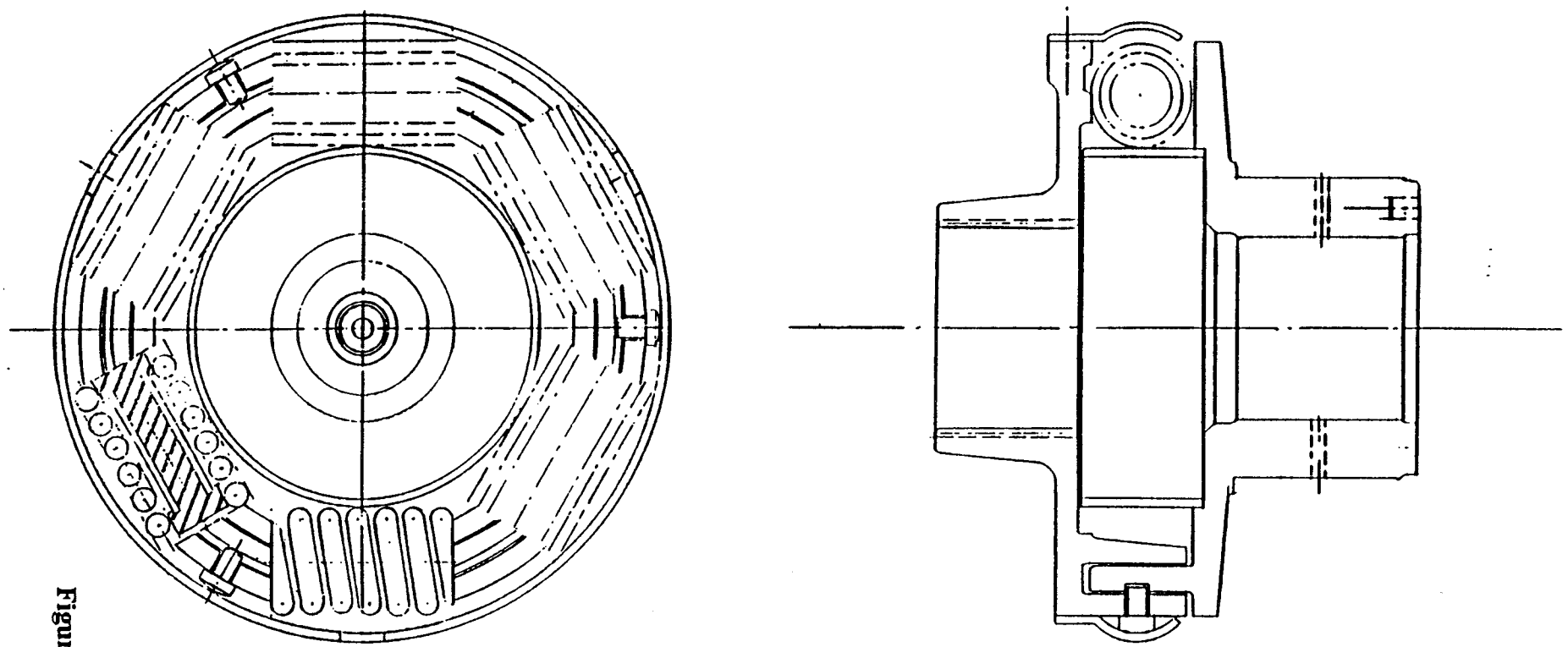


Figure No. 8

2013R NASA REFERENCE ENGINE

CLOCKWISE PROP REDUCTION GEARING

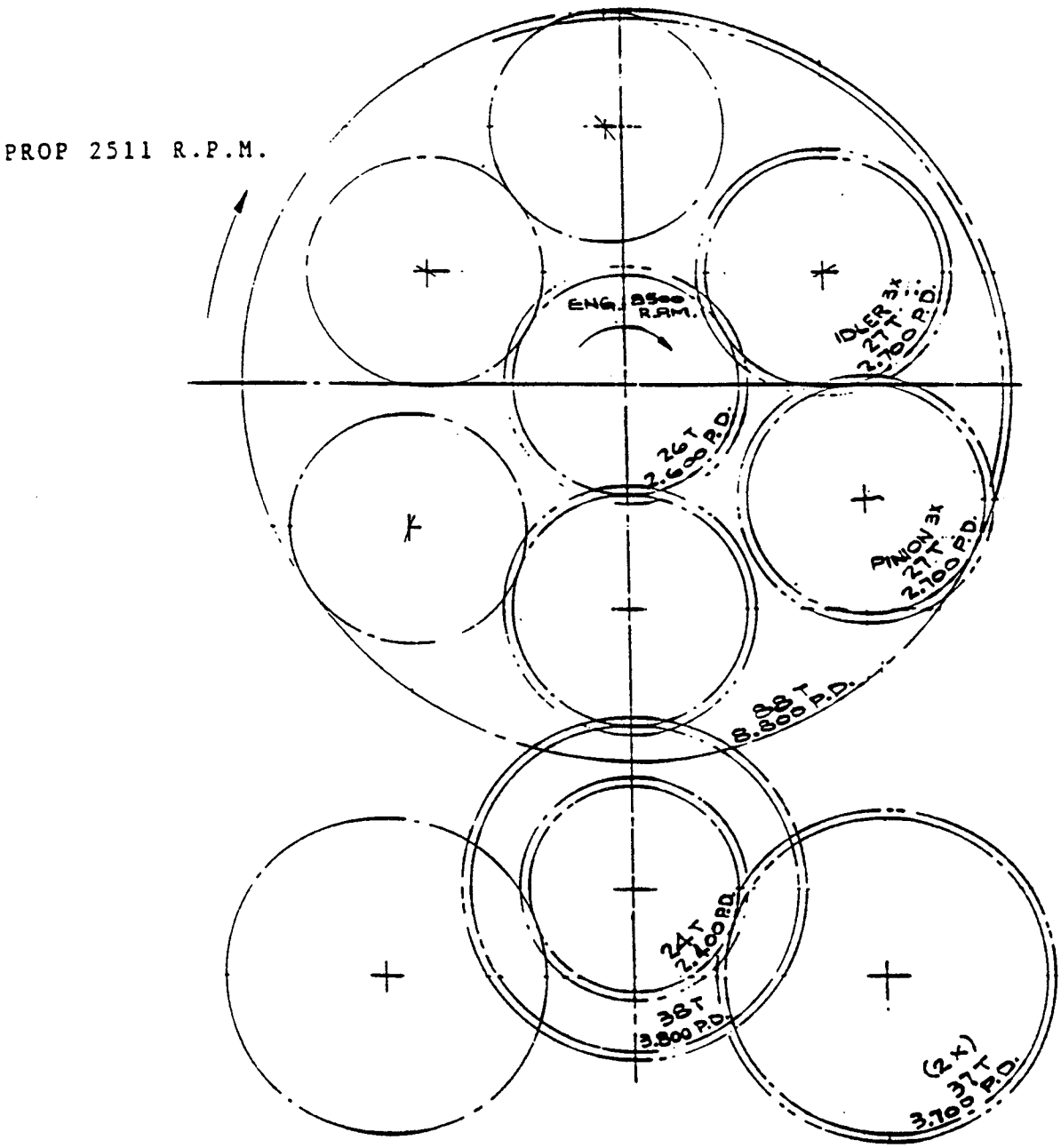


Figure No. 9

2013R NASA REFERENCE ENGINE

COUNTERCLOCKWISE PROP REDUCTION GEARING

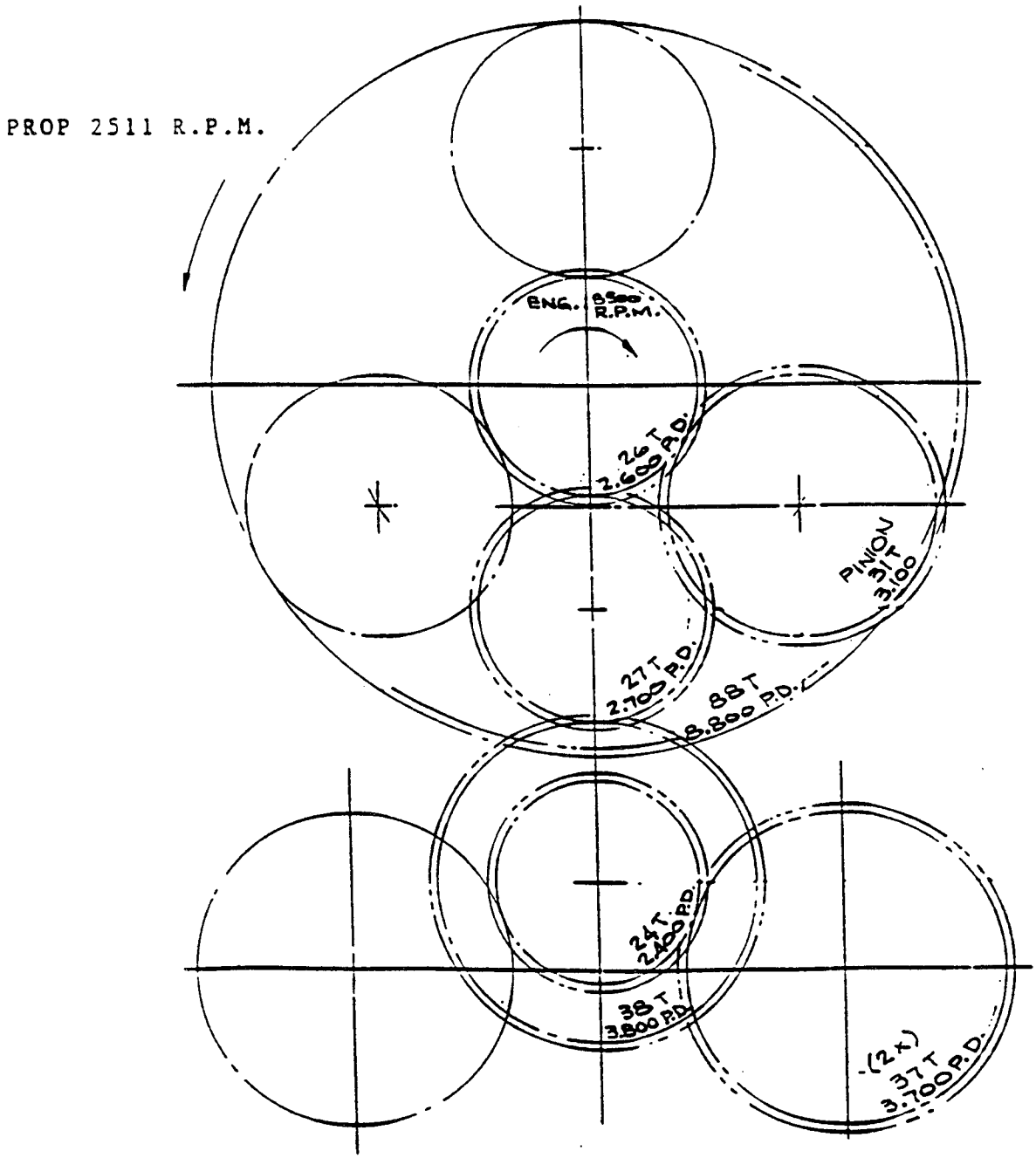


Figure No. 10

2013R NASA REFERENCE ENGINE

TURBOCHARGER SUPPORT

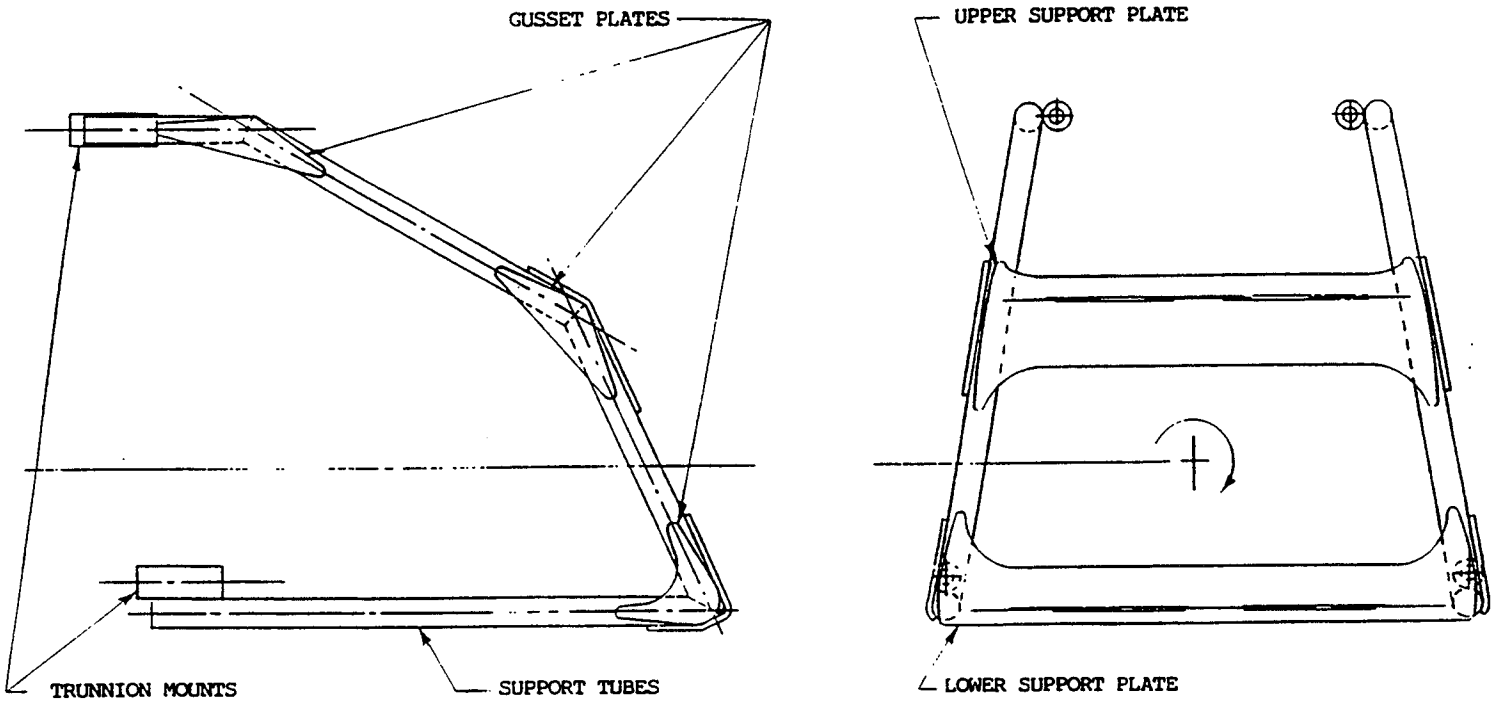


Figure No. 11

2013R NASA REFERENCE ENGINE

TURBOCHARGER/INTERCOOLER INSTALLATION

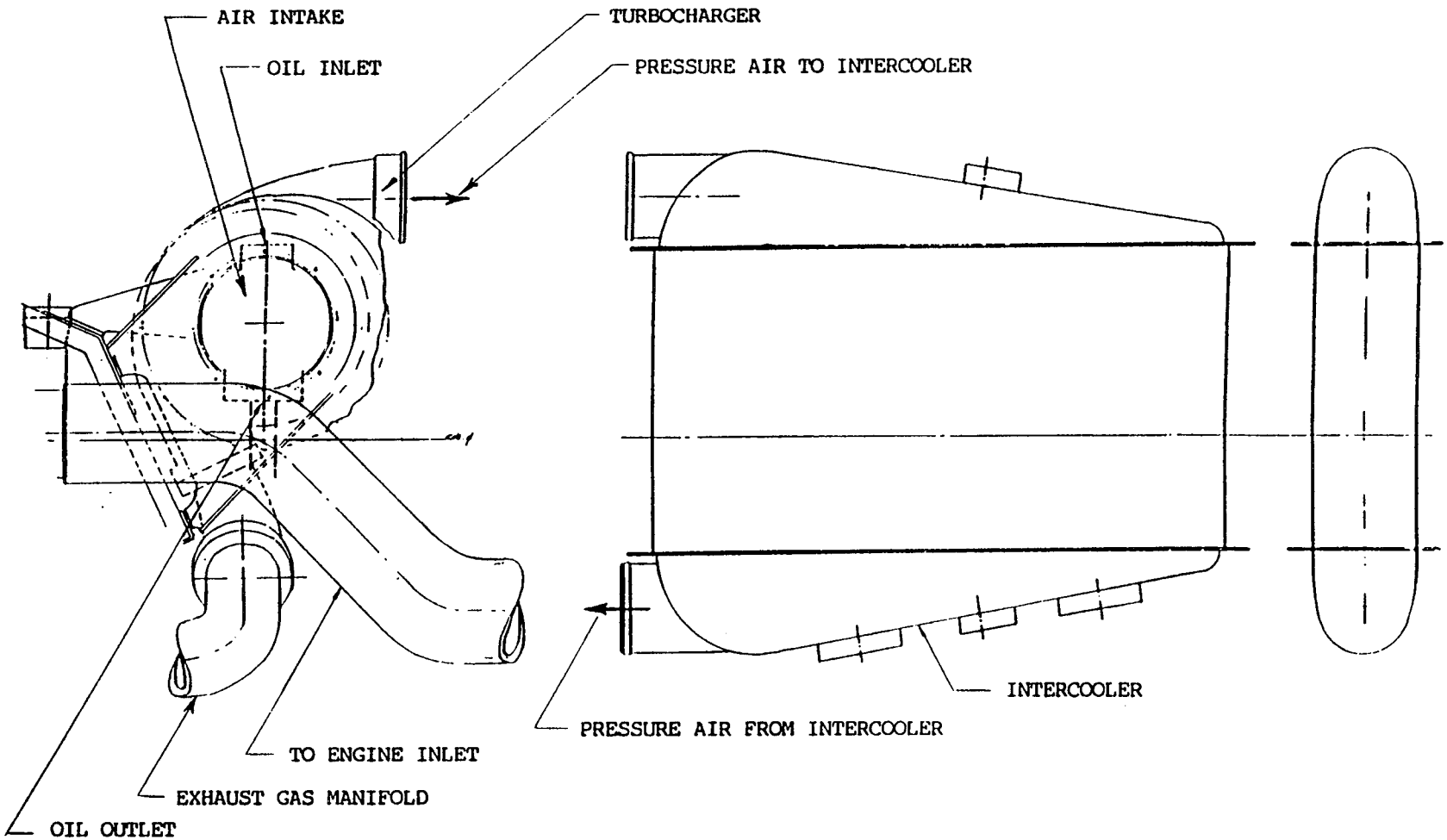


Figure No. 12

2013R NASA REFERENCE ENGINE

COOLANT FLOW SCHEMATIC THRU ENGINE

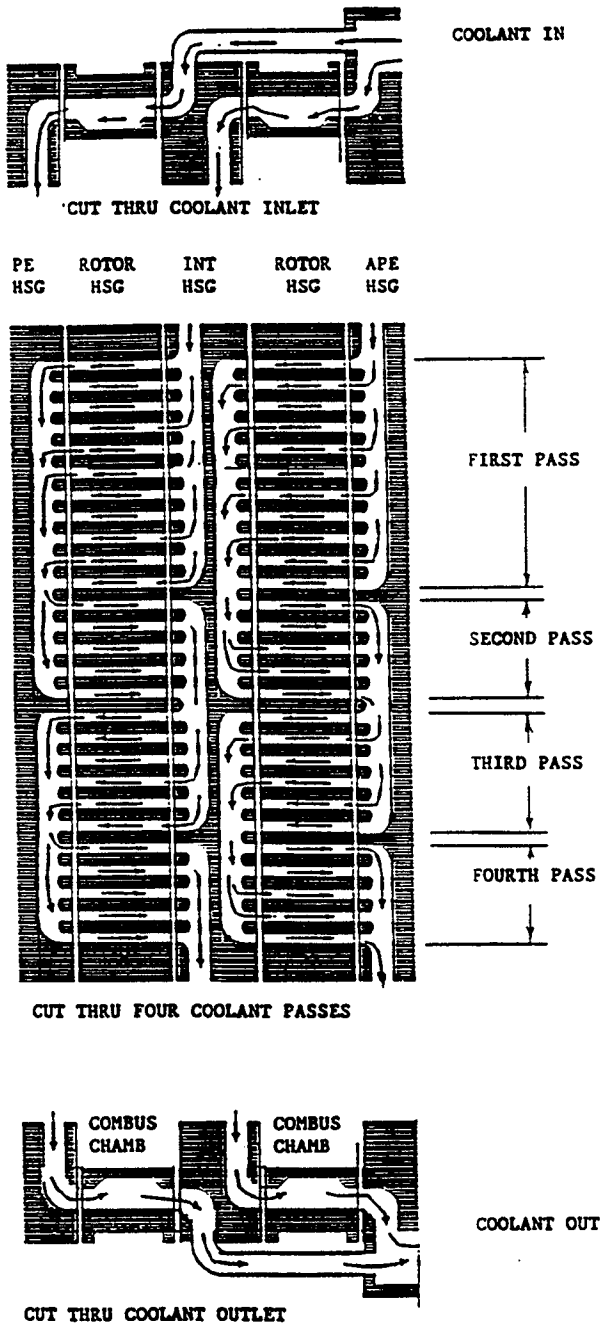


Figure No. 13

2013R NASA REFERENCE ENGINE

COOLANT FLOW THRU ROTOR HOUSING

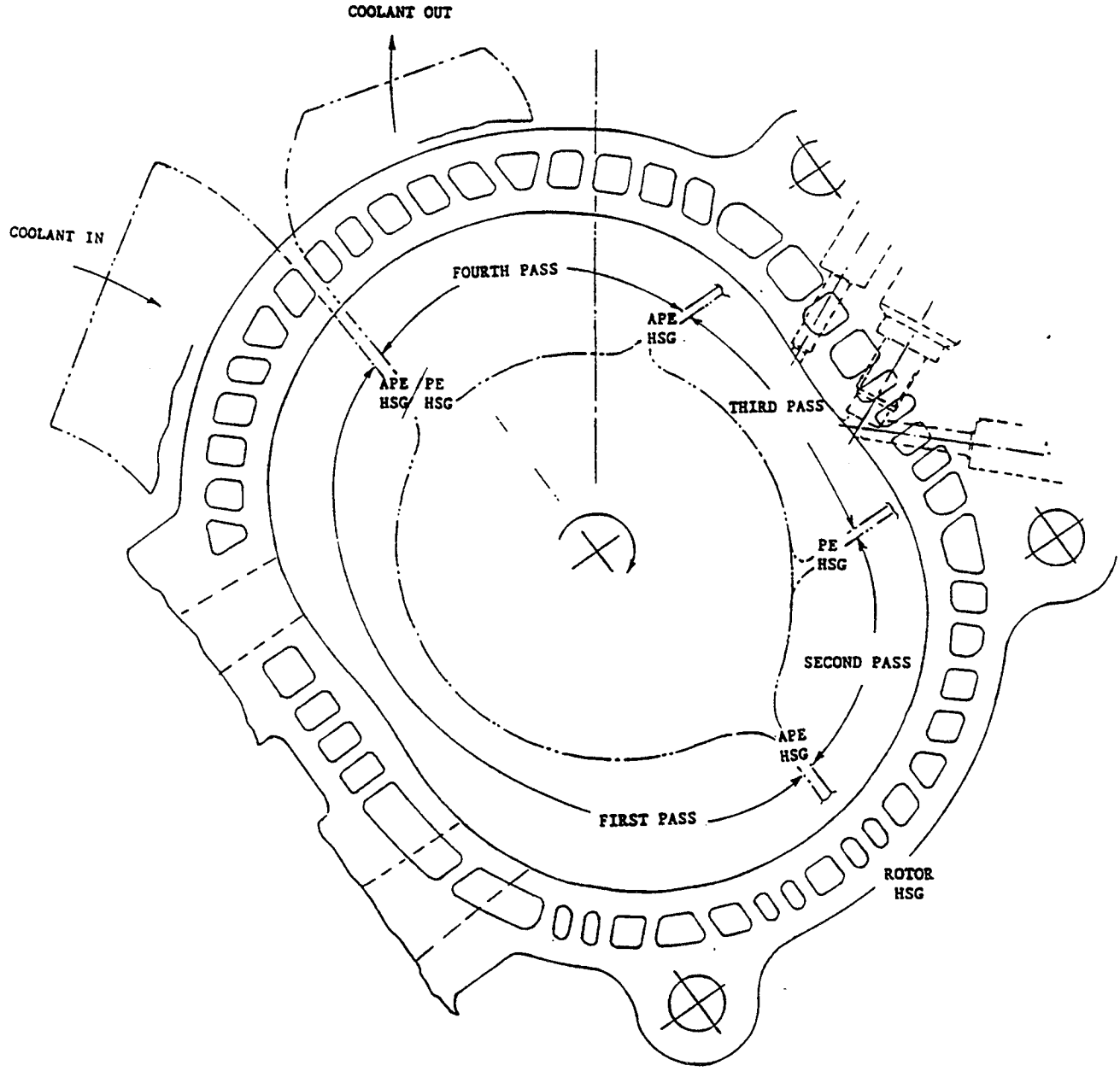


Figure No. 14

2013R NASA REFERENCE ENGINE

LUBRICATION SYSTEM

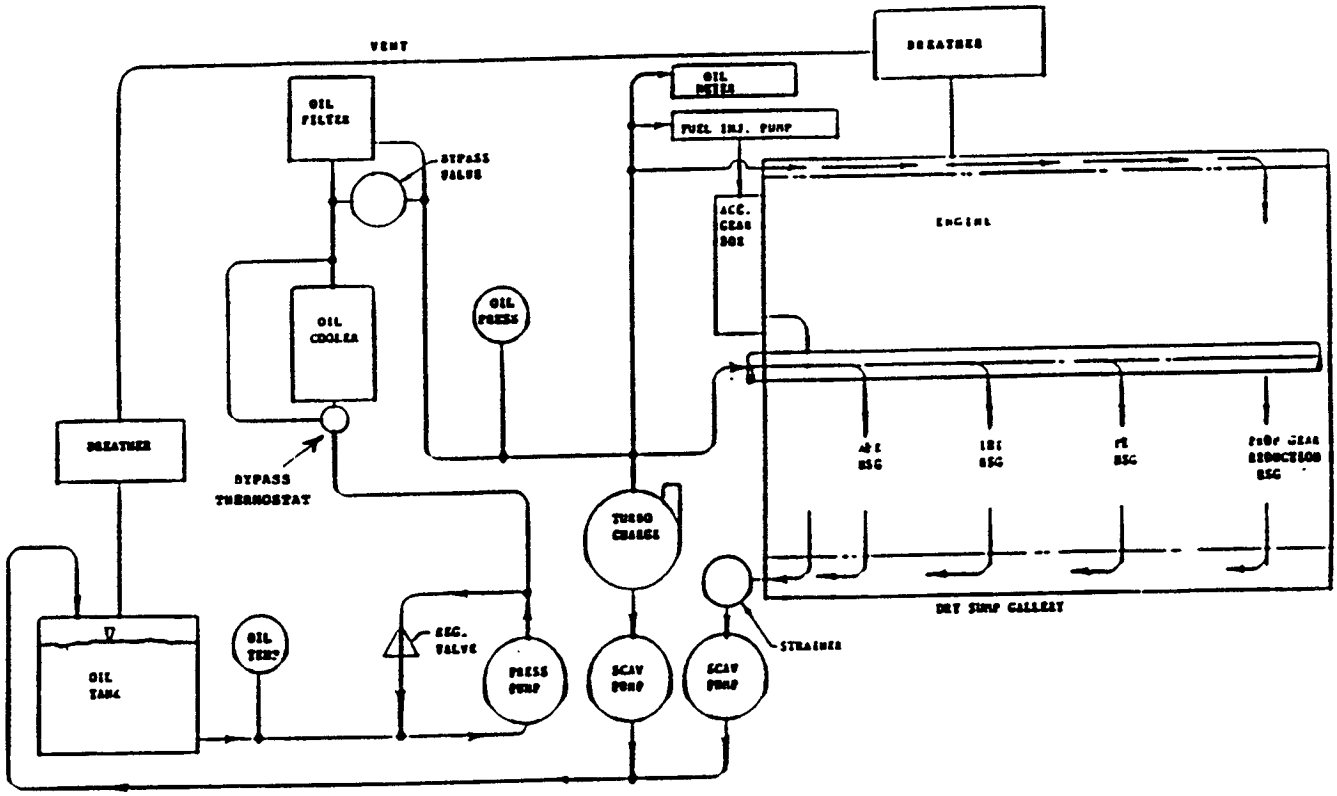


Figure No. 15

2013R NASA REFERENCE ENGINE

FUEL PUMP ADVANCE/RETARD MECHANISM

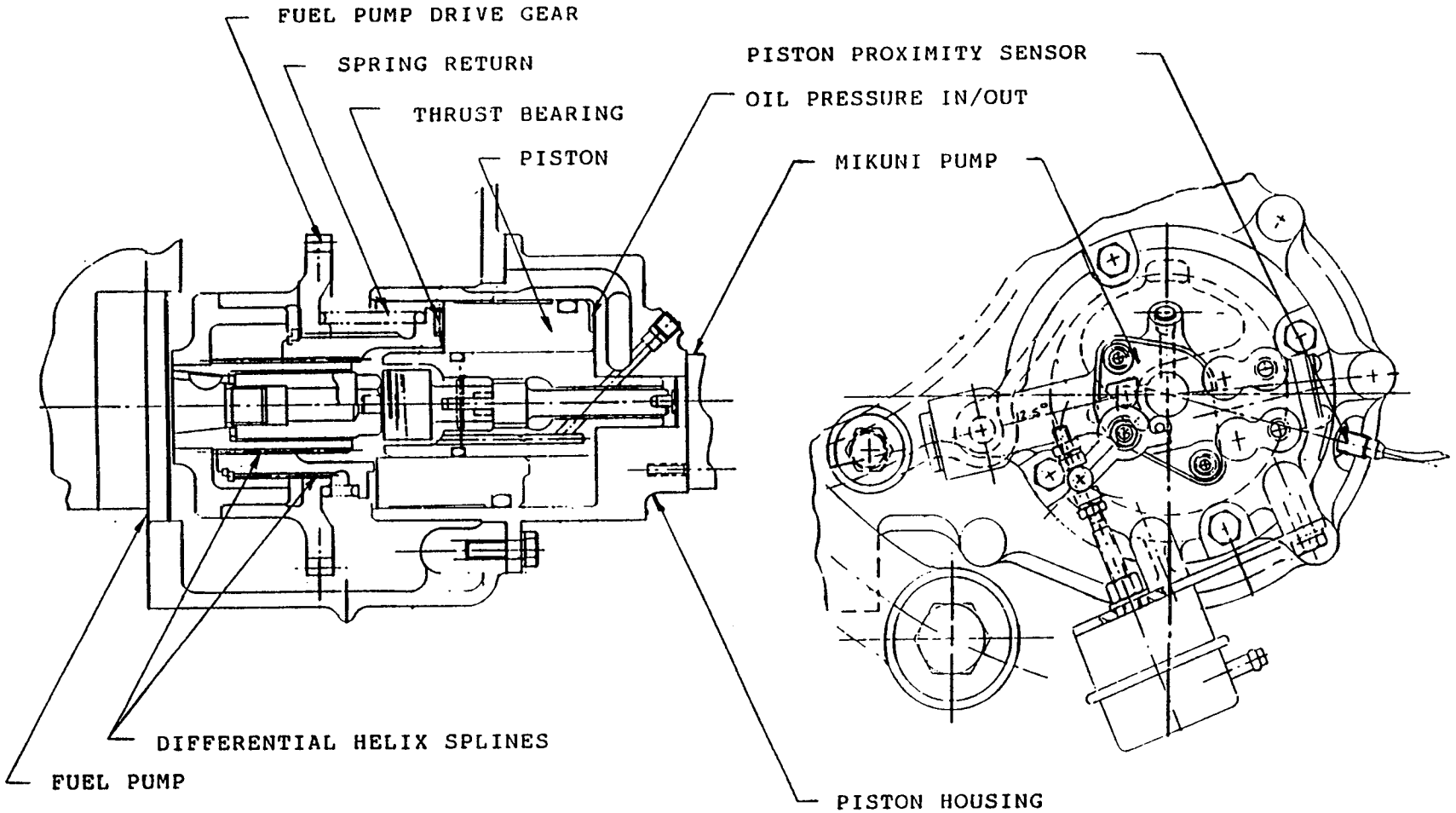


Figure No. 16

2013R NASA REFERENCE ENGINE

ENGINE WEIGHT AND C.G.

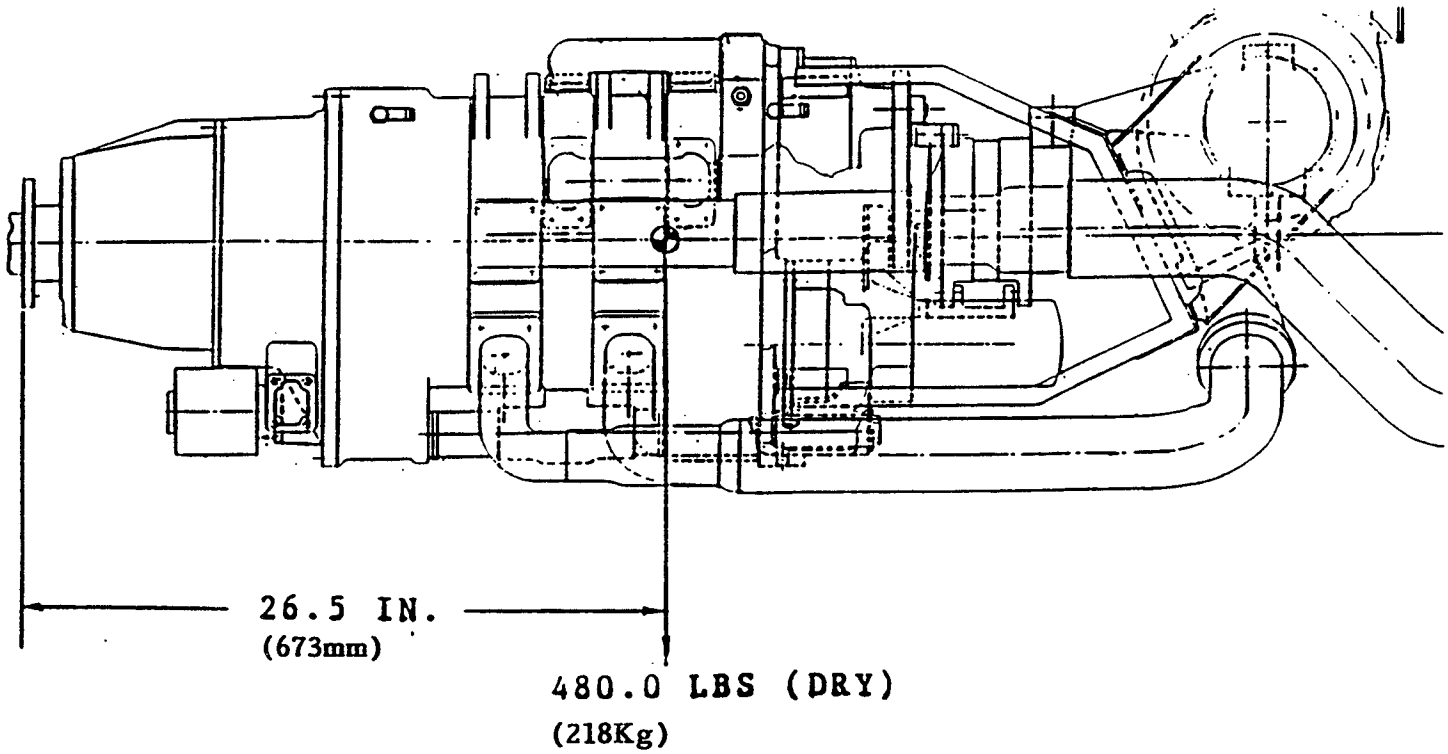


Figure No. 17

2013 NASA REFERENCE ENGINE

OPERATING DATA SUMMARY

	TAKE-OFF		75% CRUISE		
	S.L.	25,000'	S.L.	25,000'	33,000'
BHP (KW)	400 (300)	-	300 (225)	-	-
RPM	8500	-	7500	-	-
IMEP-PSI (kPa)	277.3 (1910)	-	237.2 (1634)	-	-
IHP (KW)	481 (361)	-	363 (272)	-	-
FMEP-PSI (kPa)	46.7 (322)	-	41.2 (284)	-	-
FHP (kw)	81 (61)	-	63 (47)	-	-
BMEP-PSI (kPa)	230.6 (1589)	-	196 (1350)	-	-
F/A	.0374	-	.0360	-	-
BSFC-LB/HP-HR (g/kwr)	.421 (256)	-	.424 (258)	-	-
AIRFLOW-LB/HR (KG/H)	4495 (2039)	-	3530 (1601)	-	-
P^2/P^1	2.5	6.84	2.16	5.89	8.5
P^3-IN. HG (KPA)	69.0 (233)	75.9 (257)	60.7 (205)	60.7 (205)	60.7 (205)
T^3-^{0}F (^{0}C)	140.3 (60.1)	-	140.3 (60.1)	-	-
FUEL FLOW-LB/HR (KG/H)	168.32 (76.3)	-	127.08 (57.6)	-	-
AMBIENT TEMP.-^{0}F (^{0}C)	59.0 (15)	-30.2 (-34)	59.0 (15)	-30.2 (-34)	-58.7 (-50)
AMBIENT PRESS-INHG (kPa)	29.92 (101.2)	11.10 (37.5)	29.92 (101.2)	11.10 (37.5)	7.732 (26.1)

FIGURE 18

2013R NASA REFERENCE ENGINE

ESTIMATED FUEL CONSUMPTION

RATING	HP (KW)	RPM	BSFC LB/HP-HR	GRS/KW-HR
Take-Off	400 (300)	8500	.421	256
75% Cruise	300 (225)	7500	.424	258
65% Cruise	260 (195)	7150	.429	261
55% Cruise	260 (195)	6765	.434	264
Approach	160 (120)	7150	.482	293
Taxi	40 (30)	3830	.644	392
Idle	4 (3)	1780	1.10	669
Idle	0 (0)	1780	3 lb/hr.	1.36 Kg/hr.

FIGURE 19

5.0 AIRFRAME/MISSION MODEL

PRECEDING PAGE BLANK NOT FILMED

INTRODUCTION

The Airframe/Mission Model Technology assessment of this contract was intended to identify and evaluate the general aviation application best suited to the advanced Stratified Charge Rotary Engine.

The best suited application would utilize the unique characteristics of the Stratified Charge Rotary Engine in shaping the airframe configuration and airplane mission. Further, the technology assessment would provide a method for evaluating the performance of the rotary engine in the proposed application. The Airframe/Mission Technology model assessment was subcontracted to the Beech Aircraft Corporation. Beech Aircraft has extensive experience in the development and application of new aircraft technology.

OBJECTIVE

The first objective was to define a representative airframe and airframe mission model. The airframe selected would be intended to best demonstrate the advantages and characteristics of the stratified charge rotary engine. The second objective was to define an airframe mission and mission simulation model. The simulation model would describe and evaluate the selected aircrafts' mission performance with the stratified charge rotary engine.

TECHNICAL APPROACH

The development effort to define the airframe, airframe mission, and mission simulation model was divided by the Beech Aircraft Corporation (Beech) into four discrete tasks. These tasks were:

1. Definition of a representative general aviation airplane configuration and performance characteristics.

2. Definition of general aviation type mission profiles from taxi and takeoff through climb and cruise and back to landing and taxi.

3. Definition of appropriate criteria of merit.

4. Production of a complete airplane/mission system simulation model which will evaluate the criteria of merit when used with a Deere furnished engine model.

PAGE 242 INTENTIONALLY BLANK

PRECEDING PAGE BLANK NOT FILMED

Beech provided the rationale framework required to establish airplane characteristics and mission profiles appropriate to the advantages and characteristics of the stratified charge rotary engine.

RESULTS

Each task which defined the airframe mission and mission simulation model will be addressed separately in the following sections. Complete details of the Beech analysis effort are provided in Reference 1.

1. Definition of Airplane Configuration and Performance

Definition of a representative airplane configuration and performance characteristics entailed consideration of numerous factors. Factors of primary consideration included the rotary engine lapse rate, take off field length, airplane drag coefficients, cruise speed and engine and airframe weights.

Consideration of the above factors provided an initial aircraft configuration and an initial set of design goals. The multi-engine executive transport was selected to provide the most advantageous application of the stratified charge rotary engine. The airplane configuration was then sized for the rotary engine to make the most favorable comparison to current turboprop airplanes which dominate the executive transport market.

The stratified charge rotary engine, as specified in the contract, has a significantly different power lapse rate with altitude than a turboprop. Comparisons of lapse rate with altitude for the stratified charge rotary and for a turboprop are shown in Figures 1 and 2. Figure 1 shows power versus altitude for a turboprop with the same take-off rating as the rotary engine, while Figure 2 compares the turbine and rotary engines with cruise power matched. Normally the case is considered where cruise power is comparable. This comparison indicates the turboprop provides more takeoff power for the same cruise power than the rotary engine. Thus the airplane sizing for the rotary engine tends to lead to a smaller airplane.

Take off field length is proportional to wing loading times power loading divided by maximum lift co-efficient. A maximum lift coefficient of 2.0 in the take-off configuration is considered feasible without imposing excessive drag. Figure 3 shows the allowable gross weight as a function of wing area and field length for two engines at 392 HP (294kw) each (400 hp, 300kw- 8hp, 6kw mechanical loads). A balanced field length of 4000 feet (1219m) or less was used as a design goal.

The wetted area drag coefficients of current airplanes in this class range from about .005 to .006. Advances in airfoils and construction techniques should allow a drag coefficient of .0045 and some modern airplanes approach this value. Figure 4 illustrates the total airplane wetted area versus design speed and altitude for the cruise power available from the rotary

engine. Current airplanes in this class have wetted areas in the 1100 to 1300 square feet (102-121 square meters) range. An initial cruise speed of 300 knots was selected which leads to a wetted area of 1055 square feet (98 square meters) at the engine cruise critical altitude of 33,000 feet (10 km).

The initial cruise speed selection was based on a data correlation of aircraft maximum speeds. Implied in those data was that induced drag was on the order of 10% of parasite drag. Induced drag is closer to 20% of parasite drag for the cruise at 33,000 feet (10 km). As shown in figure 5, the 300 knot goal led to an unacceptably small airplane. A goal of 280 knots gives a more practical size as shown in Figure 6. Both figures show results form a simplified synthesis program using Breguet's range equation and a weight correlation equation.

Airframe weights were approximated from a correlation of empty weight minus installed engine weight per unit wetted area. The resulting estimated weights were somewhat higher than indicated by the weight correlation equation used in the synthesis routine which had been based on turboprop airplanes. The result was some adjustment of weight goals from those shown on Figures 5 and 6.

The following design goals were selected based on the results of the above analysis.

Wetted Area	1100 Sq. Ft. (102 sq. M)
Wing Area	195 Sq. Ft. (18.1 Sq. M)
Fuel Weight	1400 lbs. (635 kg.)
Empty Weight	5100 lbs. (2313 kg.)
Take Off Gross Weight	8000 lbs. (3629 kg.)
Aspect Ratio - selected	10

An engine installation layout was made based on the heat exchanger sizes received from Sundstrand. The best arrangement was to mount the heat exchangers between the engine mount rails with cooling air entering below the exchangers and flowing upward to exits in the top of the cowl as shown in Figure 7. The heat exchangers were re-sized to better fit the available space.

Heat exchanger weights were originally based upon a liquid cooled, turbocharged engine of comparable power. The coolant radiator is approximately two times and the intercooler approximately five times the weight of comparable items for a reciprocating engine. The comparison is based upon the split intercooler for the single compression stage. Weights cited are for the core only and do not include manifolds and plumbing which will reduce further the engine weight advantage of the rotary. The engine weight savings over comparable reciprocating engines was estimated to be 100 pounds (45.4 kg). The increased weights of the heat exchangers will reduce the advantage to less than 50 pounds (22.7 kg).

Propeller sizing for the rotary engine application was strongly influenced by noise limits. Noise limits in Europe have now been reduced to 72 DBA flyover. New airplanes should be designed to be marketable worldwide.

Figure 8 shows the maximum diameter allowed as a function of RPM for 72 DBA. Figures 9 to 11 then show the resulting efficiencies for the corresponding points with the cruise RPM reduced by the engine RPM ratio of cruise to maximum RPM (7500/8500). From these curves it can be seen that a four bladed prop of 92 inches diameter (2337mm) with takeoff RPM of 1950 is near peak efficiency for all calculated flight points (gear ratio-0.229).

The initial aircraft design layouts had used a smaller propeller and the layout has been modified to accommodate the larger propeller size. Nacelles had to be moved outboard, the landing gear lengthened and the engine moved slightly forward to maintain clearance of the crew and flight controls from the 5 degree propeller cone as shown in Figure 12.

Final aircraft specifications and performances are as follows.

Wetted area,	1100 Sq. Ft. (102 Sq. M)
Wing area,	195 Sq. Ft. (18.1 Sq. M)
Fuel weight,	1300 lbs. (590 kg.)
Empty weight,	5200 lbs. (2359 kg.)
Gross weight,	8000 lbs. (3629 kg.)
Aspect ratio	10
Cruise speed (33000 ft/10 km), knots	277
Range (33000 ft/10 km) nm @	
Max cruise speed	1550 nm
Max range	1803 nm
Time to climb (33000 ft/10km), min	24

Performance estimates have been based on the expected attainable wetted area drag coefficient of 0.0045.

2. Definition of Mission Profiles

Two mission profiles were selected and are shown below. These missions are for standard day temperature conditions (ISA).

Mission 1 includes segments for taxi and take off, climb to cruise altitude, and descent to sea level. Allowances were made for a 45 minute reserve flown at long range power at cruise altitude. Cruise altitude is 25,000 feet (7.62 km) and maximum cruise power is used for the cruise segment. The climb, cruise and descent legs have a total range of 600 nautical miles.

Mission 2 is the same as Mission 1 except the climb, cruise and descent legs have a total duration of six hours and the cruise is accomplished with maximum range power.

Data set listings for these missions are included in Appendix D of Reference 1.

3. Definition of Criteria of Merit

The criteria of merit is the product of range and payload. This parameter results in a large number for a high payload carried a long distance. The larger the number the better the capability of the airplane. This parameter reflects the most common evaluation of an airplane's performance.

4. Production of Mission Analysis Simulation Model

A mission analysis simulation model was developed to allow operational evaluation of the basic aircraft configuration performance. The simulation program accounts for all phases of a flight from ground operation to cruise reserves.

The mission analysis program includes numerical representations of the engine, propeller and airframe performance. An engine model furnished by John Deere simulates engine performance. The propeller performance is predicted using a general propeller chart presented in Reference 2. The basic propeller chart was extrapolated for the low engine power operating region of some mission segments. Airplane drag is represented by a basic drag polar with skin friction and form factor drag as well as lift dependent drag.

The mission segments available in the program are ground, climb, cruise, descent and climb-cruise descent. The climb-cruise-descent segment combines the three mission flight segments to allow a time, fuel or distance constraint to be applied to the sum of the flight segment. Program output data sets to illustrate program utilization are provided in Reference 1. Complete program user input variable lists are included in Appendix A of Reference 1.

CONCLUSIONS

1. A representative, general aviation type airframe was sized and characterized. A multi-engine executive transport was selected to best demonstrate the advantages of the stratified-charge rotary engine. The airplane has a gross weight of 8000 pounds (3629 kg), a cruise speed of 277 knots at 33,000 feet (10 km), and a maximum range of 1803 nautical miles. The airplane was sized to make the most favorable comparison to current turboprop airplanes.

2. Two mission profiles were selected. Both mission include segments for taxi and take off, climb to cruise altitude of 25,000 feet (7.62km), and descent to sea level. In addition, there is a 45 minute fuel reserve. The first mission has a total range of 600 nautical miles, with maximum cruise power at cruise. The second mission has a total duration of six hours, with cruise at maximum range power.

3. The criterion of merit selected is the product of range and payload. This product reflects the most common evaluation of an airplane's performance. The larger the "product" the better the capability of the airplane.

4. A mission analysis program was written which will accept an engine performance subroutine and will provide aircraft mission performance. The program accounts for all phases of a flight from ground operation to cruise reserves. The program calculates the criterion of merit for the selected mission.

RECOMMENDATIONS

1. The analytical mission analysis program should be used concurrently in evaluating engine design alternatives. Design changes which impact engine envelope, gross weight, power output, or bsfc can be examined with the mission analysis program for effects of the changes on airplane configuration and or mission capability.

REFERENCES

1. Bernstorf, D., Zickhur, T., "Summary Report: Airplane Configuration and Analysis for the Stratified Charge Rotary Engine Study", Report #E24734, 16 Sept 1991, Beech Aircraft Corporation

2. Perkins, C.D., and Hage, R.E, "Airplane Performance, Stability and Control, "Wiley and Sons, Inc. New York, 1949

ENGINE LAPSE RATE

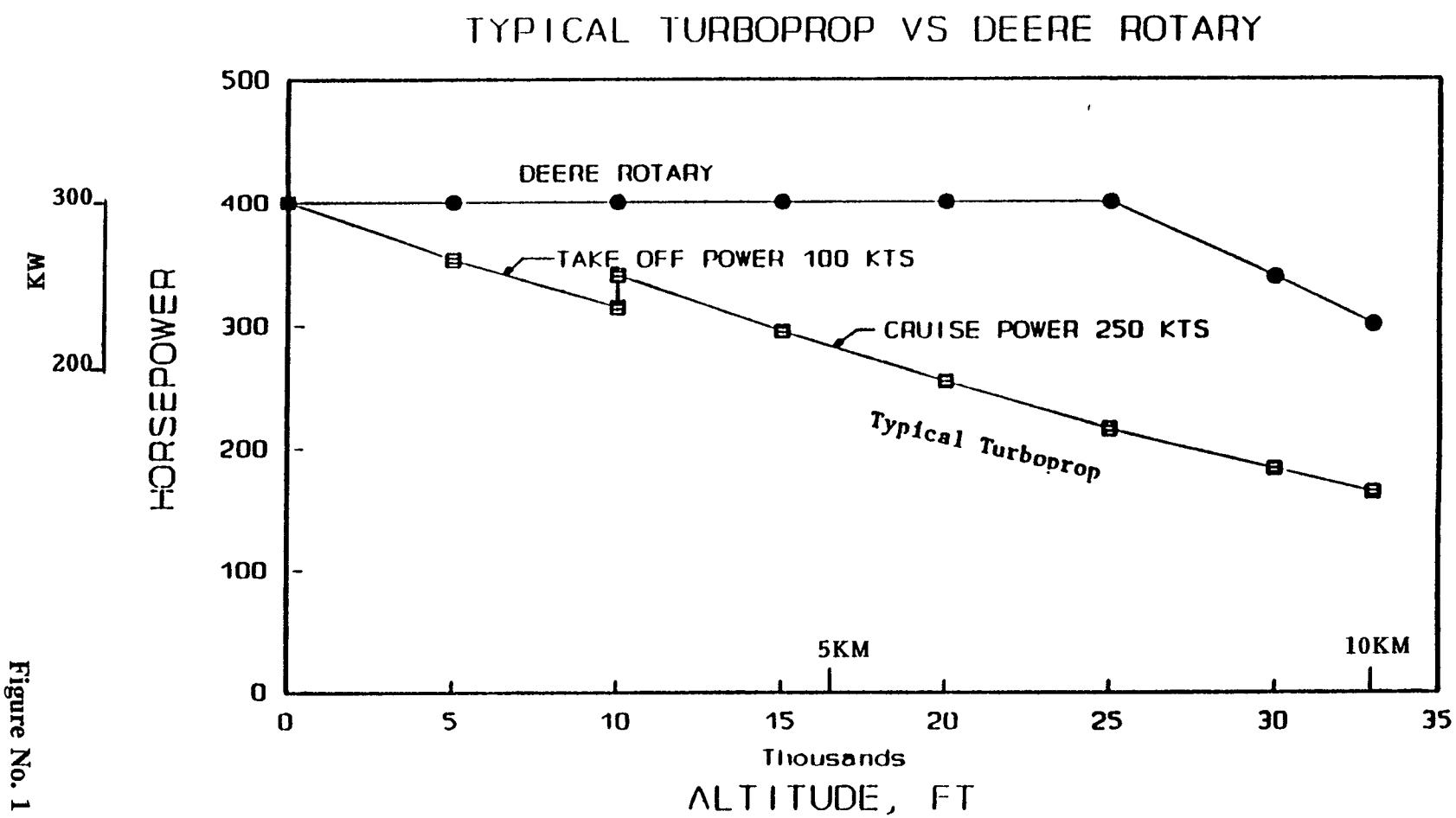


Figure No. 1

ENGINE LAPSE RATE

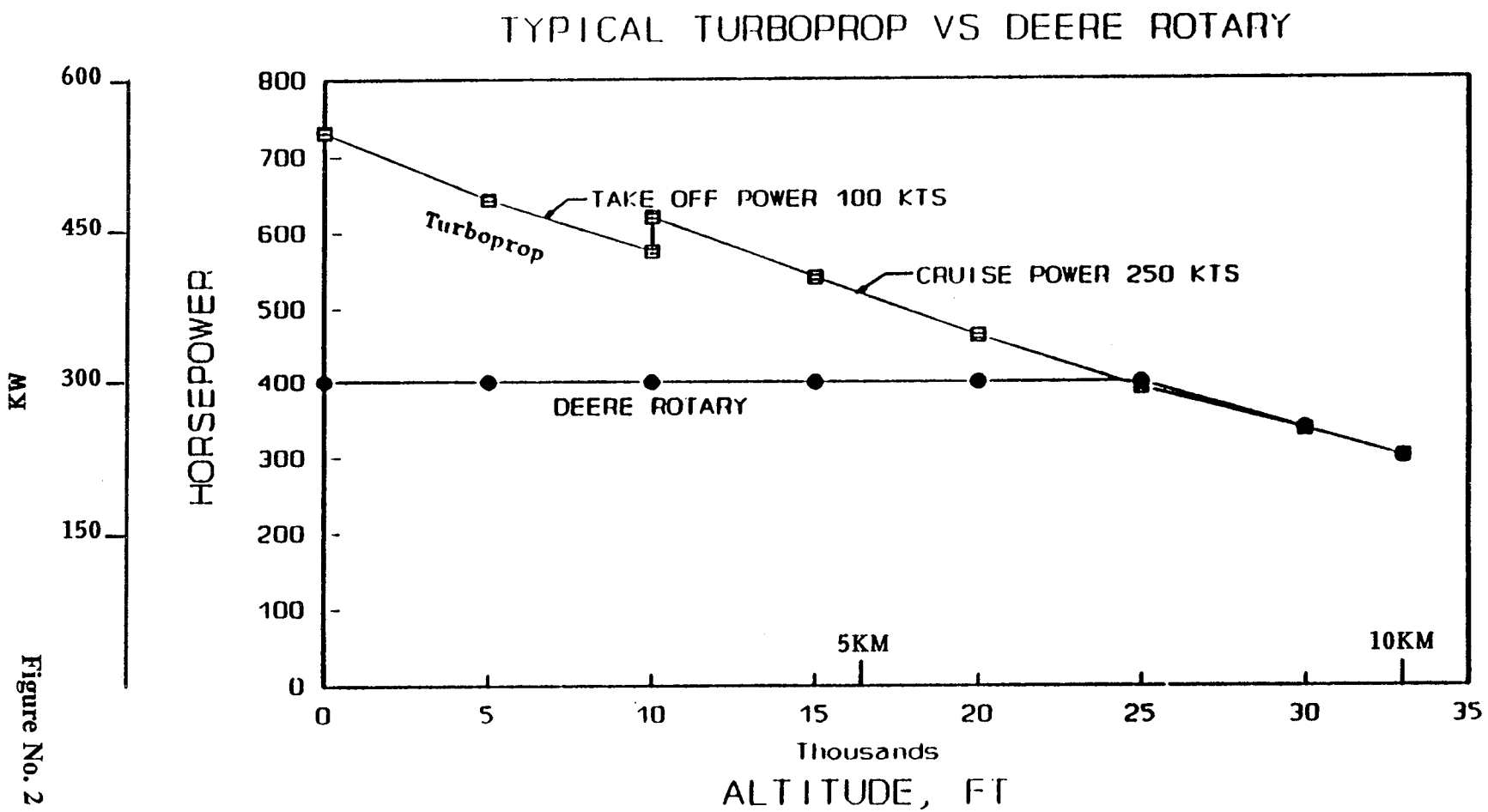


Figure No. 2

WEIGHT LIMITS FOR BALANCED FIELD LENGTH

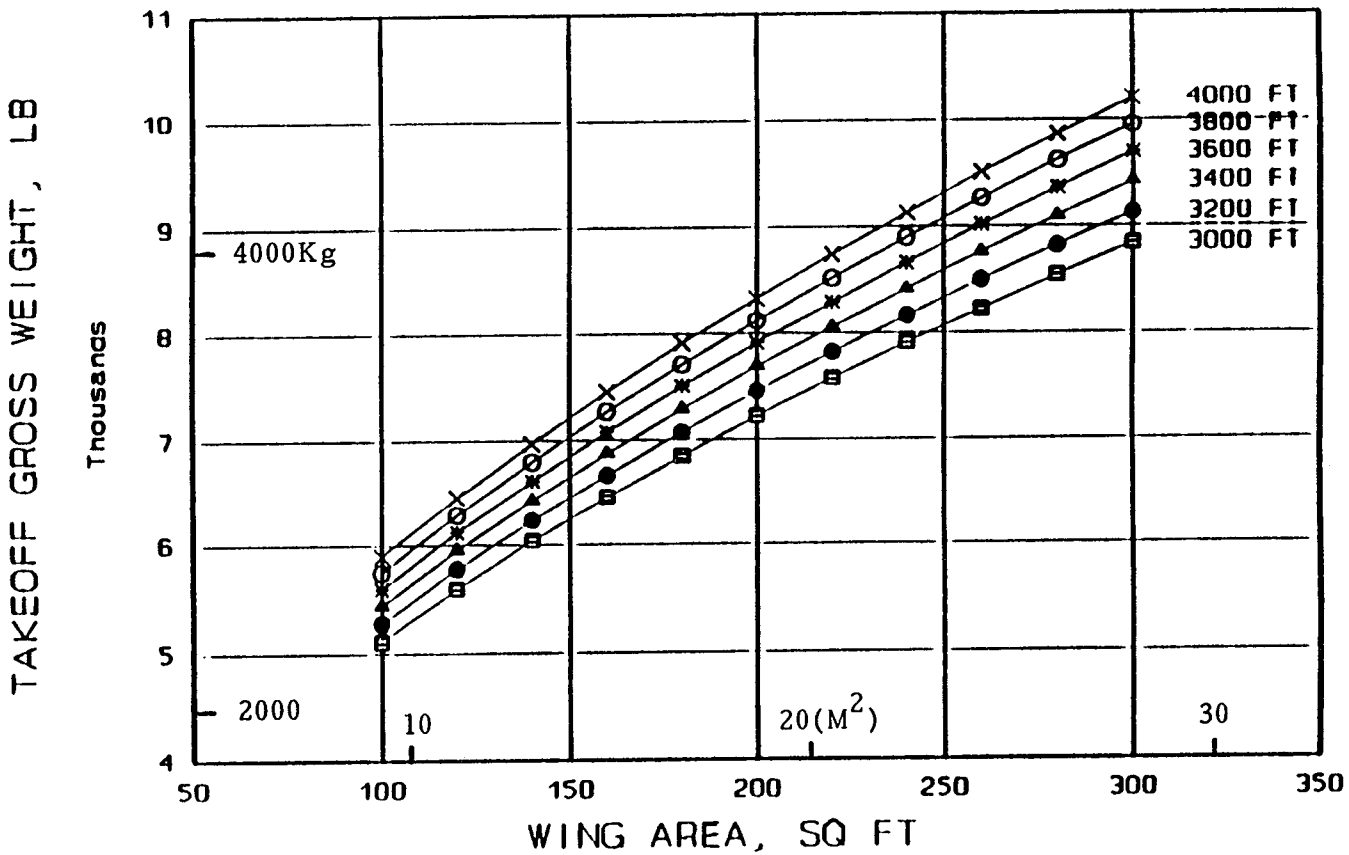
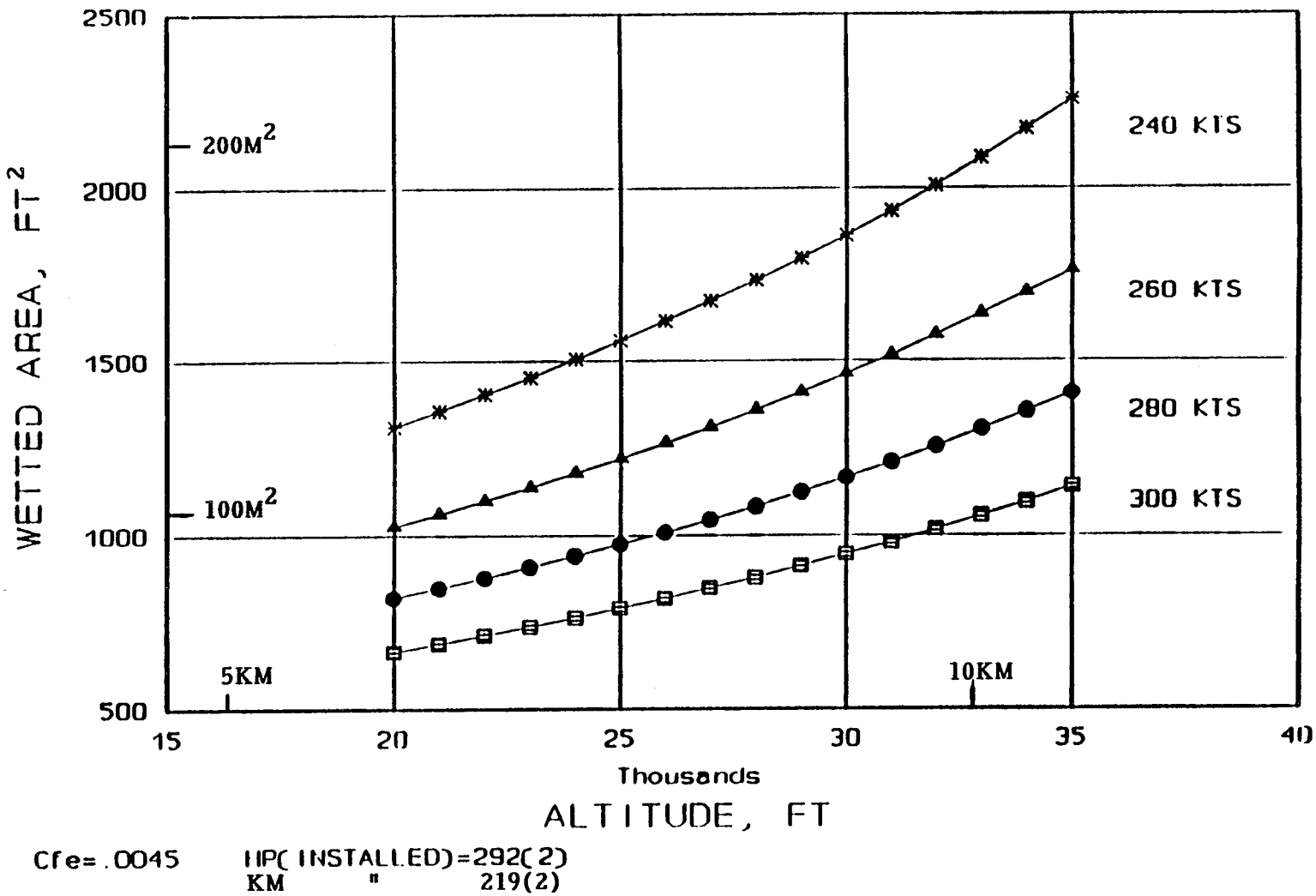


Figure No. 3

WETTED AREA SIZING



Cfe=.0045 HP(INSTALLED)=292(2)
KM " 219(2)

Figure No. 4

7/8/80

Figure No. 5

CRUISE ALTITUDE = 33000 FT (10KM)
RANGE = 1500 NMI
FIXED LOAD = 1800 LBS (816Kg)
BSFC = .354 LBS/BHP-HR (216 g/kW/Hr)
e = .8 AR = 10
V CRUISE = 280 KTS
9500
9000
8500
8000
7500
7000
4000
3750 Kg
3500
3250
GROSS WEIGHT LBS
SEA HP (610kW)
11000 FT
60
10000 FT (9049M²)
55
50
WETTED AREA (102.2M²)
WETTED AREA
8Kg/M² WING LOADING
45
40
35
30
6
7.5
10
LB/FT²

Figure No. 6

Rotary-Powered Twin Study

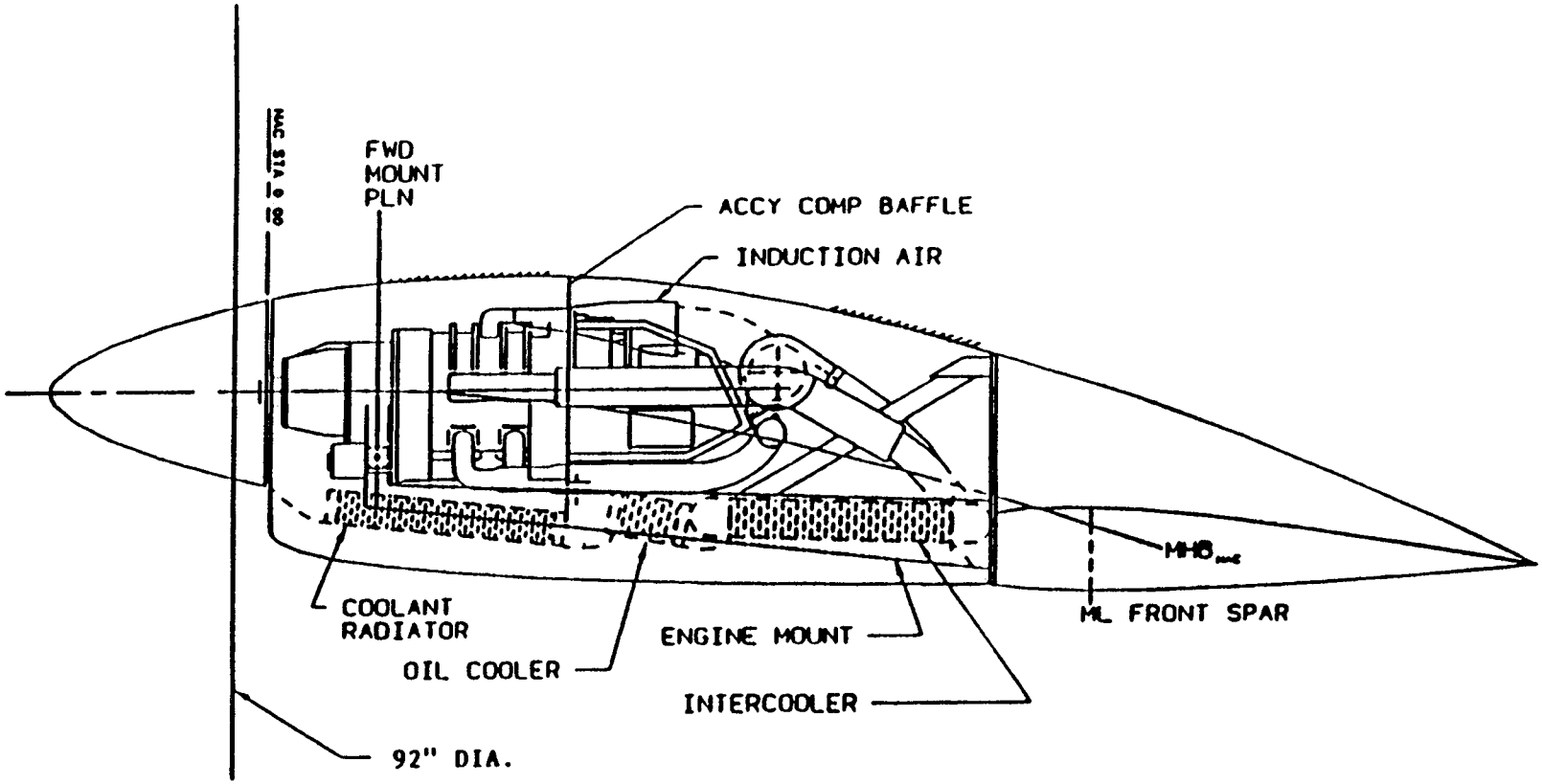


Figure No. 7

GJ Case 22Aug90
NASA.VGF

JOHN DEERE/NASA PROPELLER OPTIMIZATION
PROPELLER SIZED FOR 72 DBA FLY-OVER NOISE
AT 400BHP (300KW) 1000 FT. (304M) 119 KTAS

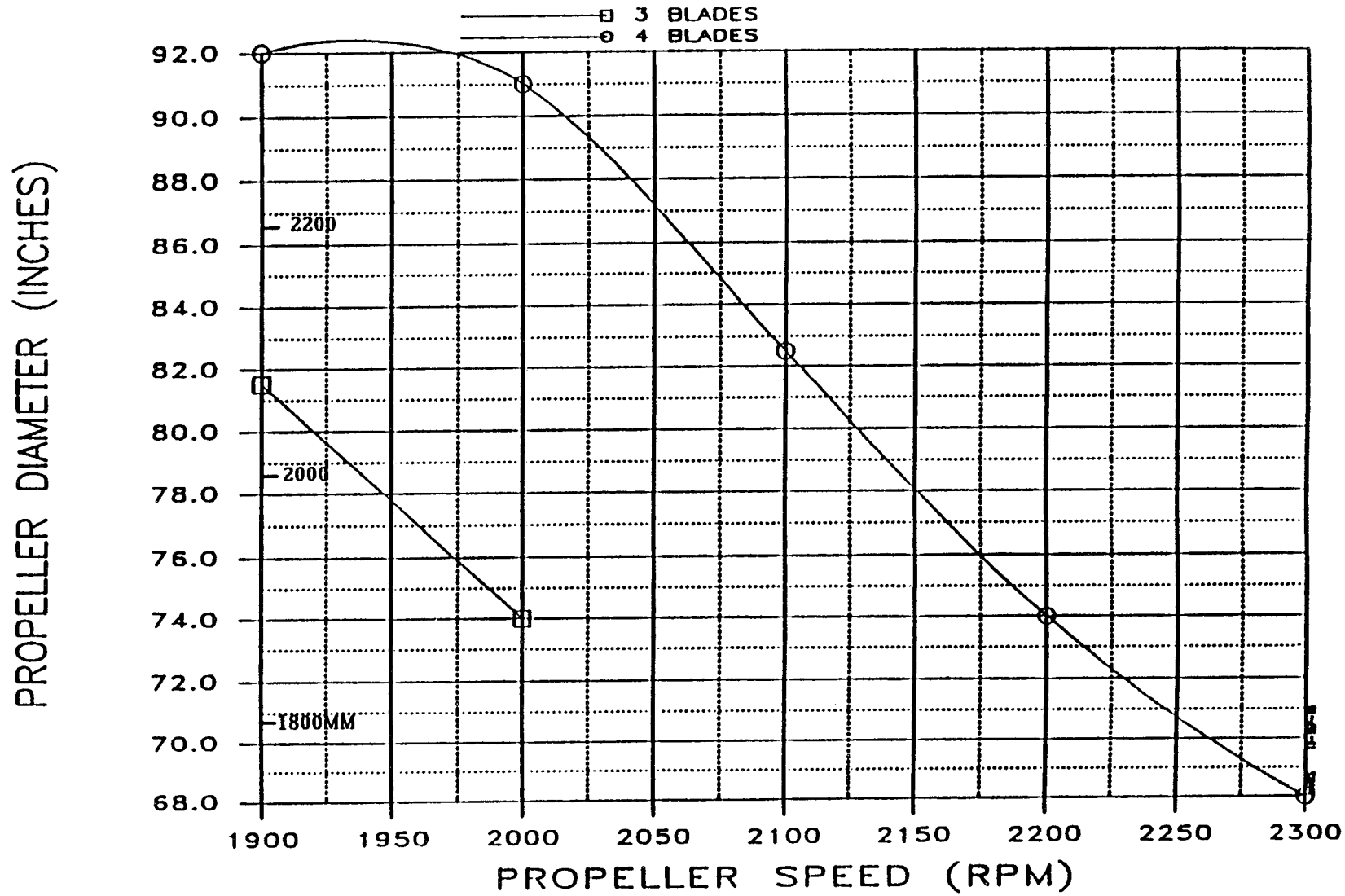


Figure No. 8

JOHN DEERE/NASA PROPELLER OPTIMIZATION
PROPELLER SIZED FOR 72 DBA FLY-OVER NOISE
TAKE-OFF, SEA LEVEL, ISA, 400SHP (300KW)
PROPELLER EFFICIENCY (ETA)
PROPELLER SPEED (RPM)
1900
1950
2000
2050
2100
2150
2200
2250
2300
0.68
0.70
0.72
0.74
0.76
0.78
0.80
0.82
3 BLADES
4 BLADES

Figure No. 9

JOHN DEERE/NASA PROPELLER OPTIMIZATION
PROPELLER SIZED FOR 72 DBA FLY-OVER NOISE
CLIMB, 25,000 FT. (7.62KM) ISA, 400SHP (300KW)

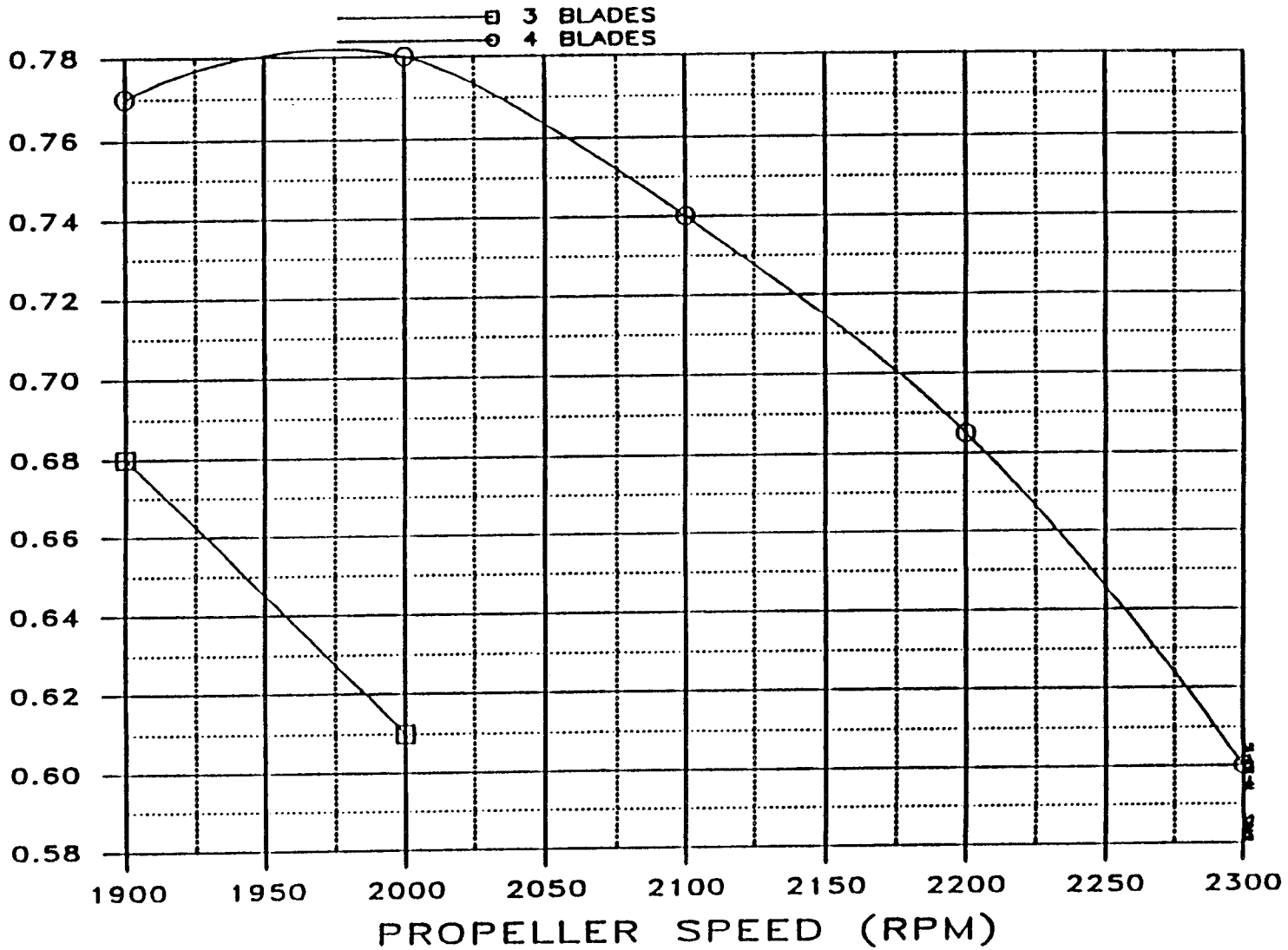


Figure No. 10

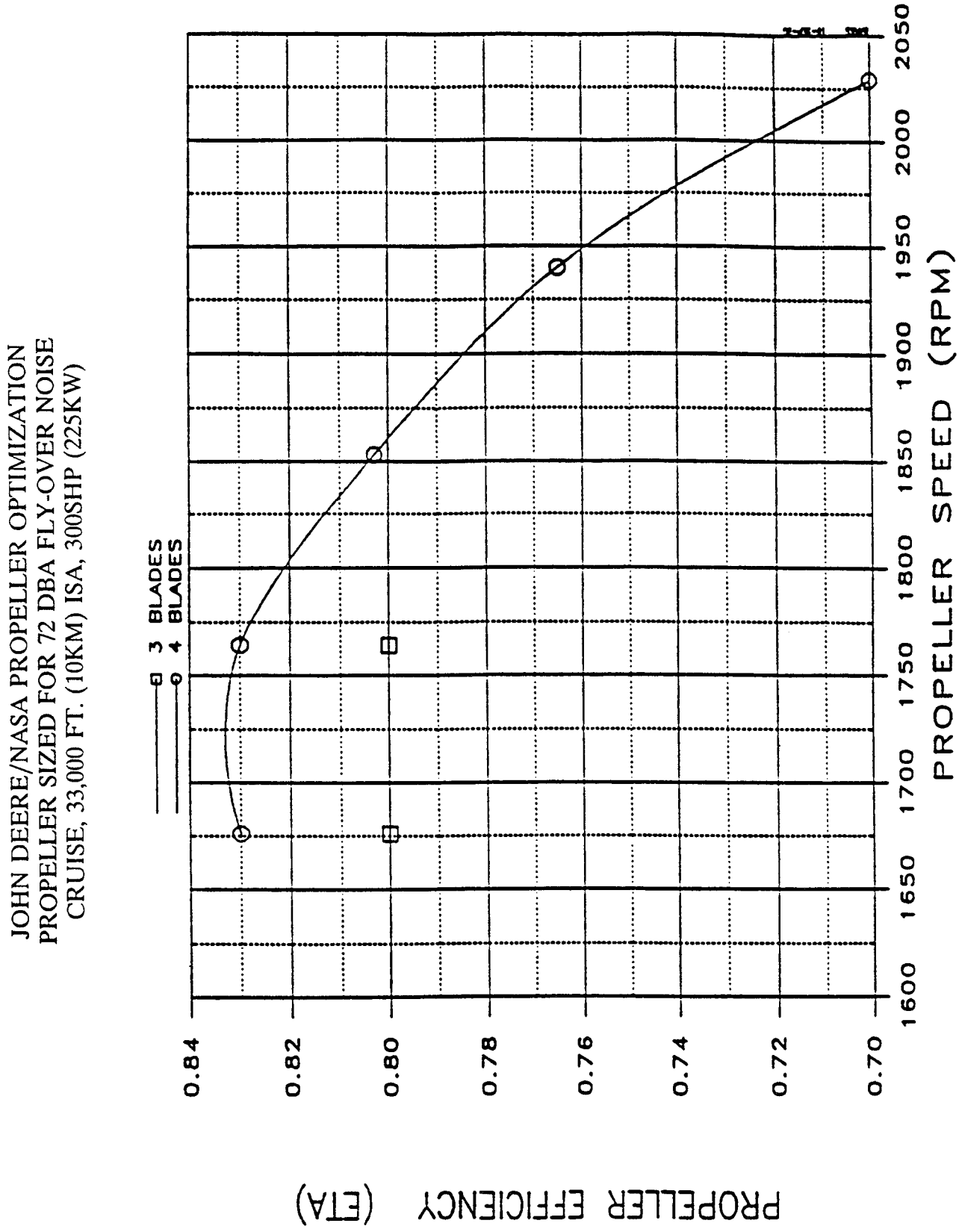

JOHN DEERE/NASA PROPELLER OPTIMIZATION
PROPELLER SIZED FOR 72 DBA FLY-OVER NOISE
CRUISE, 33,000 FT. (10KM) ISA, 300SHP (225KW)
3 BLADES
4 BLADES
PROPELLER EFFICIENCY (ETA)
0.84
0.82
0.80
0.78
0.76
0.74
0.72
0.70
1600
1650
1700
1750
1800
1850
1900
1950
2000
2050
PROPELLER SPEED (RPM)

Figure No. 11

6.0 CONTROLS SYSTEM MODEL

PRECEDING PAGE BLANK NOT FILMED

PAGE 260 INTENTIONALLY BLANK

6.0 Controls System Model

INTRODUCTION

A subcontract was placed with Douglas Aircraft Company for purposes of investigating an advanced technology automatic control system for the overall basic engine system (including management of combustion, air, coolant, lube, fuel injection, propeller and accessory systems). The activity was terminated in the initial phase, "Technology Assessment" with re-direction of the overall technology enablement program as discussed in Section 2.0 Executive Summary.

Objectives

1. Minimize fuel consumption by:

   - Integrating the control of the entire system to take advantage of coupling effects that are neglected otherwise.

   - Designing a control system that gives minimum energy performance under disturbances such as gusts, torque load or altitude changes.

2. System monitoring and protection from overspeeding or overheating.

3. Providing diagnostics and maintenance assistance by logging occurrences of operation in critical performance areas; storing the information and taking action for safe operation.

Technical Approach

The workplan defined for this task consisted of four major tasks with appropriate subtasks.

1. Technology Assessment

2. Model Development

3. control System Development

4. Reporting

The schedule and identification of subtasks is presented in Figure 1. As noted in the schedule, activity was terminated shortly after the program start.

PRECEDING PAGE BLANK NOT FILMED

PAGE 262 INTENTIONALLY BLANK

Results

1. The literature search was essentially completed in terms of identifying literature sources on rotary engine control, intermittent combustion and rotary engine modeling, multivariable control, fuel injection, ignition systems, apex seal lubrication systems, oil, coolant and fuel management systems and turbocharger control.

   - Acquired 150 Publications and Papers
   - Built Database
   - Entered Literature into Database
   - Reviewed and Documented 50% of Literature
   - Developed List of Additional Publications from References
   - Researchers Contacted
     - John Moska - University of Wisconsin
       - Engine Modelling for Real-Time Control
       - Nonlinear Control Theory Applied to Engines
     - Jeffrey Runde - General Motors, Allison Division
       - Automatic Transmission Modelling
       - Control of Automatic Transmissions

2. Discussions were held with the airframer (Beech Aircraft), the turbomachinery supplier (Sundstrand Aerospace) and the engine prime contractor (JDTI, Inc.) to acquire models and data related to the control analysis.

3. An engine system block diagram was established, Figure 2.

4. A list of controllable and measurable variables was jointly prepared with JDTI, Inc.

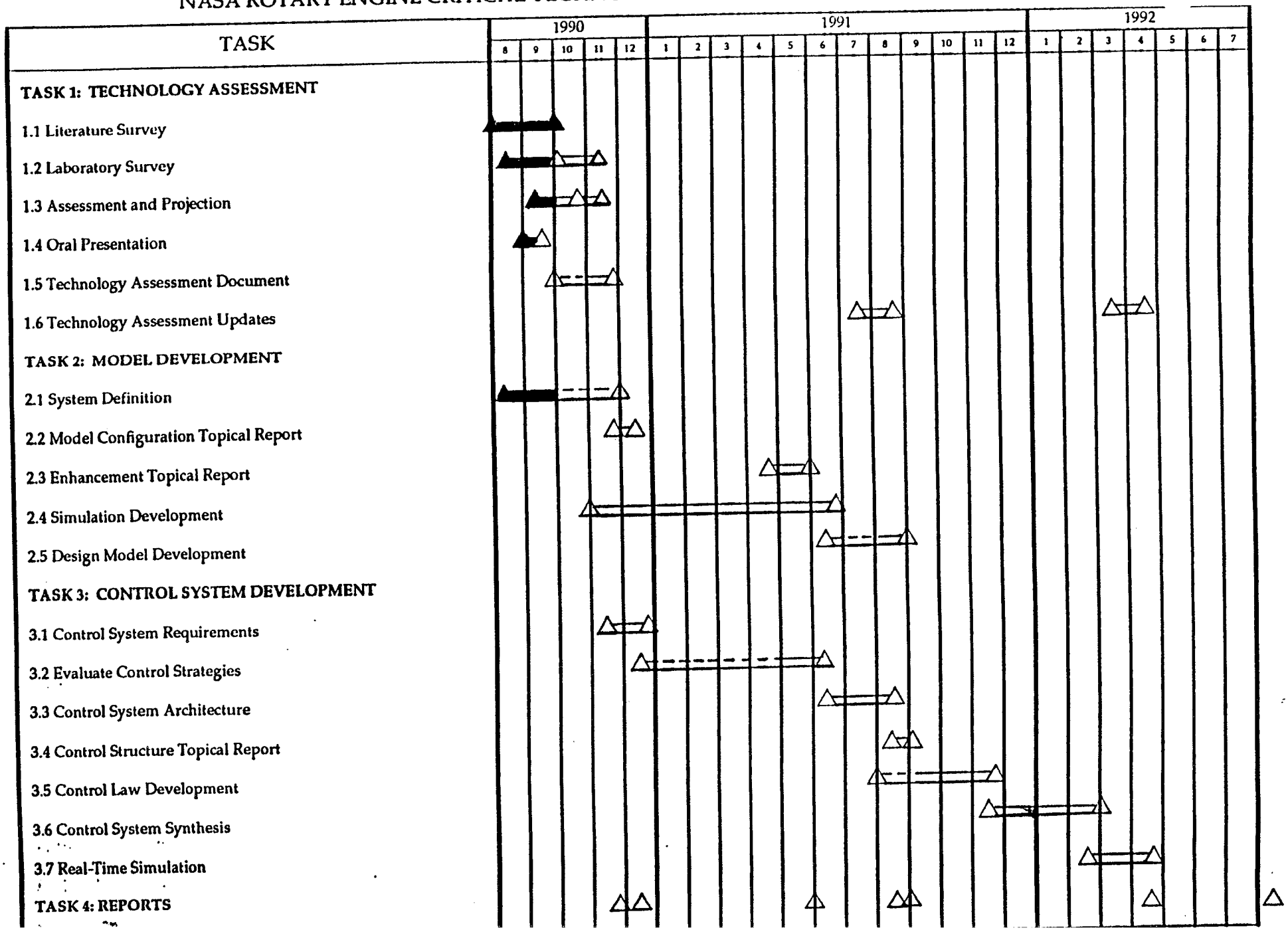
5. The MIT/Bartrand model was acquired and executed with only minor editing.

6. Simulation development was initiated.

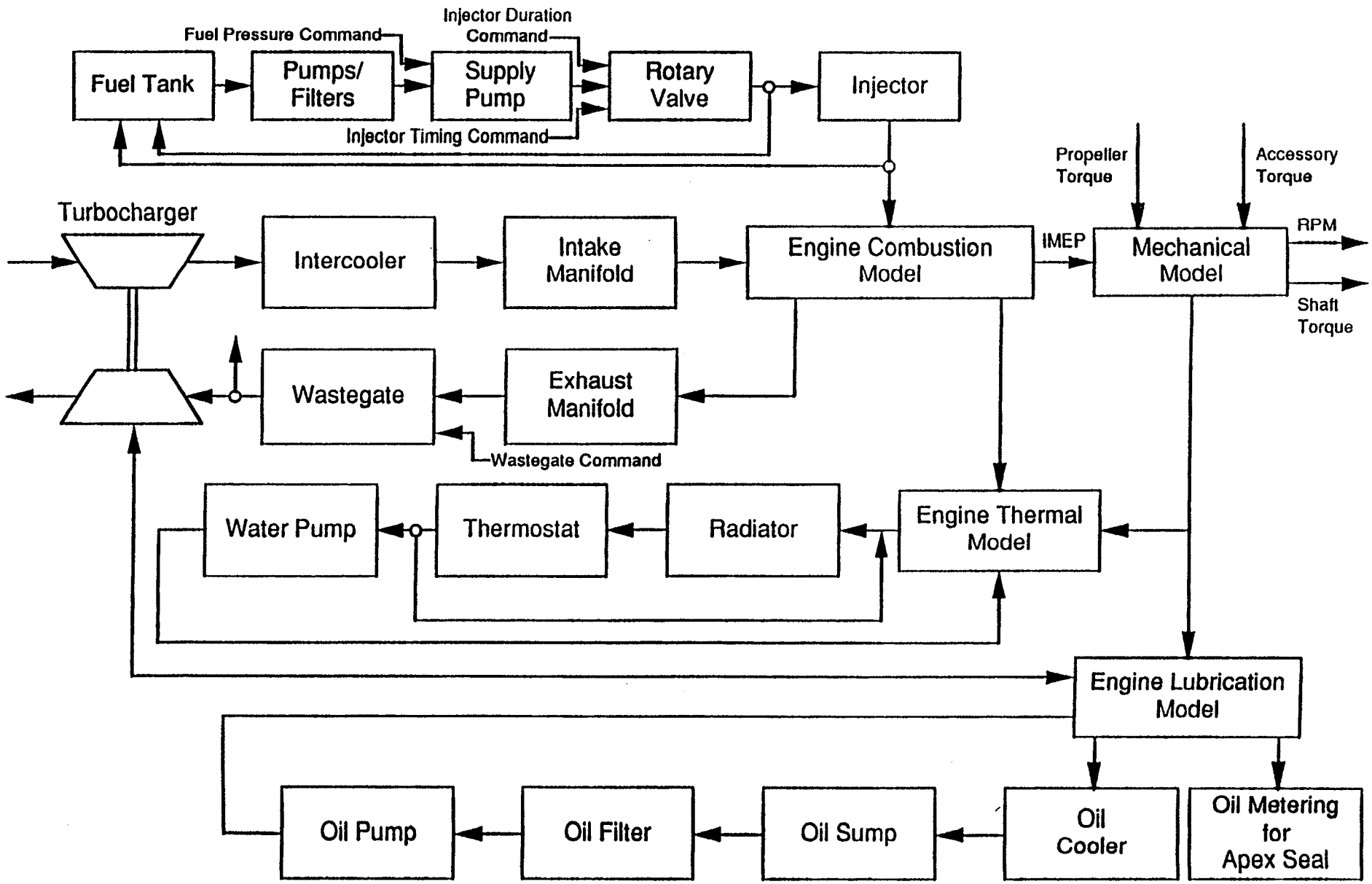
Recommendations

1. Continue to developed a simulation to describe the dynamic behavior of the Stratified Charge Rotary Engine and its subsystems. The simulation can support the development and evaluation of control laws and logic and can encompass all expected control variables, significant sensed variable and operating parameters.

NASA ROTARY ENGINE CRITICAL TECHNOL GY ENABLEMENT PROGRAM SCHEDULE



Engine System Block Diagram



7.0 TURBOMACHINERY

PRECEDING PAGE BLANK NOT FILMED

INTRODUCTION

Analytical studies of turbomachinery systems were conducted to determine the optimum overall system configuration appropriate to the critical technology enablement objectives. Primary requirements were 400 BHP (300kw) at take-off, maintained to 25,000 feet (7.57 km) and maximum cruise power (75%) maintained to 33,000 feet (10 km) altitude combined with the improved efficiency and reduced heat rejection requirements.

The task was subcontracted to Sundstrand Corporation and included asembly of component sizing and performance prediction models into a system analysis model for evaluation of candidate systems. Evaluation criteria were developed, and an optimization routine used to find the preferred configuration. The best turbomachinery configuration included a compounding turbine, which converts some of the exhaust energy to shaft power, as well as a turbocharger having two compressor stages driven by a single-stage turbine. The intake charge was intercooled between compressor stages and between the second compressor and the engine intake port. Intake manifold pressure control was effected by exhaust wastegate operations.

The System and Turbomachinery Development Task was divided into the following four subtasks:

Subtask 1 - System Analysis and Optimization.

Subtask 2 - Component and Subsystem Design

Subtask 3 - Subsystem Design

Subtask 4 - Component Verification

Subtask 1 involved analysis of various turbocharging and turbocompounding concepts and the selection of an optimum configuration.

The effort was terminated upon the completion of Subtask 1 due to redirection of the program as discussed in Section 2.0 Executive Summary.

OBJECTIVE

To identify an engine turbomachinery system capable of providing sufficient inlet air pressure boost for the Stratified Charge Rotary Engine to allow full power operation to a 25,000 foot (7.57 km) altitude, and 75 percent power for cruise up to 33,000 (10 km) feet altitude. The turbomachinery should provide the required altitude capability with minimum adverse effects upon the engine brake specific fuel consumption.

PAGE 270 INTENTIONALLY BLANK

PRECEDING PAGE BLANK NOT FILMED

TECHNICAL APPROACH

The design and sizing analysis of the turbomachinery system was divided into three phases.

1. Identify the Candidate Systems
2. Develop an Analytical Model
3. System Evaluation and Selection

The technical approach for each phase is summarized herein.

1. Identify the Candidate Systems

Models of candidate turbomachinery systems were constructed to estimate and optimize characteristics of components. These system configurations were combined into a thermodynamic analysis computer program which balances component functions and computes system parameters. A typical turbomachinery system for a rotary engine is shown in Figure 1. This system, like all systems evaluated, employs various turbine and compressor stages, heat exchangers, charge air lines, and ram air ducts. A gearbox is employed for the power turbine options. Each component type is modeled by unique component computer subroutines which predict component size and weight. Most of the routines perform heat transfer and thermodynamic analysis for the individual components.

Several types and arrangements of turbomachinery equipment were considered for the stratified charge rotary engine. The system shown in Figure 1 is an example of a simple, thermodynamically complete turbomachinery system for a turbocompounded, turbocharged engine system.

Different candidate system arrangements can be devised from this system by varying the number of compression stages, the number of turbine stages, the order in which the exhaust gases pass through the turbines, and the presence or absence of the power turbine which provides the turbocompounding.

A number of candidate system configurations were identified. Three configurations were deemed appropriate for further evaluation. These were:

1) Multiple Spool System - Composed of two conventional turbochargers, each having a single compressor stage and a single turbine stage, with intercooling after each compressor stage.

2) Multiple Stage System - Similar to the Multiple Spool System, but combines the two compressors on a single shaft driven by a single turbine.

3) Single Stage System - is similar to the above, but uses only a single stage of compression.

The three configurations were evaluated by themselves and combined with a power recovery turbine placed in the exhaust stream between the engine exhaust port and the turbocharger turbines. The power recovery turbine provides the turbocompounding effect by extracting excess power from the exhaust and adding it to the engine output shaft through a gearbox. Preliminary analysis indicates that there is significant gas power available for turbocompounding, and that this function may be necessary to achieve the engine BSFC goal. The three candidate systems selected are shown in Figure 2.

In Figure 3 are shown four other schematics which were proposed but discarded for various reasons. The first configuration is like the basic multiple spool configuration, but uses an additional valve to control the compressor flow split. This causes additional compressor matching problems without adding any performance to the system. The second schematic, REDIV Alternate 2, suggests using a variable geometry turbine instead of wastegate control and an axial/centrifugal compressor. This is thermodynamically equivalent to the multistage turbocharger at design operation, which is the only operating condition analyzed to date. Some operational (off-design) advantages may accrue from using variable geometry instead of wastegate control. Controls would be more complex, and development would be necessary. The three equal turbocharger schematic was proposed as a potential approach for constructing a ground test article to demonstrate thermodynamic performance. The additional pieces of hardware and plumbing would make it impractical for aircraft installation. The alternate turbocompound schematic illustrates the potential for positioning the power turbine last in the exhaust, instead of first. This is suggested in the literature as a technique for improving engine throttle response, because it tends to maintain turbocharger turbine pressure ratios at a more constant level. However, it also eliminates the increase in turbocharger output with increasing altitude, which is an absolute must for the aircraft engine.

2. Develop the Analytical Model

A turbomachinery system model was developed to predict the performance characteristics of each of the candidate systems. Each element within each candidate system was characterized in terms of weight, volume and performance. The system elements modeled include the turbines and compressors, heat exchangers, air ducts, exhaust pulses and gearbox. A separate system model was prepared for each of the three candidate systems.

The system analysis modeling program calculates candidate system operating conditions and provides an optimization routine. A system schematic with various configuration options is shown in Figure 4. The analysis program calculates system state points (temperature, pressure, and flow rate) at the numbered locations shown in Figure 4. The calculated state points are based on the input design conditions, design constraints, and the current values of optimization parameters. The system model then calls the various component sizing models to size the components based on the calculated state points.

An equivalent power function is calculated for each candidate system. The equivalent power function is evaluated from the resultant values (from the system analysis) of engine exit pressure, power turbine power, incurred drag and fixed weight. The equivalent power predicts the usable power (net power) supplied to the airframe.

An optimization routine is included in the system analysis computer program. The optimization routine varies the system optimization parameters until the equivalent power is maximized. A flow chart of the system model analysis program is provided in Figure 5. The system model thus maximizes equivalent power for each candidate system. Comparison of equivalent power calculated for each candidate system enables selection of a "best" turbomachinery system configuration.

3. System Evaluation and Selection

The final system evaluation and selection process encompassed the following three steps:

a. Identify the design conditions

b. Establish the optimization criteria

c. Establish parametric factors affecting system optimization criteria.

A synopsis of the above three steps is provided in the following paragraphs.

a. Identify the design conditions

Evaluation of the turbomachinery candidate systems requires establishing design conditions which constrain the system operation. The basis for the system evaluation selected is the specified full power output operation capability at 25,000 foot (7.57 km) altitude (25,000 feet (7.57km) climb). The design conditions established for the 25,000 foot (7.57 km) climb are listed in Table 1. A secondary set of assumed physical design constraints were established for the air handling ducts. These assumed design constraints are listed in Table 2. Further discussion of development of the design

condition (especially conditions downstream of the propeller wash) are provided in reference 1.

b. Establish the Optimization Criteria

Optimization of the turbomachinery system by the selected mathematical system analysis requires an objective function which varies smoothly with the independent system parameters. The turbocharger system imposes three penalties on the airframe and engine. These penalties are the system's fixed weight, the drag incurred by the ram air cooled heat exchangers, and the back pressure imposed at the engine exhaust. An optimization algorithm must balance the benefits of increased propulsive power or efficiency provided by the turbomachinery against the penalties incurred. The ram drag of the system, drag due to lift incurred by system weights, engine power changes due to exhaust pressure changes, and power turbine power contributions can all be combined into a single expression for net output power due to the turbomachinery system.

The NASA contract for development of the stratified charge rotary engine set goals for power, weight, and fuel consumption of the entire system. However, allotments for the turbomachinery were not specified, nor was any guidance provided in evaluating system tradeoffs. The "best" turbomachinery for the purposes of this contract will therefore be the one which maximizes installed thrust minus drag.

The net effect of the turbomachinery system on engine shaft power available for propulsion is obtained by converting net drag to a (negative) thrust power and adding this value to the net power. The final expression of equivalent power provides the numerical basis for evaluation of the candidate systems.

Table 1
Design Conditions
25,000 ft. (7.57km) climb

Ambient	
Pressure	5.46 psia (37.62 kPa)
Temperature	6.71° F (-14° C)
Mach number	0.267
Downstream of Propeller	
Pressure (Psia)	5.84 psia (40.2 kPa)
Total Temperature	16.14 ° F (-8.8° C)
Mach number	0.311
Engine air requirements	
Inlet temperature	140.00 ° F (60° C)
Inlet flow rate	70.55 lbm/min (32 Kg/Min)
Inlet Pressure	34.90 psia (240 kPa)
Exit temperature	1154.00 ° F (623° C)
Exit flow rate	72.84 lbm/min (35 Kg/min)
Engine parameters	
Propeller efficiency	0.83
Displaced volume	0.046 ft^3 (.0013m^3)
Engine Speed (rpm)	8500.00
Exit pressure for 400 HP (300kw)	30.60 psia (211 kPa)
Aircraft lift over drag	11.20

Table 2
Assumed Design Constraints

Charge Air Ducts	
Compression side	
Length	5.00 ft (1.52m)
Material	Al
Wall thickness	0.03125 in. (.794mm)
Density	172.80 lbm/ft^3 (2.19 kg/m^3)
conductivity (Btu/hr ft ° F)	110.00
Expansion side	
Length	3.00 ft (0.91m)
Material	Steel
Wall thickness	0.03125 in (0.79mm)
Density	499.50 lbm/ft^3 (6.34 kg/m^3)
Conductivity (Btu/hr ft ° F)	8.67
Insulation	
Density	11.90
Conductivity (BTU/hr ft ° F)	0.10
Inlet and Exit	
Inlet diffuser half angle (deg)	10.00
Exit nozzle half angle (deg)	10.00
Ratio of nozzle exit to freestream momentum	1.0
Heat loss to surroundings	
Heat transfer coefficient (Btu/hr ft^2 ° F)	2.0
Ram air heat exchanger cooling duct	
Inlet diffuser half angle (deg)	10.00
Angle of exit flow relative to free stream	0.00

c. Establish Parametric Evaluation Factors

Nine parameters have been identified which affect the optimization function, as well a: penalty factors of weight, drag, and engine exhaust pressure. Some parameters affect one or two of these penalty factors. The optimization parameters are listed below along a description of the penalty factors they affect.

1.	First stage compression ration	affects system weight and engine exit pressure (net power); affects heat exchanger size which has only slight effect on incurred drag
2.	Intercooler charge air exit temperature	same effects as above
3.	Inter/aftercooler charge air side pressure drop	trades heat exchanger weight against engine exit pressure (net power); affects heat exchanger size which has only slight effect on incurred drag
4.	Duct mach number	trades duct weight against engine exit pressure (net power); no effect on incurred drag
5.	Power supplied to prop shaft from power turbine	affects power turbine weight (and system weight slightly) and engine exit pressure (net power); no effect on incurred drag
6.	Expansion side duct insulation thickness	trades weight of insulation against engine exit pressure (net power); no effect on incurred drag
7.	Inter/aftercooler air side pressure drop	trades weight of heat exchangers against ram air drag; no effect on engine exit pressure (net power)
8.	Intercooler air flow rate	trades weight of heat exchangers against ram air drag; no effect on engine exit pressure (net power)
9.	Aftercooler air flow rate	trades weight of heat exchangers against ram air drag; no effect on engine exit pressure (net power)

ORIGINAL PAGE IS
OF POOR QUALITY

The effects of each of the optimization parameters was examined individually. Several were found to have optima which fell into narrow ranges and could be fixed for system optimization studies.

The dual stage turbocharger system (two compressor stages driven by one turbine stage) was used for evaluating the effects of insulation thickness, pressure ratio split, intercooler charge air exit temperature, and air side pressure drop and flow rate through the intercooler and aftercooler on net drag, net power and equivalent power. Turbocompounding was not included, inter/aftercooler charge air side pressure drop was set to 0.125 psid, and duct Mach number was set to 0.175 for this set of optimization studies.

Insulation Thickness:

As insulation is added to the exhaust ducts, less thermal energy is lost and lower engine back pressure is required to drive the turbines, resulting in a net power increase. However, duct weight and net drag increase. The net effect is for equivalent power to drop as insulation thickness is increased. Therefore, insulation thickness is set to zero since this leads to maximum equivalent power.

Compressor Pressure Ratio Split:

Over a wide range of the other optimization parameters, the first stage compression ratio (Pr) is optimal between 3.6 and 3.8 for maximum equivalent power. Pressure ratio was, therefore, fixed at 3.7.

Ram Air Heat Exchanger Pressure Drop:

As intercooler and aftercooler air side pressure drop (ΔPc) increases, heat exchanger weight decreases but ram air drag increases. Only net drag is effected. A value of ΔPc of 0.1 psid was found to be optimal for minimum net drag.

Intercooling:

The intercooler charge air exit temperature was examined for its effect on net power, net drag, and equivalent power. For each exit temperature the inter/aftercooler ram air flow rates are optimized for minimum net drag. Over an exit temperature range from 140.0° F to 210.0 ° F (60 to 99 ° C), the resultant equivalent power is constant within 0.7%. The charge air exit temperature is set to 150.0° F (66° C) since it yields high net power. The intercooler and aftercooler flow rates for which net drag is minimized for the 150.0° F (66° C) exit temperature are 53.3 and 54.7 lbm/min (24.2 and 24.8 kg/min) respectively.

Charge Air Heat Exchanger/Duct Pressure Drop:

The optimal values of intercooler/aftercooler charge air pressure drop, duct mach number, and turbocompounding power remain to be determined. The previously discussed optimization parameters will remain fixed for this analysis. The power turbine is placed upstream of the turbocharger as this minimizes power turbine weight with little effect on the turbocharger. Normalized parameters for heat exchanger pressure drop and Mach number were utilized to allow varying the two parameters together systematically. Normalized pressure drops from 0.05 to 0.25 psid (0.34 to 1.72 kPa) and normalized Mach numbers from 0.10 to 0.30 were examined. As the pressure drop and Mach number increase the heat exchangers and duct weights decrease, which result in a net drag decrease. However, power must be expended to overcome the increased charge air pressure drops, and thus net power is decreased. The resultant equivalent power curves, shown with net power and net drag curves in Figure 6, are nearly flat with a slight maximum between 25 and 50% of the pressure drop range. The equivalent power decreases at higher pressure drops. thus values of 0.125 psid (0.86 kPa) and 0.175 Mach number are chosen for charge air pressure drop and duct Mach number respectively.

Power Turbine Power:

Power turbine power is indicated by the coding numbers on the curves, in tens of horsepower (e.g., the curve having the numeral "4" embedded in it indicates a fixed power turbine power of 40 horsepower). With increasing power turbine power, net power increases. Net drag at first increases; there is a jump in weight, and thus in net drag from zero power (no turbine or gearbox) to finite power output. Then net drag decreases as increasing power turbine pressure ratios (at fixed flow) result in faster, smaller turbines. Equivalent power decreases with the initial addition of hardware between zero and non-zero turbine power, then increases. Net and equivalent power increase monotonically with increasing power turbine power, seemingly indicating very large power availability. However, there is probably a practical limit at back pressures sufficiently high (exhaust pressures near engine inlet pressure) to cause engine scavenging difficulties. The inlet and exhaust pressures specified by REDIV (34.9 and 30.6 psia (240 and 211 kPa), respectively) are shown on the net power plot. they show a practical power turbine maximum design power to be in the 50-60 horsepower (37.5-45 kw) range (with NO pulse effects), with resulting equivalent power of 35-40 horsepower (26.2-30kw).

Figure 7 shows the effect of ΔP_{hx} and M_d, again using the parameter k, at various levels of turbocompounding power, on net drag, net power, and equivalent power with initial estimates of pressure pulse effects included. The trends are the same as those with pressure pulse effects neglected, however the levels of available power turbine power are increased to 65-80 horsepower (48.7-60kw). Both net power and equivalent power are increased by 15-20 horsepower (11.25-15 kw) by pulse effects. (Although incomplete, the pressure pulse analysis indicated that even higher turbine powers should be available with pulse recovery.)

In summary, the power turbine analysis shows equivalent power gains of 35 horsepower (26.2 kw) (minimum, steady flow) to 60 horsepower (45 kw) (maximum, initial pulse analysis), or more. These gains represent recovery of 12-20 percent of the rotary engine shaft power from its wasted exhaust energy; inclusion of the power turbine in the optimum system would seem to be mandatory. Some further pulse analysis, in conjunction with installation design, is needed to quantify the achievable turbocompounding benefit.

RESULTS

The system analysis program was used to characterize the three candidate systems previously shown in Figure 2. These systems are the multiple spool, multistage, and single stage turbochargers, each in a system utilizing a power turbine upstream of the turbocharger(s) for turbocompounding. The calculated equivalent powers for the three optimized systems are shown in Figure 8.

The dual stage configuration leads to the highest value of equivalent power by a modest amount (16 percent higher than that of the dual spool). The single stage system, expected to be potentially the best, falls midway between the others. Relative to the dual stage configuration, the single stage system suffers from somewhat poorer thermodynamic performance (no intercooling) as well as high aftercooler weight resulting from the need to use steel materials at the high compressor outlet temperature.

Since the equivalent power does not indicate a clear advantage for one of the configurations, others factors, such as reliability, cost, off design performance, should be considered. Table 3 lists some of the other advantages and disadvantages of the three configurations.

Table 3

System Configuration Tradeoffs

Dual spool	-	Largest regions of shaft speed where speed match is possible. Allows each turbine and compressor to be run at near optimal speed for best efficiency.
	-	Lowest engine back pressure
	-	Good performance range for off-design operation
	-	Most complex, highest weight
Dual stage	-	Smaller region of shaft speed where speed match is possible. More difficult to get all turbomachinery elements to optimal speed for best efficiency
	-	Good performance range for off-design operation
	-	Low engine back pressure
	-	Simple and low weight
Single stage	-	Simple and low weight
	-	High engine back pressure
	-	Narrower performance range for off-design operation
	-	Very narrow region of shaft speed where speed match is possible. May not be possible to get both wheels to optimal speed for best efficiency
	-	High compressor and turbine tip speeds (high stress)

CONCLUSIONS

1. The dual stage turbocharging configuration with an upstream turbocompounding (power) turbine is preferred for its high equivalent power, good off-design operating performance range, and reasonable simplicity. The recovery of pulse power leads to substantial increases in power turbine output, so the system should be designed to fully utilize this power. The power turbine can provide at least 60 to 80 hp (45 to 60 kw), while keeping the engine back pressure between 30.6 psia and 34.9 psia (211 and 240 kPa).

2. The selected turbomachinery system configuration incorporates a turbocharger consisting of two compressor stages and one turbine stage on a single shaft, intercooling after each compressor stage, and a compounding turbine upstream of the turbocharger (at the engine exhaust). The system is estimated to weigh 206.50 lbm (93.66 Kg), to impose a net ram drag of 5.05 lbf (22.46N) on the aircraft, and to produce 49.4 hp (37 kw) of shaft power through turbocompounding (increasing engine output).

3. The contract for development of the SCRE turbomachinery system set goals for power output, weight and fuel consumption of the entire engine system. Allotments for the turbomachinery system were not known, nor was any guidance provided for establishing priorities among available design tradeoffs. Re-evaluation of the engine total system and turbomachinery priorities may result in selection of a different configuration for the turbomachinery system.

RECOMMENDATIONS

Additional analytical efforts are needed to better quantify exhaust pulse effects, which apparently will significantly affect turbomachinery sizing and power output. Additionally, an off-design system analysis should be performed to learn how the proposed system configuration(s) perform at lower altitudes and lower throttle settings. These conditions will determine control schedules and may have an impact on proper turbomachinery matching.

REFERENCE

Volume II, Appendix C

Engineering Report, "Turbomachinery System Analysis For Stratified Charge Rotary Engine Critical Technology Enablement", R.O. Brennan, Sundstrand Aerospace Corporation, 4 October 91.

LIST OF FIGURES

FIGURE 1 TURBOCOMPOUND ENGINE

FIGURE 2 TURBOCOMPOUND CANDIDATE SYSTEMS

FIGURE 3 ALTERNATE CANDIDATE SYSTEMS

FIGURE 4 TURBOMACHINERY SYSTEM STATE POINTS

FIGURE 5 SYSTEM ANALYSIS PROGRAM FLOW CHART

FIGURE 6 EFFECT OF CHARGE AIR PRESSURE DROP (NO PULSE EFFECTS)

FIGURE 7 EFFECT OF CHARGE AIR PRESSURE DROP (WITH PULSE EFFECTS)

FIGURE 8 SYSTEM COMPARISON

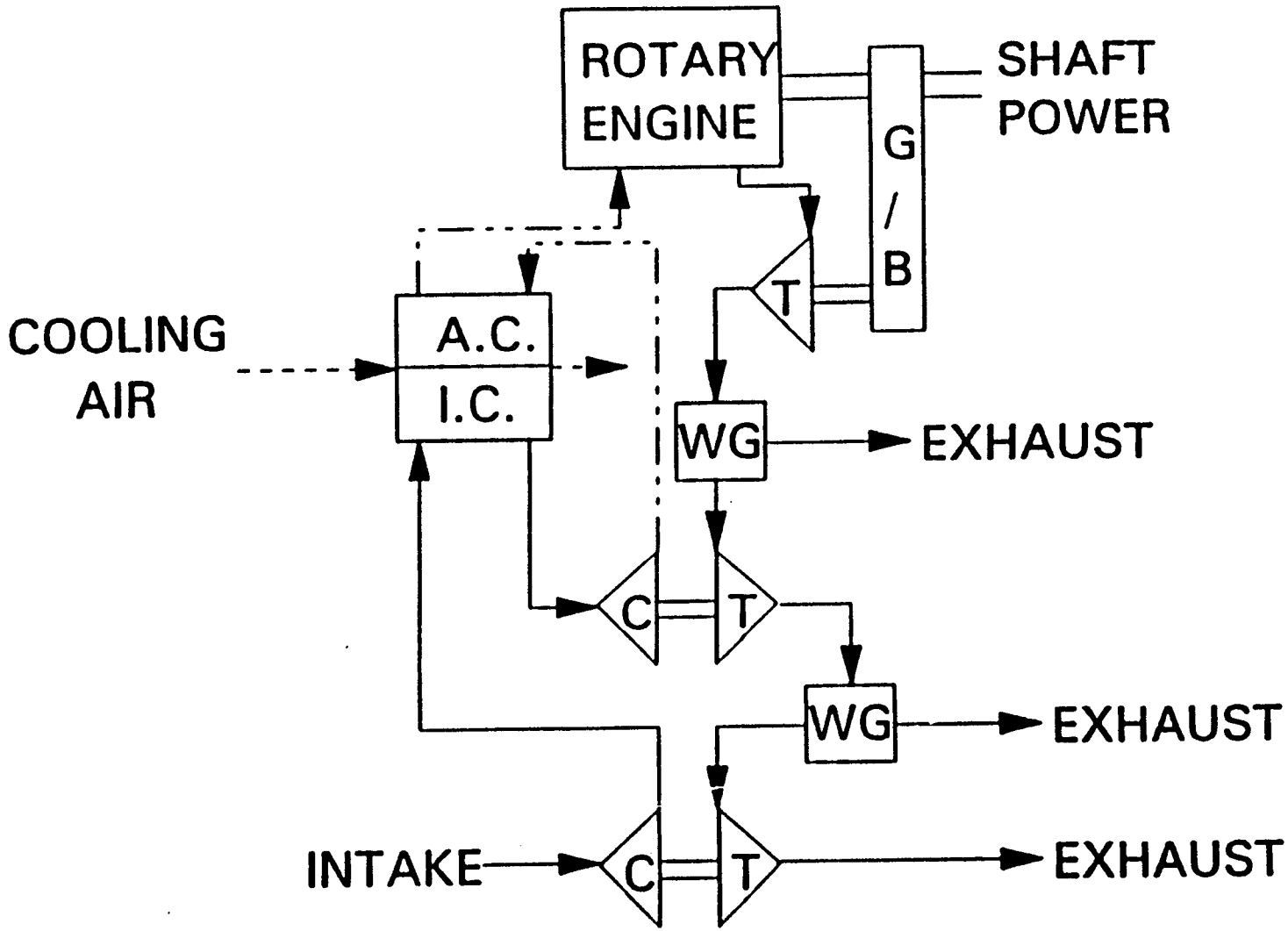
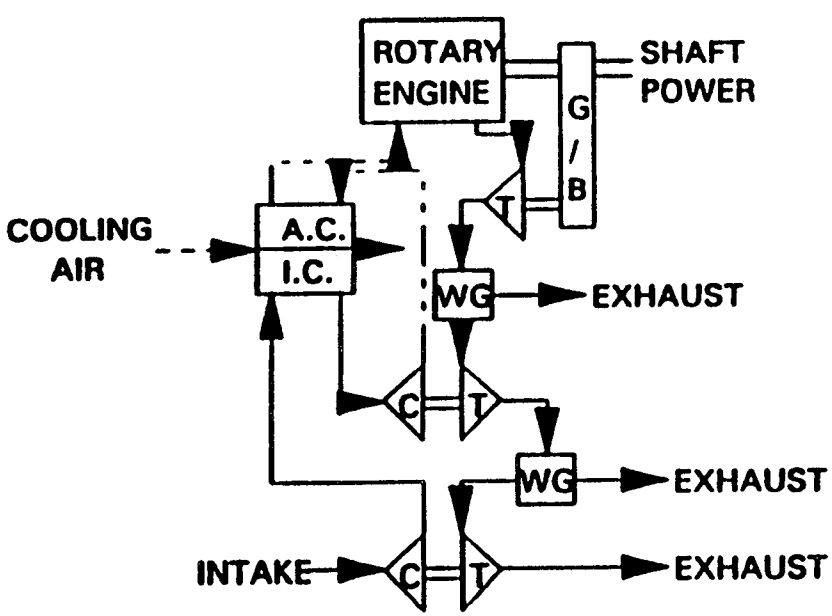
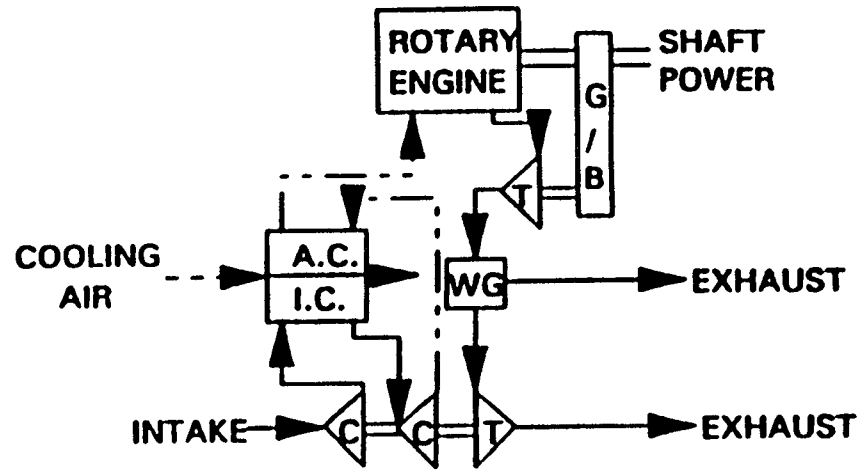


FIGURE 1. TURBOCOMPOUND ENGINE

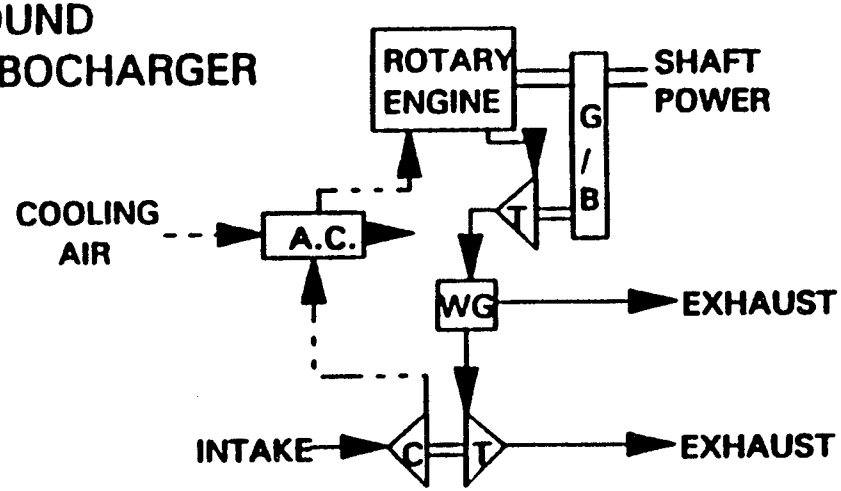
Figure No. 1



TURBOCOMPOUND
MULTIPLE SPOOL TURBOCHARGER



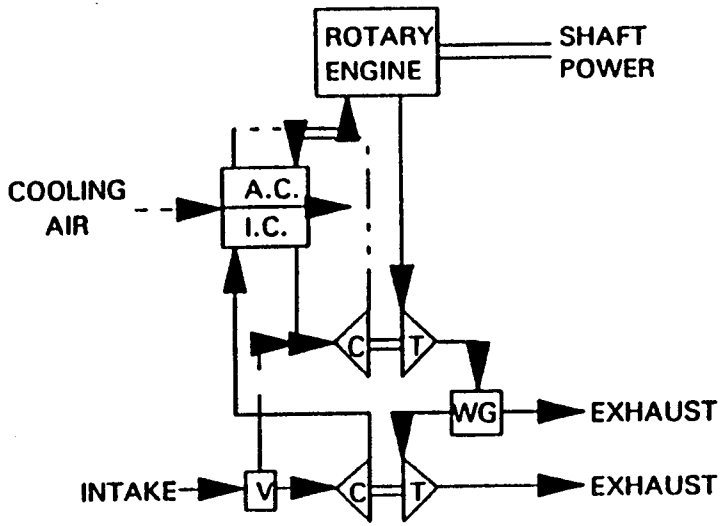
TURBOCOMPOUND
MULTIPLE STAGE TURBOCHARGER



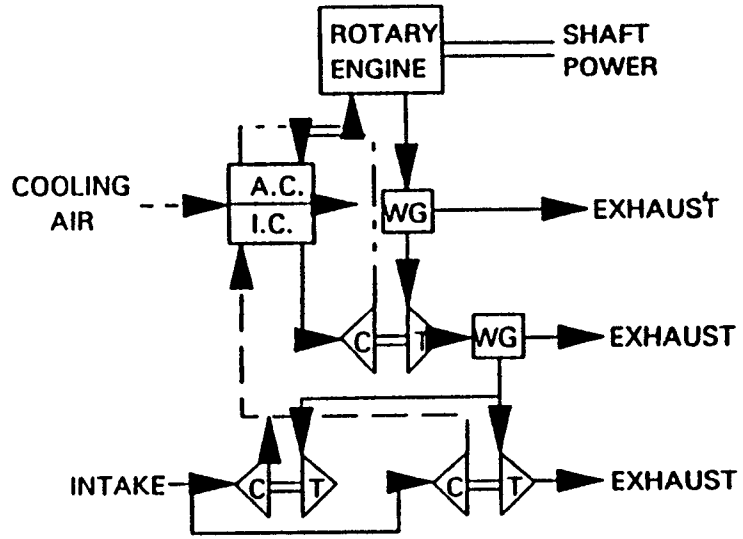
TURBOCOMPOUND
SINGLE STAGE TURBOCHARGER

TURBOCOMPOUND CANDIDATE SYSTEMS

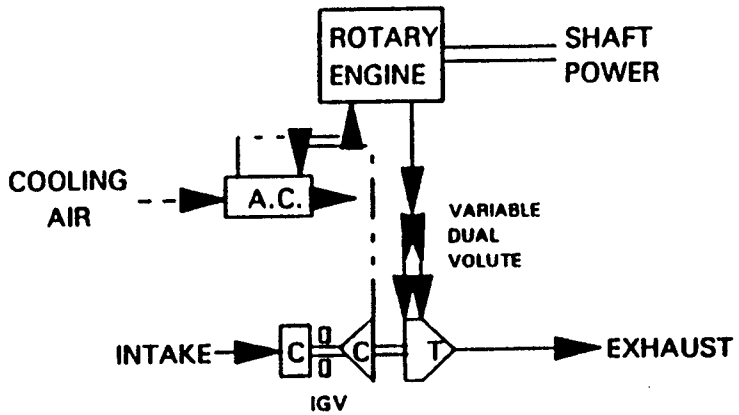
Figure No. 2



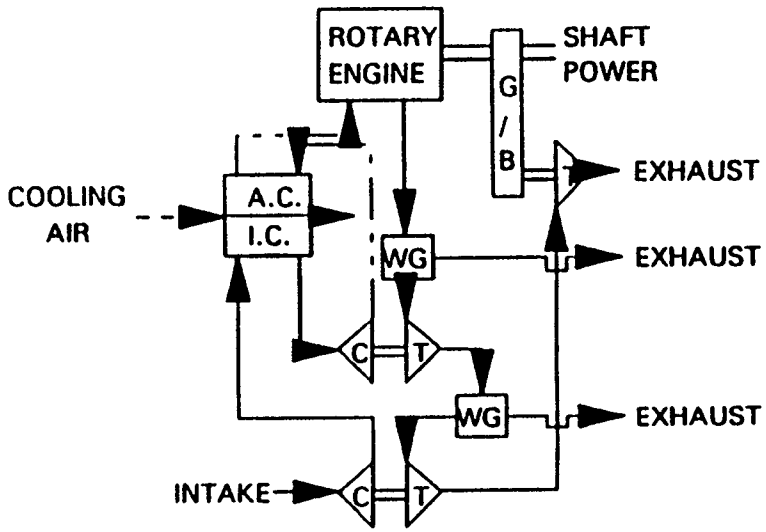
REDIV ALTERNATE 1



3 EQUAL TURBOCHARGERS



REDIV ALTERNATE 2



ALTERNATE TURBOCOMPOUND ENGINE

Figure No. 3

ALTERNATE CANDIDATE SYSTEMS

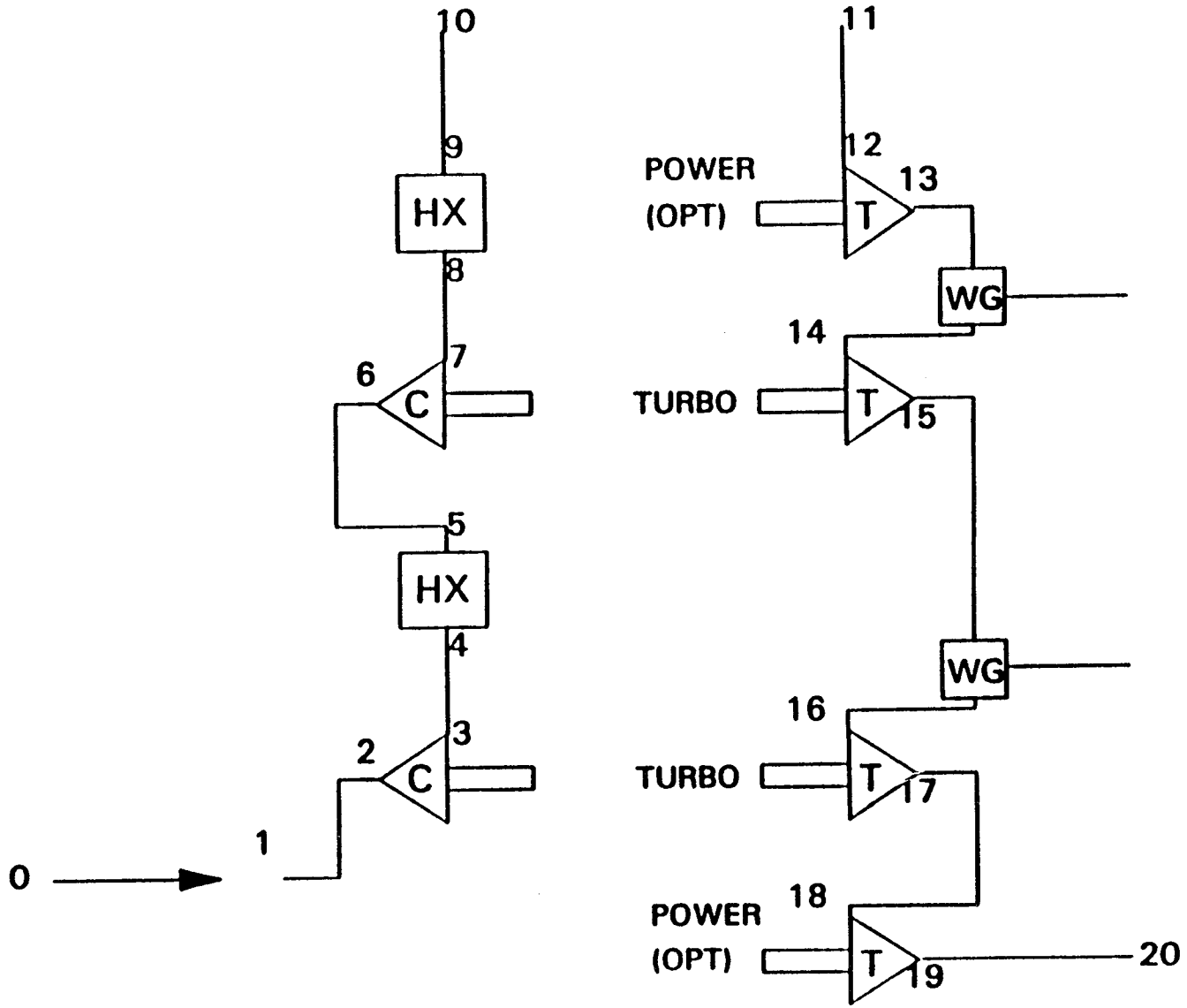


Figure No. 4

TURBOMACHINERY SYSTEM STATE POINTS

Figure No. 5

SYSTEM ANALYSIS PROGRAM FLOW CHART

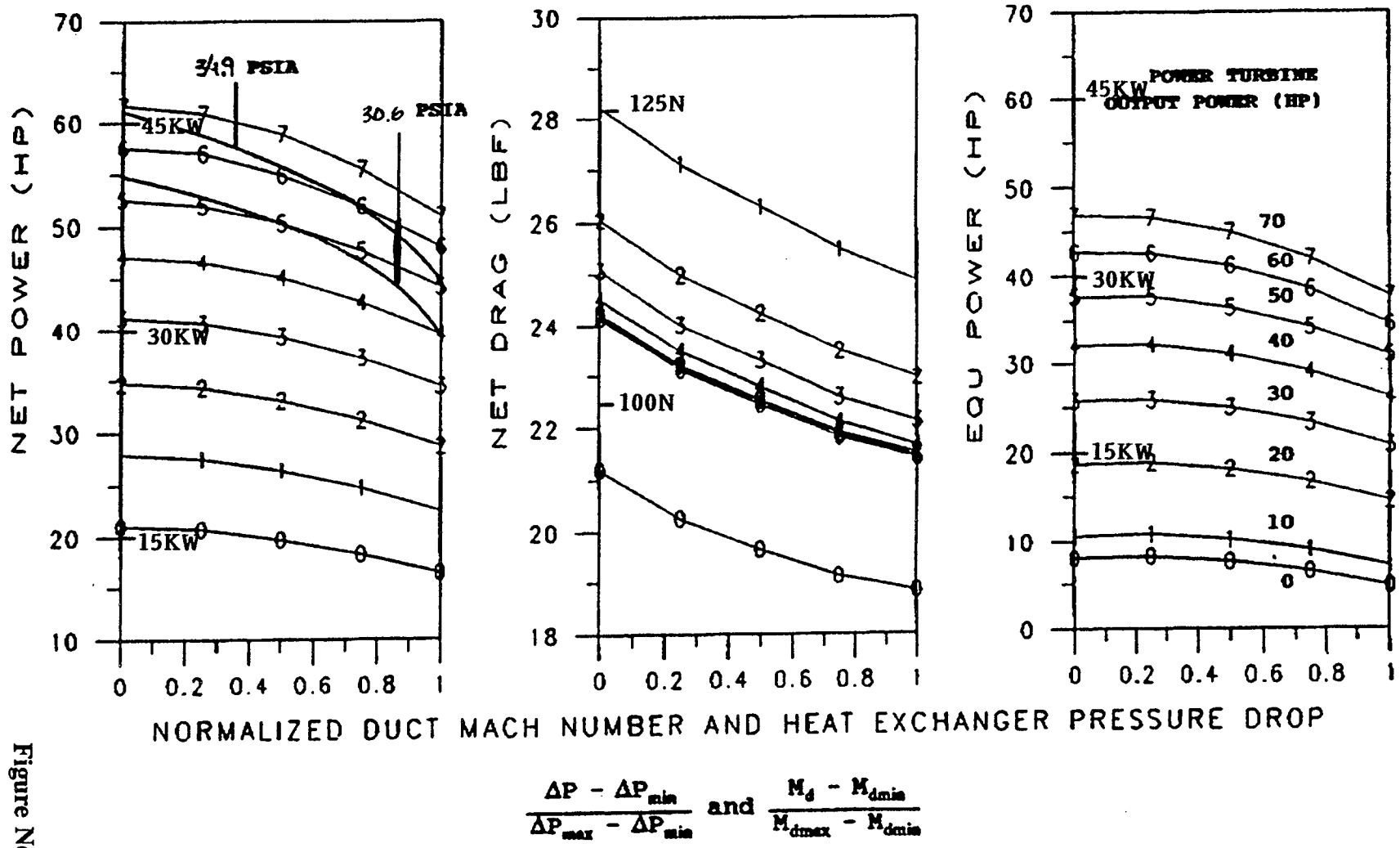


Figure No. 6

EFFECT OF CHARGE AIR PRESSURE DROP (NO PULSE EFFECTS)

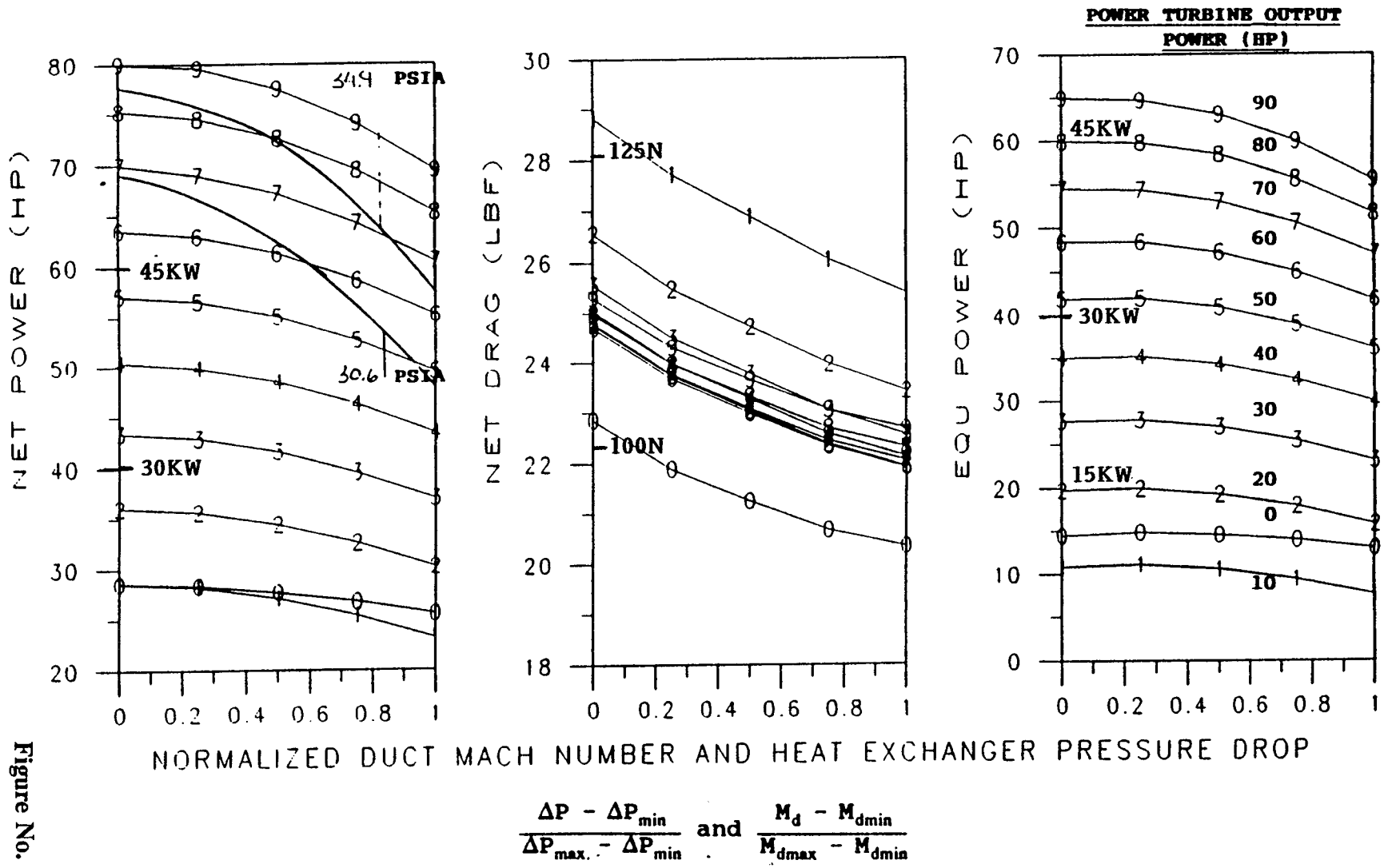


Figure No. 7

EFFECT OF CHARGE AIR PRESSURE DROP (WITH PULSE EFFECT)

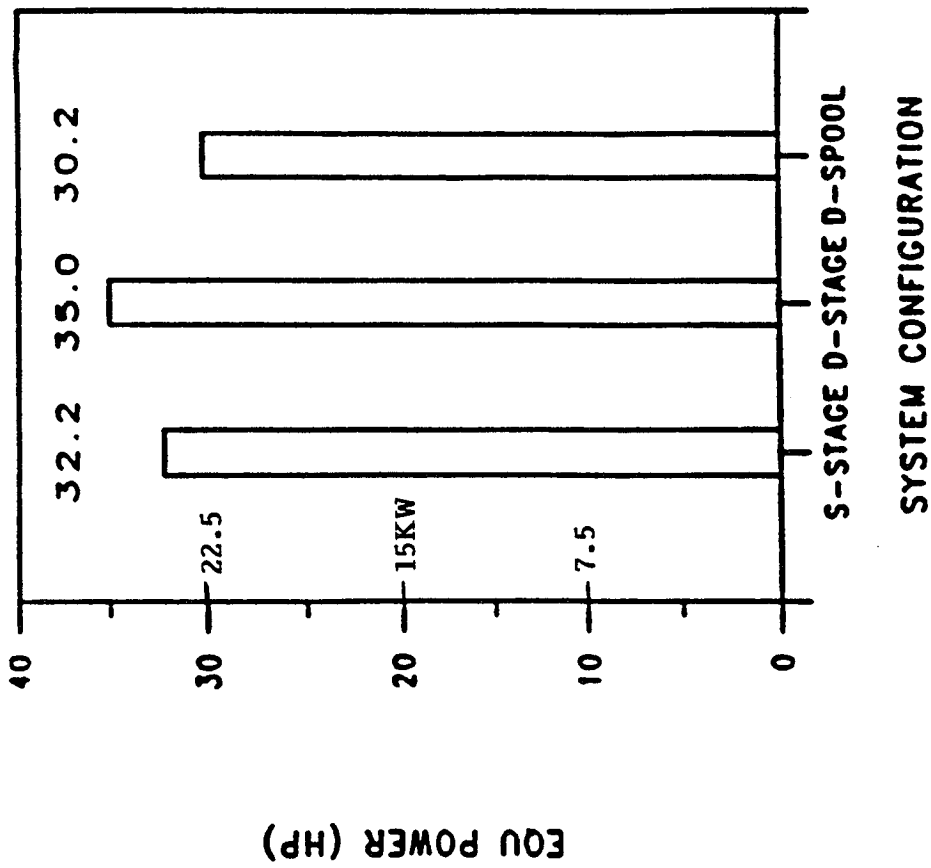

SYSTEM COMPARISON
SYSTEM CONFIGURATION
S-STAGE D-STAGE D-SPOOL
EOU POWER (HP)
40
30
20
10
0
22.5
15KW
7.5
32.2
35.0
30.2

Figure No. 8

8.0 UNIVERSITY COORDINATION

THIS PAGE BLANK NOT FILMED

INTRODUCTION

During the time period of this program basic research o rotary engines were being carried out at Carnegie-Mellon University, Michigan State University, Princeton University and at Sverdrup Technologies. This work complemented the development work at John Deere Technologies International. The basic work was analytical (at Carnegie-Mellon, Princeton and Sverdrup) and experimental (at Michigan State University). References 1-9 are publications which illustrate the nature of the work at these places. The work at Princeton is covered separately in Section 3.2 and Appendix A of this report.

OBJECTIVES

The objectives of this task were:

1. Coordinate the work at these different centers so that analytical and experimental studies would complement each other; and

2. Transfer information when applicable to more applied critical technology enablement efforts including research rig engine testing for confirmation and correlation.

TECHNICAL APPROACH

A 'Rotary Engine Research Coordinating Committee' which had been established during phase II of the NASA program was the main forum for exchange of technical information. Meetings were held bi-annually in different locations. Two meetings were held in 1990 (the first at NASA and the second at Michigan State University). A third meeting was held in May 1992 at John Deere Technologies International. At these meetings the latest analytical and experimental results were presented and discussed. The experimental program was set up so that in addition to obtaining fundamental information regarding rotary engine flowfields, results could be used to validate the computer codes. Results from the use of the computer codes are presented in Section 3.2, and in the references listed herein..

RESULTS

The University coordination conducted during this program permitted an open exchange of ideas and directions in analytical and experimental efforts. These exchanges resulted in a more focused multi-pronged thrust toward improving combustion and airflow condition contributing to higher efficiencies.

PRECEDING PAGE BLANK NOT FILMED

PAGE 294 INTENTIONALLY BLANK

CONCLUSIONS

The university coordination was complementary to the experimental research conducted in this program and permitted the utilization of advanced theoretical and experimental technologies.

REFERENCES

1. Hamady, F., Stuecken, T. and Schock, H., "Airflow Visualization and LDV Measurements in a Motored Rotary Engine Assembly part 1: Flow Visualization," SAE Paper No. 900030.

2. Chouinard, E., Hamady, F. and Schock, H., "Airflow Visualization and LDV Measurements in a Motored Rotary Engine Assembly Part 2: LDV Measurements," SAE Paper No. 900031

3. Bartrand, T.A., And Willis, E.A., "Performance of a Supercharged Direct-Injection Stratified-Charge Rotary Combustion Engine," paper presented at the Joint Symposium on General Aviation Systems co-sponsored by the AIAA and FAA at Ocean City, NJ, April 1990.

4. Raju, M.S. and Willis, E.A., "Computational Experience with a 3-D Rotary Engine Combustion Model," paper presented at the Joint Symposium on General Aviation systems co-sponsored by the AIAA and FAA at Ocean City, NJ, 1990.

5. Morita, T., Hamady, F., Stuecken, T., Somerton, C. and Schock, H., "Fuel-Air Mixing Visualization in a Motored Rotary Engine Assembly," SAE Paper No. 910704.

6. Hamady, F., DeFilippis, M., Stuecken, T. and Schock, H., "Experimental Analysis of Blowby and Flow Field Interaction in a Motored Rotary Engine," SAE Paper NO. 910893.

7. Li, Z., Shih, T.I-P, Schock, H. and Willis, E., "A Numerical Study on the Effects of Apex Seal Leakage on Wankel Engine Flow Fields," SAE Paper No. 910703.

8. Raju, M.S. and Willis, E., "Three-Dimensional Analysis and Modeling of a Wankel Engine," SAE Paper No. 910701.

9. Li, Z., Steinthorsson, E., Shih, T.i-P. and Nguyen, H.l., "Modeling and Simulation of Wankel Engine Flowfields," SAE Paper No. 900029.

9.0 CONCLUSIONS AND RECOMMENDATIONS

9.0 CONCLUSIONS AND RECOMMENDATIONS

Conclusions

Significant progress was made in key critical technology areas.

- Advanced, higher speed CFD capability was achieved.
- Correlation between 3-d combustion modeling and experimental hardware performance results was achieved.
- Power density equivalent to 400 BHP (300kw) in a twin rotor 0.7ℓ /rotor displacement engine was demonstrated.
- Fuel consumption reduction equivalent to 0.375 lbs/BHP-hr (228 gr/kw-hr) referred to a twin rotor 0.7ℓ /rotor displacement engine was demonstrated.
- Major system understanding and directions for future improved systems were established including
    - fuel injection systems
    - turbocharging systems
    - control systems
    - airframe and missions
- Directions were established for lightweight, improved rotor designs
- An overall aircraft engine reference design was completed, suitable for a baseline reference configuration

Recommendations

- Continue experimental testing and analysis to evaluate items designed and procured but not tested as a result of curtailment of this program
    - leading pocket rotor
    - re-entrant pocket rotor
    - intake and exhaust port variations
- Continue the technology enablement effort to permit preparation of and evaluation of several iterations of the twin rotor configuration over the full operational range of start, idle, taxi, climb, cruise and take-off power and speed conditions.

O:\WORK\DETEMP\MOUNT.6

PAGE 298 INTENTIONALLY BLANK

PRECEDING PAGE BLANK NOT FILMED

10.0 LISTING OF APPENDICES (VOLUME II)

PRECEDING PAGE BLANK NOT FILMED

10.0 LISTING OF APPENDICES (SEPARATE VOLUME)

APPENDIX A: NEW IMPROVED COMPUTATIONAL FLUID DYNAMICS (CFD) CODES/DETAILED ILLUSTRATIONS

APPENDIX B: FEASIBILITY ANALYSIS-ROTATING VALVE HIGH PRESSURE COMMON RAIL SYSTEM

APPENDIX C: TURBOMACHINERY SYSTEM ANALYSIS FOR STRATIFIED CHARGE ROTARY ENGINE CRITICAL TECHNOLOGY ENABLEMENT; REPORT NO. AER 3485, SUNDSTRAND AEROSPACE CORPORATION, 4 OCTOBER 91

PRECEDING PAGE BLANK NOT FILMED

302 INTENTIONALLY BLANK

REPORT DOCUMENTATION PAGE

Form Approved
OMB No. 0704-0188

Public reporting burden for this collection of information is estimated to average 1 hour per response, including the time for reviewing instructions, searching existing data sources, gathering and maintaining the data needed, and completing and reviewing the collection of information. Send comments regarding this burden estimate or any other aspect of this collection of information, including suggestions for reducing this burden, to Washington Headquarters Services, Directorate for Information Operations and Reports, 1215 Jefferson Davis Highway, Suite 1204, Arlington, VA 22202-4302, and to the Office of Management and Budget, Paperwork Reduction Project (0704-0188), Washington, DC 20503.

1. AGENCY USE ONLY (*Leave blank*)	2. REPORT DATE	3. REPORT TYPE AND DATES COVERED
	August 1992	Final Contractor Report

4. TITLE AND SUBTITLE

Stratified Charge Rotary Engine Critical Technology Enablement
Volume I

5. FUNDING NUMBERS

WU–505–62–1
C–NAS3–25945

6. AUTHOR(S)

C.E. Irion and R.E. Mount

7. PERFORMING ORGANIZATION NAME(S) AND ADDRESS(ES)

Rotary Power International, Inc.
P.O. Box 128
Wood-Ridge, New Jersey 07075

8. PERFORMING ORGANIZATION REPORT NUMBER

E–8831

9. SPONSORING/MONITORING AGENCY NAME(S) AND ADDRESS(ES)

National Aeronautics and Space Administration
Lewis Research Center
Cleveland, Ohio 44135–3191

10. SPONSORING/MONITORING AGENCY REPORT NUMBER

NASA CR–189106

11. SUPPLEMENTARY NOTES

Project Manager, Paul T. Kerwin, Propulsion Systems Division, NASA Lewis Research Center, organization code 2703, (216) 433–3409.

12a. DISTRIBUTION/AVAILABILITY STATEMENT

Unclassified - Unlimited
Subject Category 07

12b. DISTRIBUTION CODE

13. ABSTRACT (*Maximum 200 words*)

This report summarizes results of a critical technology enablement effort with the stratified charge rotary engine (SCRE) focusing on a power section of 0.67 liters (40 cu. in.) per rotor in single and two rotor versions. The work is a continuation of prior NASA Contracts NAS3–23056 and NAS3–24628. Technical objectives are multi-fuel capability, including civil and military jet fuel and DF-2, fuel efficiency of 0.355 Lbs/BHP-Hr. at best cruise condition above 50% power, altitude capability of up to 10Km (33,000 ft.) cruise, 2000 hour TBO and reduced coolant heat rejection. Critical technologies for SCREs that have the potential for competitive performance and cost in a representative light-aircraft environment were examined. Objectives were: the development and utilization of advanced analytical tools, i.e. higher speed and enhanced three dimensional combustion modeling; identification of critical technologies; development of improved instrumentation, and to isolate and quantitatively identify the contribution to performance and efficiency of critical components or subsystems.

14. SUBJECT TERMS

Stratified charge; Rotary; Engine; Aircraft; Fuel injection; CFD computer codes; Flow visualization; Multi-fuel

15. NUMBER OF PAGES
305

16. PRICE CODE
A14

17. SECURITY CLASSIFICATION OF REPORT	18. SECURITY CLASSIFICATION OF THIS PAGE	19. SECURITY CLASSIFICATION OF ABSTRACT	20. LIMITATION OF ABSTRACT
Unclassified	Unclassified	Unclassified	